TECHNISCHE UNIVERSITÄT KAISERSLAUTERN

Faruk Keskin

**Precoding for MIMO
multi-user mobile radio downlinks**

HS

Faruk Keskin
Seydlitzstraße 17
D - 67061 Ludwigshafen

Precoding for MIMO
multi-user mobile radio downlinks

deutscher Titel:

Sendesignalvorverarbeitung für Mehrteilnehmer-
Mobilfunkabwärtsstrecken mit MIMO-Antennen

Beim Fachbereich Elektrotechnik und Informationstechnik

der Technischen Universität Kaiserslautern

zur Verleihung des akademischen Grades

Doktor–Ingenieur (Dr.–Ing.)

eingereichte Dissertation

von

Dipl.–Ing. Faruk Keskin

D 386

Tag der Einreichung:	27.06.2007
Tag der mündlichen Prüfung:	08.10.2007

Dekan des Fachbereichs
Elektrotechnik und
Informationstechnik: Prof. Dr.–Ing. S. Liu

Vorsitzender der
Prüfungskommission: Prof. Dr.–Ing. H. Schotten

1. Berichterstatter: Prof. Dr.–Ing. habil. Dr.–Ing. E.h. P.W. Baier
2. Berichterstatter: Prof. Dr.–rer. nat. Dr. h.c. H. Rohling

Vorwort

Die vorliegende Arbeit entstand in der Zeit von Dezember 2005 bis Juni 2007 im Rahmen meiner Tätigkeit als wissenschaftlicher Mitarbeiter am Lehrstuhl für hochfrequente Signalübertragung und -verarbeitung der Technischen Universität Kaiserslautern. Ich möchte all jenen danken, die mich bei der Entstehung dieser Arbeit unterstützt haben.

Mein besonderer Dank gilt Herrn Prof. Dr.–Ing. habil. Dr.–Ing. E.h. P. W. Baier für die Anregung, die Betreuung und die Förderung meiner Arbeit. Durch seine stete Diskussionsbereitschaft sowie durch zahlreiche Ratschläge und Hinweise hat er wesentlich zum Gelingen dieser Arbeit beigetragen.

Herrn Prof. Dr. rer. nat. Dr. h.c. H. Rohling danke ich für das Interesse an meiner Arbeit und für die Übernahme des Korreferats. Weiterhin danke ich dem Vorsitzenden der Promotionskommission, Herrn Prof. Dr.–Ing. H- Schotten.

Den ehemaligen Kollegen an dem Lehrstuhl für hochfrequente Signalübertragung und -verarbeitung danke ich für eine angenehme Arbeitsatmosphäre und für viele fruchtbare Diskussionen, die mir oftmals weitergeholfen haben. Ein besonderer Dank ergeht an die Herren Dr.–Ing. habil. M. Meurer und Dipl.-Wirtsch.-Ing. J. Hahn für die erfolgreiche Zusammenarbeit in gemeinsamen Projekten und viele hilfreiche Hinweise. Ebenso danke ich allen Studenten, die im Rahmen ihrer Studien-, Diplom- und Masterarbeiten sowie als wissenschaftliche Hilfskräfte unter meiner Anleitung Beiträge zu dieser Arbeit geleistet haben. Hierbei sei insbesondere den Herren A. Egelhof und M. Bauer gedankt.

Die wissenschaftlichen Grundlagen meiner Arbeit konnten im Rahmen eines DFG-Forschungsvorhabens im Schwerpunktprogramm AKOM (Adaptivität in heterogenen Kommunikationsnetzen mit drahtlosem Zugang) entwickelt werden. Dafür danke ich der DFG. In meine Dissertation sind auch Ergebnisse eingeflossen, die aus der Kooperation des Lehrstuhls mit der Fa. Siemens entstanden, u.a. im BMBF-Projekt 3GET (Third Generation Evolving Technologies). Für diese Förderung sowie zahlreiche konstruktive Anregungen sei den Herren Dr.–Ing. E. Schulz und Dipl.-Ing. W. Zirwas herzlich gedankt.

Der Technischen Universität Kaiserslautern danke ich für die Möglichkeit, die leistungsfähigen Rechner des Regionalen Hochschulrechenzentrums Kaiserslautern (RHRK) für meine Forschungsarbeiten zu benutzen. Den Mitarbeitern des RHRK gilt mein Dank für die Beratung in Software- und Hardwarefragen.

Nicht zuletzt möchte ich mich bei meiner Familie und meinen Freunden bedanken, die mir immer ein großer Rückhalt waren. Ganz besonders herzlich danke ich meinen Eltern. Sie haben mir das Studium ermöglicht und mir immer ihre uneingeschränkte Unterstützung zukommen lassen. Ihnen widme ich diese Arbeit.

Kaiserslautern, im Juni 2007   Faruk Keskin

Contents

Chapter 1

Introduction

1.1 Receiver orientation versus transmitter orientation in radio transmission

This thesis deals with certain aspects of radio transmission systems with the focus on future multi-user mobile radio downlinks (DL) incorporating Multiple-Input Multiple-Output (MIMO) antenna systems. As a precondition of the investigations to be performed in the thesis, first some basic structural properties specific of the considered transmission systems have to be worked out. In doing so we resort to the equivalent low-pass representation of the considered bandpass systems [SJ67, Hay83, BBC87] and refer the reader to the conventions and nomenclature introduced in [Qiu05]; specifically, certain relations between the dimensions of the complex vectors and complex matrices occurring in the course of the thesis have to be fulfilled [Lue96, GvL96], which for the sake of brevity are not always explicitly mentioned. Fig. 1.1 shows the generic structure of the considered systems which consist of the transmitter (Tx), the channel (Ch), the noise adder (NA) and the receiver (Rx). The overall task of the system is the transfer of the data $\mathfrak{a}$ from the transmitter input to the receiver output, where we obtain the data $\hat{\mathfrak{a}}$. This transfer should be as reliable as possible. This means that it would be desirable that $\hat{\mathfrak{a}}$ becomes equal to $\mathfrak{a}$. However, due to the added noise, in general this equality cannot be strictly guaranteed. $\hat{\mathfrak{a}}$ cannot be more than an estimate of $\mathfrak{a}$, that is transmission errors have to be accepted. The occurrence of such errors can be quantified by the error probability

$$P_{\mathrm{e}} = \mathrm{Prob}\left(\hat{\mathfrak{a}} \neq \mathfrak{a}\right). \tag{1.1}$$

In the structure of Fig. 1.1 the performance of the transmitter can be characterized by the transmit operator $\mathcal{M}\left(\mathfrak{a}\right)$, which assigns to the data $\mathfrak{a}$ the complex transmit vector

$$\underline{\mathbf{t}} = \mathcal{M}\left(\mathfrak{a}\right) \in \mathbb{C}^{Q \times 1}. \tag{1.2}$$

Under $\mathcal{M}\left(\mathfrak{a}\right)$ we subsume transmitter typical procedures as for instance FEC coding, modulation etc. $\underline{\mathbf{t}}$ of (1.2) is fed into the channel, which is assumed to be linear so that it can be characterized by the channel matrix [Bel63, BMWT00, MBW$^+$00, BQT$^+$03]

$$\underline{\mathbf{H}} \in \mathbb{C}^{Z \times Q}. \tag{1.3}$$

At its output the channel yields the undisturbed receive vector

$$\underline{e} = \underline{H}\,\underline{t} \in \mathbb{C}^{Z \times 1}. \tag{1.4}$$

In radio communications the assumption of said linearity of the channel is justified as long as its fluctuations with time are sufficiently slow, a requirement equivalent to a negligible impact of the Doppler effect [FK03]. In the noise adder, $\underline{e}$ of (1.4) is corrupted by the noise vector $\underline{\tilde{n}}$. This produces at the output of the noise adder the disturbed receive vector

$$\underline{r} = \underline{e} + \underline{\tilde{n}} \in \mathbb{C}^{Z \times 1}, \tag{1.5}$$

which is then delivered to the receiver. Based on $\underline{r}$ the receiver, which is characterized by the receive operator $\mathcal{D}\left(\underline{r}\right)$, generates the estimate

$$\hat{\mathfrak{a}} = \mathcal{D}\left(\underline{r}\right) \tag{1.6}$$

of the sent data $\mathfrak{a}$. The elements of the vectors $\underline{t}$, $\underline{e}$, $\underline{n}$ and $\underline{r}$ represent sample values of physical signals [BQT+03]. Depending on whether single carrier [MBW+00, QTM02, QMBW04] or multi-carrier transmission [SWBC02, WLM+03] systems are considered, it is more convenient and obvious to take these sample values in the time or frequency domains, respectively. The channel matrix $\underline{H}$ of (1.3) establishes input-output relations between

- temporal signal samples in the former case - then $\underline{H}$ can be termed convolution matrix, and

- spectral signal samples, that is complex amplitudes, in the latter case - then $\underline{H}$ can be designated as matrix of transfer function values.
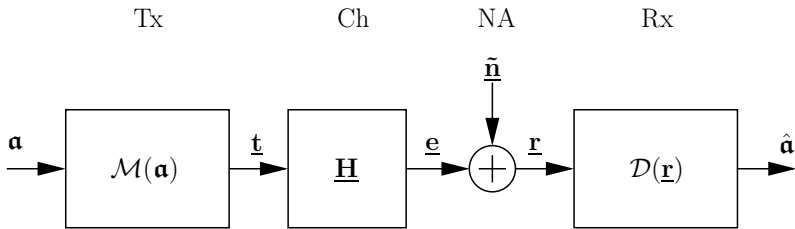
Fig. 1.1. Generic structure of the considered transmission systems

$\mathfrak{a}$ can take on R different realizations $\mathfrak{a}^{(1)} \ldots \mathfrak{a}^{(R)}$, that is

$$\mathfrak{a} \in \left\{ \mathfrak{a}^{(1)} \ldots \mathfrak{a}^{(R)} \right\}, \tag{1.7}$$

which are all assumed to occur with the same probability $1/R$. The transmitter assigns to each of these realizations $\mathfrak{a}^{(r)}$, $r = 1 \ldots R$ a realization $\underline{t}^{(r)}$ of $\underline{t}$, that is

$$\underline{t} \in \left\{ \underline{t}^{(1)} \ldots \underline{t}^{(R)} \right\}. \tag{1.8}$$

It is self-evident that, for given properties of the noise vector $\underline{\tilde{n}}$, the performance of transmission systems with the structure shown in Fig. 1.1 not only depends on the operators $\mathcal{M}(\mathfrak{a})$ and $\mathcal{D}(\underline{r})$, but also on the properties of the channel, that is, in our case, on the channel matrix $\underline{H}$. The structure shown in Fig. 1.1 gives the impression that the transmit operator $\mathcal{M}(\mathfrak{a})$ and the receive operator $\mathcal{D}(\underline{r})$ are set without any consideration of the channel properties, and, indeed, this would be a possible rationale of system design, which sometimes is termed 'blind' (with respect to $\underline{H}$) [MFP97, Hug00, LSF03, LHS03]. However, if knowledge of the channel properties - such knowledge is also termed channel state information (CSI) - is available, then its appropriate consideration in system design and operation can be expected to enhance the system performance. Concerning such a consideration of CSI, three main approaches exist, which are illustrated in Figs. 1.2 a to c and can be characterized as follows [QTMJ03, BQT+03, MBQ04]: CSI is taken into account when determining the algorithms and/or parametrizations of

- both the transmit and the receive operators in the concept of Fig. 1.2 a. For this concept the attribute 'channel oriented (CO)' has been coined due to the determining influence of CSI on both the transmit and receive operators.

- The receive operator in the concept of Fig. 1.2 b. This concept is also said to be transmitter oriented (TO), because the transmit operator ('master') can be a priori set without taking into account CSI, whereas the receive operator ('slave') depends on CSI and the transmit operator.

- The transmit operator in the concept of Fig. 1.2 c. This concept is also termed receiver oriented (RO), because the receive operator ('master') can be a priori set without taking into account CSI, whereas the transmit operator ('slave') depends on CSI and the receive operator.

In the case of a time varying channel, CSI should be made available to the receiver and/or transmitter in the structures of Figs. 1.2 a to c, respectively, in an on-line fashion, that is during system operation. In Figs. 1.2 a to c this is visualized by a direct connection
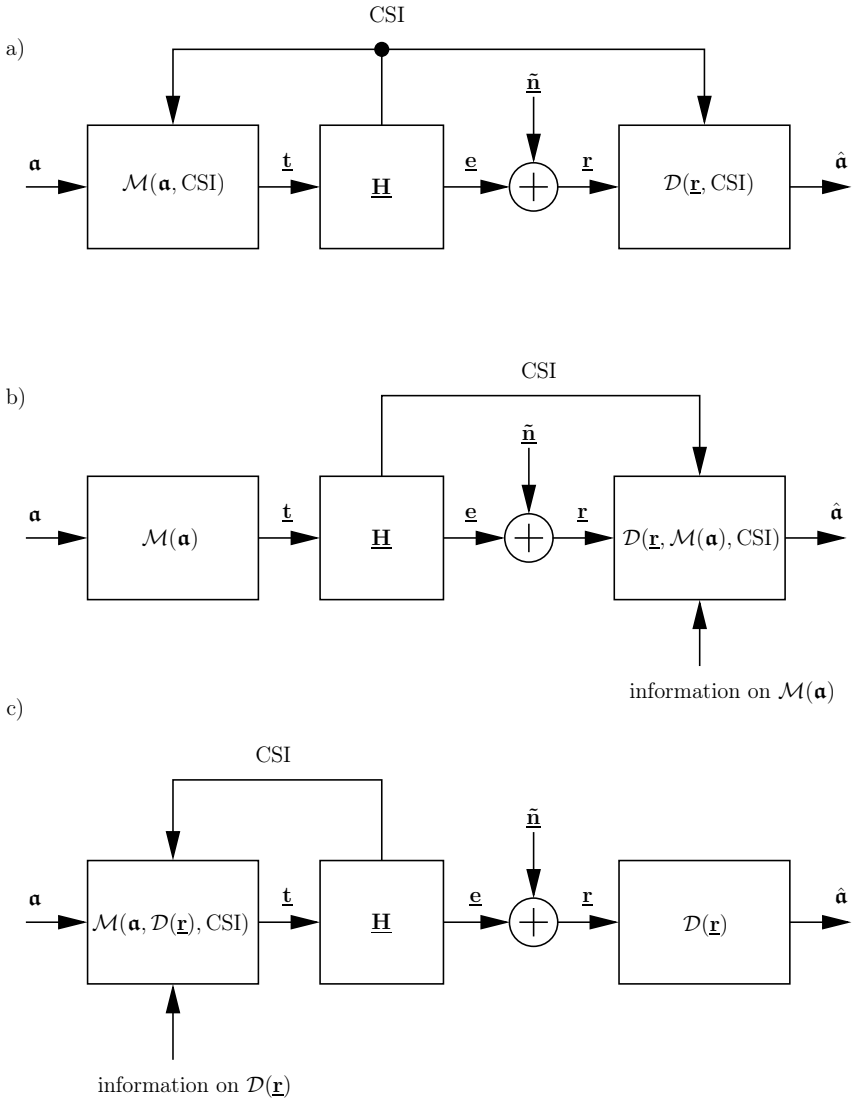
Fig. 1.2. Transmission concepts
  a) Channel oriented (CO)
  b) Transmitter oriented (TO)
  c) Receiver oriented (RO)

from the channel to the receiver and/or transmitter, respectively. For clarification, this connection does not symbolize a physical link from the channel to the receiver and/or transmitter, but only indicates the provision of CSI irrespective of how this is effected. In contrast to said provision of CSI, the information on $\mathcal{M}(\mathfrak{a})$ to the receiver in the case of TO or on $\mathcal{D}(\underline{r})$ to the transmitter in the case of RO could be performed off-line, because once $\mathcal{M}(\mathfrak{a})$ or $\mathcal{D}(\underline{r})$, respectively, are set, these operators are kept constant, at least in the 'pure' schemes TO or RO.

As one approach to CO, it could be based on the Singular Value Decomposition (SVD) of $\underline{\mathbf{H}}$ [JVP98, MTWB01, CM04], possibly in combination with waterfilling [CT91]. TO has the potential to lead to relatively low cost transmitters, whereas the receivers tend to be more complex [MBW+00, BQT+03, MBQ04]. The opposite is true for RO [VJ98, BMWT00, PMWB00, CM02]. Therefore, concerning mobile radio systems with their strong demand of low cost mobile terminals (MT),

- TO should be chosen for the uplink (UL), and

- RO for the downlink (DL).

Because the topic of this work are future mobile radio DLs, we concentrate throughout the thesis on RO with its inherent complexity advantage for this direction of data transmission. However, it should be mentioned that in today's operational mobile radio systems not only the UL, but also the DL still invariably rely on the scheme TO.

1.2 Requirements of low transmit power and low receive signal dynamics

When designing radio transmission systems, first of all - depending on the envisaged application - two vital and, therefore, primary requirements have to be borne in mind:

- The application specific required data rates should be guaranteed, and

- the error probability P_e of (1.1) should not exceed a given upper bound.

In addition, there exist quite a number of other, quasi secondary requirements [Meu05]. In this thesis we will focus on two rather important ones of them:

- The transmit power needed to meet said vital requirements should be as small as possible, and

- the amplitude dynamics of the receive signals, that is the variance of their amplitudes, should be kept low.

Low transmit power is desirable both with respect to diminishing the electromagnetic immission as a possible source of health hazards, and to the mitigation of interference to other radio links; as another beneficial effect, also the consumption of primary power goes down with decreasing transmit power. Concerning the requirement of low amplitude dynamics of the received signals, it should be remembered that these dynamics have a direct impact on the required amplitude resolution and, therefore, on the word length of the A/D converters at the receiver inputs and of the subsequent digital signal processing. For clarification it should be mentioned that here by 'amplitude dynamics' we do not mean the amplitude fluctuations of the received signals caused by fading, which can be at least partially compensated by power control, but the amplitude dynamics inherent in the signal structure which remain despite of power control. As another demand on radio transmission systems, the amplitude dynamics of the transmitted signals should be low [MR98, Wun03, HL05]. However, this issue is beyond the scope of this thesis, even though the presented approaches to modelling and conceiving RO transmission systems would be a good basis for tackling this problem as well [Jia04, HRF06].

As stated in Section 1.1, the topic of the thesis are MIMO multi-user mobile radio DLs based on RO. We now can formulate the problems addressed in the thesis more precisely as follows: Minimization of the required transmit powers of such systems under observation of the additional aspect of low amplitude dynamics of the received signals with a view to possibly reduce these dynamics.

1.3   Transmission systems with a linear inner section

We reconsider the generic system structure of Fig. 1.1. Most transmission systems studied today result by specialising this structure as illustrated in Fig. 1.3. In this structure the transmit operator $\mathcal{M}(\mathbf{a})$ and the receive operator $\mathcal{D}(\underline{\mathbf{r}})$ are built up in a specific manner, which we are now going to describe. In the transmit operator $\mathcal{M}(\mathbf{a})$, to each realization $\mathbf{a}^{(r)}$, $r = 1 \ldots R$, of $\mathbf{a}$ a complex vector

$$\underline{\mathbf{d}}^{(r)} = \left(\underline{d}_1^{(r)} \ldots \underline{d}_N^{(r)} \right)^{\mathrm{T}} \tag{1.9}$$

is uniquely assigned, the N components $\underline{d}_n^{(r)}$ of which are all taken from the same set

$$\mathbb{V} = \{ \underline{v}_1 \ldots \underline{v}_M \} \tag{1.10}$$

$\hat{\underline{\mathbf{a}}}$

$\underline{\mathbf{a}}$

Tx   Ch   NA   Rx

$\mathcal{M}(\underline{\mathbf{a}})$ modulator   demodulator   quantizer

$\mathcal{D}(\underline{\mathbf{r}})$

unique assignment

$\underline{\mathbf{a}}^{(r)} \rightarrow \underline{\mathbf{d}}^{(r)}$

$\underline{\mathbf{d}}^{(r)}$

$\underline{\mathbf{M}}$

$\underline{\mathbf{t}}^{(r)}$

$\underline{\mathbf{H}}$

$\underline{\mathbf{e}}^{(r)}$ $\underline{\tilde{\mathbf{n}}}$ $\underline{\mathbf{r}}^{(r)}$

$\underline{\mathbf{D}}$

$\underline{\mathbf{d}}_{\mathrm{Rx}}$

$\mathcal{Q}(\underline{\mathbf{d}}_{\mathrm{Rx}})$

linear inner section
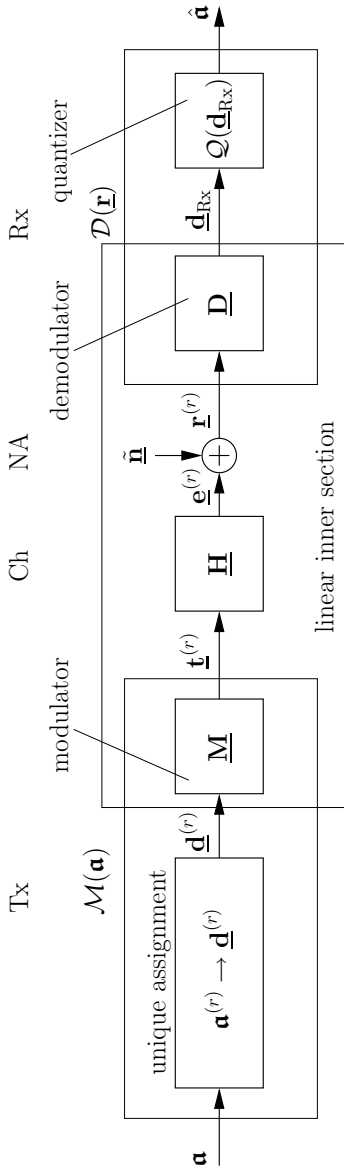
Fig. 1.3. Transmission system with a linear inner section

of M discrete valued representatives $\underline{v}_1 \ldots \underline{v}_M$, which we term unique representative values (the attribute unique will become clear in Chapter 2). The parameter M is called cardinality of the set $\mathbb{V}$ of (1.10). We term $\mathbb{V}$ representative set of $\mathfrak{a}$. In order to enable a unique data representation of the R realizations $\mathfrak{a}^{(r)}$ of $\mathfrak{a}$ by R representative vectors $\underline{d}^{(r)}$, the representative vectors of two different realizations $\mathfrak{a}^{(r)}$ and $\mathfrak{a}^{(r')}$, $r' \neq r$, of $\mathfrak{a}$ have to differ in at least one of their N components. Due to this requirement the relation

$$R \leq M^N \tag{1.11}$$

has to be fulfilled. In the case of the sign of equality, for given values of M and N the maximum possible number of data realizations $\mathfrak{a}^{(r)}$ is accommodated, which means that the data realizations $\mathfrak{a}^{(r)}$ are represented by the vectors $\underline{d}^{(r)}$ of (1.9) without redundancy. Otherwise, we would have redundancy in the sense of block channel encoding.

In the structure of Fig. 1.3 the transmit vector $\underline{t}^{(r)}$ pertaining to $\mathfrak{a}^{(r)}$ is obtained from $\underline{d}^{(r)}$ of (1.9) in a linear manner, namely by feeding $\underline{d}^{(r)}$ into a modulator described by a matrix

$$\underline{M} \in \mathbb{C}^{Q \times N} \tag{1.12}$$

termed modulator matrix, which yields

$$\underline{t}^{(r)} = \left(\underline{t}_1^{(r)} \ldots \underline{t}_Q^{(r)} \right)^{\mathrm{T}} = \underline{M}\,\underline{d}^{(r)} \in \mathbb{C}^{Q \times 1}. \tag{1.13}$$

In $\underline{t}^{(r)}$ of (1.13) the contribution of each of the N components $\underline{d}_n^{(r)}$ of $\underline{d}^{(r)}$ of (1.9) is contained in the form of a component-specific transmit vector, which in the receiver may or may not cause interference on components $\underline{d}_{n'}^{(r)}$, $n \neq n'$, of $\underline{d}^{(r)}$, that is these vectors can be designed as non-interfering. Let us designate column n of a matrix in brackets as $[\cdot]_{(n)}$. Then, the component-specific transmit vector $\underline{t}_n^{(r)}$ can be expressed as, see (1.13),

$$\underbrace{[\underline{M}]_{(n)}\underline{d}_n^{(r)}}_{\underline{t}_{0,n}^{(r)}} = \underline{t}_n^{(r)}. \tag{1.14}$$

We term $\underline{t}_{0,n}^{(r)}$ of (1.14) normalized component-specific transmit vector.

The receive operator $\mathcal{D}\left(\underline{r}\right)$ consists of a linear part which we term demodulator and which is characterized by the demodulator matrix

$$\underline{D} \in \mathbb{C}^{N \times Z}, \tag{1.15}$$

and a quantizer described by a quantization operator $\mathcal{Q}(.)$, which has to be non-linear by nature.

In the structure of Fig. 1.3 the four components modulator, channel, noise adder and demodulator constitute what we term the linear inner section of the system. With $\underline{\mathbf{d}}^{(r)}$ of (1.9) and the noise vector $\underline{\tilde{\mathbf{n}}}$ we obtain at the demodulator output the vector

$$\underline{\mathbf{d}}_{\mathrm{Rx}} = \underline{\mathbf{D}}\,\underline{\mathbf{H}}\,\underline{\mathbf{M}}\,\underline{\mathbf{d}}^{(r)} + \underbrace{\underline{\mathbf{D}}\,\underline{\tilde{\mathbf{n}}}}_{\underline{\mathbf{n}}} = \underline{\mathbf{D}}\,\underline{\mathbf{H}}\,\underline{\mathbf{M}}\,\underline{\mathbf{d}}^{(r)} + \underline{\mathbf{n}} \in \mathbb{C}^{N \times 1}. \tag{1.16}$$

1.4 Rationale Zero Forcing

1.4.1 Receive Zero Forcing and Transmit Zero Forcing

For a given channel matrix $\underline{\mathbf{H}}$ we can choose the modulator matrix $\underline{\mathbf{M}}$ and the demodulator matrix $\underline{\mathbf{D}}$ in such a way that

$$\underline{\mathbf{D}}\,\underline{\mathbf{H}}\,\underline{\mathbf{M}} = \mathbf{I}^{N \times N} \tag{1.17}$$

holds. In this case follows from (1.16)

$$\underline{\mathbf{d}}_{\mathrm{Rx}} = \underline{\mathbf{D}}\,\underline{\mathbf{H}}\,\underline{\mathbf{M}}\,\underline{\mathbf{d}}^{(r)} + \underline{\mathbf{D}}\,\underline{\tilde{\mathbf{n}}} = \underline{\mathbf{D}}\,\underline{\mathbf{H}}\,\underline{\mathbf{t}}^{(r)} + \underline{\mathbf{D}}\,\underline{\tilde{\mathbf{n}}} = \underline{\mathbf{d}}^{(r)} + \underline{\mathbf{D}}\,\underline{\tilde{\mathbf{n}}} = \underline{\mathbf{d}}^{(r)} + \underline{\mathbf{n}}, \tag{1.18}$$

that is the vector $\underline{\mathbf{d}}^{(r)}$ applied to the input of the modulator re-appears at the output of the demodulator free from any interference between its components $\underline{d}_n^{(r)}$, $n = 1 \ldots N$, and is only disturbed by the additive noise $\underline{\mathbf{n}}$ equal to $\underline{\mathbf{D}}\,\underline{\tilde{\mathbf{n}}}$. In other words, the transmission system becomes transparent with respect to the representative vectors $\underline{\mathbf{d}}^{(r)}$. Said absence of interference is accomplished by forcing interference to zero due to a specific choice of $\underline{\mathbf{M}}$ and $\underline{\mathbf{D}}$. Therefore, this approach is known as Zero Forcing (ZF) [VJ98, MBW$^+$00, MBQ04]. In general the noise vector $\underline{\mathbf{n}}$ in (1.16) is non-white; it would be white only if the Gram matrix $\underline{\mathbf{D}}\,\underline{\mathbf{D}}^{\mathrm{H}}$ would be proportional to the identity matrix $\mathbf{I}^{N \times N}$. The perfect nulling of interference by ZF could be bargained for a reduced impact of the noise vector $\underline{\tilde{\mathbf{n}}}$ with a view to minimize the joint disturbance by interference and noise. Examples would be systems employing Minimum Mean Square Error (MMSE) approach [KSS99, CM02, PHS03, HPS05a]. However the advantage of such approaches over ZF is only marginal [MBQ04, KB07b] and, therefore, they are left aside in this thesis.

The components of $\underline{\mathbf{d}}^{(r)}$, which compose the undisturbed part of $\underline{\mathbf{d}}_{\mathrm{Rx}}$ of (1.18), can be considered the landing points aspired by ZF in the complex plane. Therefore, sometimes in this thesis the synonym "landing points" is used for these components.

We now reconsider the concepts TO and RO explained in Section 1.1 for the special case of transmission systems with a linear inner section, see Fig. 1.3. In the case of such systems, a priori setting the transmit operator $\mathcal{M}(\mathfrak{a})$ in the sense of TO means that the modulator matrix $\underline{\mathbf{M}}$ of (1.12) is a priori given. Then, based on (1.17) the demodulator

matrix

$$\underline{\mathbf{D}} = \left[(\underline{\mathbf{H}}\,\underline{\mathbf{M}})^{\mathrm{H}}\,\underline{\mathbf{H}}\,\underline{\mathbf{M}} \right]^{-1} (\underline{\mathbf{H}}\,\underline{\mathbf{M}})^{\mathrm{H}} \tag{1.19}$$

results from $\underline{\mathbf{M}}$ and $\underline{\mathbf{H}}$ [VJ98, MBW$^+$00, MBQ04]. By this $\underline{\mathbf{D}}$ the variances of the components of $\underline{\mathbf{n}}$ of (1.16) are minimized under the side condition of nulling interference. Due to the fact that in this case interference is forced to zero in the receiver by suitably processing the receive vector $\underline{\mathbf{r}}$ of (1.5), we speak of Receive Zero Forcing (RxZF). A priori setting the receive operator $\mathcal{D}\left(\underline{\mathbf{r}}\right)$ in the sense of RO means in transmission systems with a linear inner section that the demodulator matrix $\underline{\mathbf{D}}$ is a priori set. Then, we obtain via (1.17) from $\underline{\mathbf{H}}$ and $\underline{\mathbf{D}}$ the modulator matrix

$$\underline{\mathbf{M}} = (\underline{\mathbf{D}}\,\underline{\mathbf{H}})^{\mathrm{H}} \left[\underline{\mathbf{D}}\,\underline{\mathbf{H}}\,(\underline{\mathbf{D}}\,\underline{\mathbf{H}})^{\mathrm{H}} \right]^{-1} \tag{1.20}$$

[MBQ04], by which the required transmit energy is minimized under the side condition of nulling interference. In this case the occurrence of interference on the receiver side is forced to zero already in the transmitter by properly choosing the transmit vector $\underline{\mathbf{t}}$ of (1.2), and, therefore, we speak of Transmit Zero Forcing (TxZF). With $\underline{\mathbf{M}}$ of (1.20) the normalized composed-specific transmit vectors of (1.14) become non-interfering.

$\underline{\mathbf{D}}$ of (1.19) and $\underline{\mathbf{M}}$ of (1.20), see [Lue96], are special versions of the Moore-Penrose inverses $[\underline{\mathbf{H}}\,\underline{\mathbf{M}}]^{+}$ of $\underline{\mathbf{H}}\,\underline{\mathbf{M}}$ and $[\underline{\mathbf{D}}\,\underline{\mathbf{H}}]^{+}$ of $\underline{\mathbf{D}}\,\underline{\mathbf{H}}$, respectively, obtained for the case

$$N \leq \min\left(Q, Z\right), \tag{1.21}$$

which throughout this thesis is assumed to be fulfilled. If (1.21) would not be fulfilled, then one should resort to a more general form of the Moore-Penrose inverse [Lue96], which no longer leads to exact spot landings on the desired landing points, that is ZF could no longer be achieved. (1.21) is a necessary, but not sufficient condition that the matrix inversions in (1.19) and (1.20) exist. Despite the fulfillment of (1.21) the matrices to be inverted could be singular. However, in this thesis we exclude such singular matrices.

As mentioned at the end of Section 1.1, we concentrate on RO in this thesis. We now concretize this statement as follows: The considered RO systems shall have a linear inner section as shown in Fig. 1.3 and resort to TxZF as characterized by (1.20). Under these premises, we obtain, by combining the structures of Figs. 1.2 c and 1.3, the structure shown in Fig. 1.4, which is of interest in this thesis.

1.4.2   Performance criteria

In [Trö03, Qiu05] performance criteria for RxZF and TxZF are introduced. Even though these criteria are not quite adequate for evaluating RO systems based on TxZF, which form
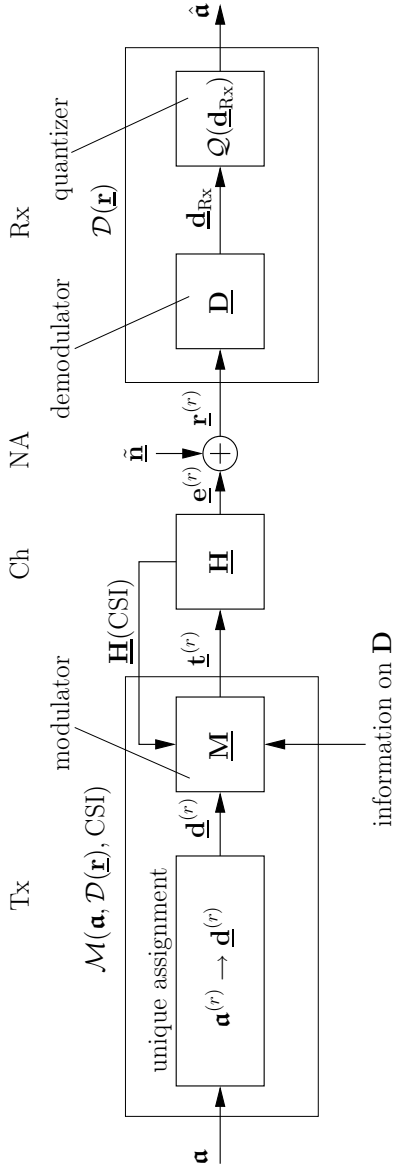
Fig. 1.4. RO transmission with unique data representation

the main focus of this thesis, the author believes that is would be elucidating to briefly revisit these criteria in what follows with a view to clearly elaborate analogies between RxZF and TxZF. Said criteria are relative, because they are based on the quantitative comparison of RxZF and TxZF with reference systems. For simplicity, we assume in these comparisons and also in the further course of this thesis that the received noise vector $\underline{\tilde{n}}$ in (1.5) is stationary and white with the variance σ^2 of the real and imaginary parts of its components, that is

$$\underline{\mathbf{R}}_{\underline{\tilde{n}}} = \mathrm{E}\left\{\underline{\tilde{n}}\,\underline{\tilde{n}}^{\mathrm{H}}\right\} = 2\sigma^2 \cdot \mathbf{I}^{Z \times Z}\,. \tag{1.22}$$

However, the following considerations could be readily extended to cases with a non-white stationary noise vector $\underline{\tilde{n}}$ as well. We further assume in the present subsection that the matrices $\underline{\mathbf{H}}$, $\underline{\mathbf{M}}$ and $\underline{\mathbf{D}}$ are fixed so that, when performing averaging, only the time variance of the data $\mathbf{a}$ and the noise vector $\underline{\tilde{n}}$ play a role.

As explained in [Kle96, Trö03], in the case of RxZF the obvious reference system would be the Receive Matched Filter (RxMF), which is characterized by the demodulator matrix [MBQ04]

$$\underline{\mathbf{D}}_{\mathrm{RxMF}} = \left(\mathrm{diag}\left[(\underline{\mathbf{H}}\,\underline{\mathbf{M}})^{\mathrm{H}}\,\underline{\mathbf{H}}\,\underline{\mathbf{M}}\right]\right)^{-1}(\underline{\mathbf{H}}\,\underline{\mathbf{M}})^{\mathrm{H}}\,. \tag{1.23}$$

The RxMF minimizes the variances of the real and imaginary parts of the N components of the noise vector $\underline{n}$ contained in the components of $\underline{d}_{\mathrm{Rx}}$ of (1.16) without taking into account interference. With $\underline{\mathbf{R}}_{\underline{\tilde{n}}}$ of (1.22) and $\underline{\mathbf{D}}_{\mathrm{RxMF}}$ of (1.23) these variances can be expressed as

$$\sigma^2_{\mathrm{RxMF},n} = \tfrac{1}{2} \cdot \left[\mathrm{E}\left\{\underline{\mathbf{D}}_{\mathrm{RxMF}}\underline{\tilde{n}}\,\underline{\tilde{n}}^{\mathrm{H}}\underline{\mathbf{D}}_{\mathrm{RxMF}}^{\mathrm{H}}\right\}\right]_{n,n} = \tfrac{1}{2} \cdot \left[\underline{\mathbf{D}}_{\mathrm{RxMF}}\underline{\mathbf{R}}_{\underline{\tilde{n}}}\underline{\mathbf{D}}_{\mathrm{RxMF}}^{\mathrm{H}}\right]_{n,n}$$

$$= \sigma^2\left[\left(\mathrm{diag}\left[(\underline{\mathbf{H}}\,\underline{\mathbf{M}})^{\mathrm{H}}\,\underline{\mathbf{H}}\,\underline{\mathbf{M}}\right]\right)^{-1}(\underline{\mathbf{H}}\,\underline{\mathbf{M}})^{\mathrm{H}}\,\underline{\mathbf{H}}\,\underline{\mathbf{M}}\left(\mathrm{diag}\left[(\underline{\mathbf{H}}\,\underline{\mathbf{M}})^{\mathrm{H}}\,\underline{\mathbf{H}}\,\underline{\mathbf{M}}\right]\right)^{-1}\right]_{n,n} \tag{1.24}$$

$$= \sigma^2\left[\left(\mathrm{diag}\left[(\underline{\mathbf{H}}\,\underline{\mathbf{M}})^{\mathrm{H}}\,\underline{\mathbf{H}}\,\underline{\mathbf{M}}\right]\right)^{-1}\right]_{n,n} = \sigma^2/\left[(\underline{\mathbf{H}}\,\underline{\mathbf{M}})^{\mathrm{H}}\,\underline{\mathbf{H}}\,\underline{\mathbf{M}}\right]_{n,n}\,.$$

Now we consider the variances of the real and imaginary parts of the components of the noise vector $\underline{n}$ contained in $\underline{d}_{\mathrm{Rx}}$ of (1.16) for the RxZF. In this case, we obtain with $\underline{\mathbf{R}}_{\underline{\tilde{n}}}$ of (1.22) and $\underline{\mathbf{D}}$ of (1.19)

$$\sigma^2_n = \tfrac{1}{2} \cdot \left[\mathrm{E}\left\{\underline{\mathbf{D}}\,\underline{\tilde{n}}\,\underline{\tilde{n}}^{\mathrm{H}}\underline{\mathbf{D}}^{\mathrm{H}}\right\}\right]_{n,n} = \tfrac{1}{2} \cdot \left[\underline{\mathbf{D}}\,\underline{\mathbf{R}}_{\underline{\tilde{n}}}\underline{\mathbf{D}}^{\mathrm{H}}\right]_{n,n}$$

$$= \sigma^2\left[\left[(\underline{\mathbf{H}}\,\underline{\mathbf{M}})^{\mathrm{H}}\,\underline{\mathbf{H}}\,\underline{\mathbf{M}}\right]^{-1}(\underline{\mathbf{H}}\,\underline{\mathbf{M}})^{\mathrm{H}}\,\underline{\mathbf{H}}\,\underline{\mathbf{M}}\left[(\underline{\mathbf{H}}\,\underline{\mathbf{M}})^{\mathrm{H}}\,\underline{\mathbf{H}}\,\underline{\mathbf{M}}\right]^{-1}\right]_{n,n} \tag{1.25}$$

$$= \sigma^2\left[\left[(\underline{\mathbf{H}}\,\underline{\mathbf{M}})^{\mathrm{H}}\,\underline{\mathbf{H}}\,\underline{\mathbf{M}}\right]^{-1}\right]_{n,n}\,.$$

As the performance criterion, the ratios of the N noise variances σ_n^2 and $\sigma_{\mathrm{RxMF},n}^2$ occurring in the cases of RxZF and RxMF are proposed, which we term component specific noise raises of RxZF [Trö03]. For the component $\underline{d}_{\mathrm{Rx},n}$ of (1.16) the component specific noise raise becomes [Trö03, Kle96] with (1.24) and (1.25)

$$\delta_n = \frac{\sigma_n^2}{\sigma_{\mathrm{RxMF},n}^2} = \left[(\underline{\mathbf{H}}\,\underline{\mathbf{M}})^{\mathrm{H}}\,\underline{\mathbf{H}}\,\underline{\mathbf{M}}\right]_{n,n} \left[\left[(\underline{\mathbf{H}}\,\underline{\mathbf{M}})^{\mathrm{H}}\,\underline{\mathbf{H}}\,\underline{\mathbf{M}}\right]^{-1}\right]_{n,n} \geq 1\,. \qquad (1.26)$$

In [Trö03, Kle96] δ_n of (1.26) is termed SNR degradation. Averaging over all N values δ_n of (1.26) would give the mean noise raise

$$\delta = \frac{1}{N}\sum_{n=1}^{N}\delta_n = \frac{1}{N}\cdot\mathrm{trace}\left\{\left[(\underline{\mathbf{H}}\,\underline{\mathbf{M}})^{\mathrm{H}}\,\underline{\mathbf{H}}\,\underline{\mathbf{M}}\right]^{-1}\mathrm{diag}\left((\underline{\mathbf{H}}\,\underline{\mathbf{M}})^{\mathrm{H}}\,\underline{\mathbf{H}}\,\underline{\mathbf{M}}\right)\right\} \geq 1\,. \qquad (1.27)$$

A performance criterion for RxZF similar to δ of (1.27) would be the ratio

$$\bar{\delta} = \mathrm{trace}\left\{\left[(\underline{\mathbf{H}}\,\underline{\mathbf{M}})^{\mathrm{H}}\,\underline{\mathbf{H}}\,\underline{\mathbf{M}}\right]^{-1}\right\} / \mathrm{trace}\left\{\left(\mathrm{diag}\left[(\underline{\mathbf{H}}\,\underline{\mathbf{M}})^{\mathrm{H}}\,\underline{\mathbf{H}}\,\underline{\mathbf{M}}\right]\right)^{-1}\right\} \geq 1 \qquad (1.28)$$

of the sum of the noise variances pertaining to the N components $\underline{d}_{\mathrm{Rx},n}$ of (1.16) in the cases of RxZF and RxMF. $\bar{\delta}$ of (1.28) could be termed overall noise raise.

In analogy to the just considered case of RxZF, the obvious reference system for TxZF would be the Transmit Matched Filter (TxMF), which is characterized by the modulator matrix [EN93, ESN93, MBQ04]

$$\underline{\mathbf{M}}_{\mathrm{TxMF}} = (\underline{\mathbf{D}}\,\underline{\mathbf{H}})^{\mathrm{H}}\left(\mathrm{diag}\left[\underline{\mathbf{D}}\,\underline{\mathbf{H}}\,(\underline{\mathbf{D}}\,\underline{\mathbf{H}})^{\mathrm{H}}\right]\right)^{-1}. \qquad (1.29)$$

The TxMF minimizes for each of the N components $\underline{d}_n^{(r)}$ of $\underline{\mathbf{d}}^{(r)}$ of (1.9) the required transmit energy $T_{\mathrm{TxMF},n}$ without taking into account the occurrence of interference. The N transmit energies $T_{\mathrm{TxMF},n}$ are termed component specific transmit energies. With the components $\underline{d}_n^{(r)}$ of $\underline{\mathbf{d}}^{(r)}$ of (1.9) and $\underline{\mathbf{M}}_{\mathrm{TxMF}}$ of (1.29) these energies can be expressed as

$$T_{\mathrm{TxMF},n}^{(r)} = \tfrac{1}{2}\left|\underline{d}_n^{(r)}\right|^2\left[\underline{\mathbf{M}}_{\mathrm{TxMF}}^{\mathrm{H}}\underline{\mathbf{M}}_{\mathrm{TxMF}}\right]_{n,n}$$

$$= \tfrac{1}{2}\left|\underline{d}_n^{(r)}\right|^2\left[\left(\mathrm{diag}\left[\underline{\mathbf{D}}\,\underline{\mathbf{H}}\,(\underline{\mathbf{D}}\,\underline{\mathbf{H}})^{\mathrm{H}}\right]\right)^{-1}\underline{\mathbf{D}}\,\underline{\mathbf{H}}\,(\underline{\mathbf{D}}\,\underline{\mathbf{H}})^{\mathrm{H}}\left(\left[\mathrm{diag}\underline{\mathbf{D}}\,\underline{\mathbf{H}}\,(\underline{\mathbf{D}}\,\underline{\mathbf{H}})^{\mathrm{H}}\right]\right)^{-1}\right]_{n,n} \qquad (1.30)$$

$$= \tfrac{1}{2}\left|\underline{d}_n^{(r)}\right|^2\left[\left(\mathrm{diag}\left[\underline{\mathbf{D}}\,\underline{\mathbf{H}}\,(\underline{\mathbf{D}}\,\underline{\mathbf{H}})^{\mathrm{H}}\right]\right)^{-1}\right]_{n,n} = \tfrac{1}{2}\left|\underline{d}_n^{(r)}\right|^2 / \left[\underline{\mathbf{D}}\,\underline{\mathbf{H}}\,(\underline{\mathbf{D}}\,\underline{\mathbf{H}})^{\mathrm{H}}\right]_{n,n}.$$

Now we consider the required transmit energies $T_n^{(r)}$ in the case of the TxZF. With $\underline{\mathbf{M}}$ of

(1.20) we obtain

$$
T_n^{(r)} = \tfrac{1}{2} \left| \underline{d}_n^{(r)} \right|^2 \left[\mathbf{\underline{M}}^{\mathrm{H}} \mathbf{\underline{M}} \right]_{n,n}
$$

$$
= \tfrac{1}{2} \left| \underline{d}_n^{(r)} \right|^2 \left[\left[\mathbf{\underline{D}}\,\mathbf{\underline{H}}\,(\mathbf{\underline{D}}\,\mathbf{\underline{H}})^{\mathrm{H}} \right]^{-1} \mathbf{\underline{D}}\,\mathbf{\underline{H}}\,(\mathbf{\underline{D}}\,\mathbf{\underline{H}})^{\mathrm{H}} \left[\mathbf{\underline{D}}\,\mathbf{\underline{H}}\,(\mathbf{\underline{D}}\,\mathbf{\underline{H}})^{\mathrm{H}} \right]^{-1} \right]_{n,n} \tag{1.31}
$$

$$
= \tfrac{1}{2} \left| \underline{d}_n^{(r)} \right|^2 \left[\left[\mathbf{\underline{D}}\,\mathbf{\underline{H}}\,(\mathbf{\underline{D}}\,\mathbf{\underline{H}})^{\mathrm{H}} \right]^{-1} \right]_{n,n} .
$$

As the performance criterion, the ratios of the N transmit energies $T_n^{(r)}$ and $T_{\mathrm{TxMF},n}^{(r)}$ required in the cases of TxZF and TxMF are proposed, which we term component specific energy raises of TxZF. For the component $\underline{d}_n^{(r)}$ of $\mathbf{\underline{d}}^{(r)}$ of (1.9) the energy raise, which is independent of the value of $\underline{d}_n^{(r)}$, becomes with (1.30) and (1.31)

$$
\eta_n = \frac{T_n^{(r)}}{T_{\mathrm{TxMF},n}^{(r)}} = \left[\left[\mathbf{\underline{D}}\,\mathbf{\underline{H}}\,(\mathbf{\underline{D}}\,\mathbf{\underline{H}})^{\mathrm{H}} \right]^{-1} \right]_{n,n} \left[\mathbf{\underline{D}}\,\mathbf{\underline{H}}\,(\mathbf{\underline{D}}\,\mathbf{\underline{H}})^{\mathrm{H}} \right]_{n,n} \geq 1 . \tag{1.32}
$$

In [BQT$^+$03, WMZ04, MWQ04] the reciprocal value of η_n is considered and termed transmit efficiency of TxZF. Averaging over all N values η_n would give the mean energy raise

$$
\eta = \frac{1}{N} \sum_{n=1}^{N} \eta_n = \frac{1}{N} \cdot \mathrm{trace} \left\{ \left[\mathbf{\underline{D}}\,\mathbf{\underline{H}}\,(\mathbf{\underline{D}}\,\mathbf{\underline{H}})^{\mathrm{H}} \right]^{-1} \mathrm{diag} \left(\mathbf{\underline{D}}\,\mathbf{\underline{H}}\,(\mathbf{\underline{D}}\,\mathbf{\underline{H}})^{\mathrm{H}} \right) \right\} \geq 1 . \tag{1.33}
$$

Under the assumption that all N magnitudes $\left| \underline{d}_n^{(r)} \right|$ are equal, another performance criterion for TxZF similar to η of (1.33) would be the ratio

$$
\bar{\eta} = \frac{\displaystyle\sum_{n=1}^{N} T_n^{(r)}}{\displaystyle\sum_{n=1}^{N} T_{\mathrm{TxMF},n}^{(r)}} = \mathrm{trace} \left\{ \left[\mathbf{\underline{D}}\,\mathbf{\underline{H}}\,(\mathbf{\underline{D}}\,\mathbf{\underline{H}})^{\mathrm{H}} \right]^{-1} \right\} / \mathrm{trace} \left\{ \left(\mathrm{diag} \left[\mathbf{\underline{D}}\,\mathbf{\underline{H}}\,(\mathbf{\underline{D}}\,\mathbf{\underline{H}})^{\mathrm{H}} \right] \right)^{-1} \right\} \geq 1
$$
$$
\tag{1.34}
$$

of the sum of the required transmit energies $T_n^{(r)}$ of (1.31) and $T_{\mathrm{TxMF},n}^{(r)}$ of (1.30) pertaining to the N components of $\underline{d}_n^{(r)}$ of $\mathbf{\underline{d}}^{(r)}$ of (1.9) in the cases of TxZF and TxMF, respectively. $\bar{\eta}$ of (1.34) could be termed overall energy raise.

In order to point out an interesting duality of the schemes RxZF and TxZF, we consider the simple case of unitary square channel matrices

$$
\mathbf{\underline{H}}\,\mathbf{\underline{H}}^{\mathrm{H}} = \mathbf{\underline{H}}^{\mathrm{H}}\mathbf{\underline{H}} = \mathbf{I}^{N \times N} \tag{1.35}
$$

and assume that between the modulator matrix $\underline{\mathbf{M}}$ of (1.23) to (1.28) and the demodulator matrix $\underline{\mathbf{D}}$ of (1.29) to (1.34) the relation

$$\underline{\mathbf{M}}^{\mathrm{H}}\underline{\mathbf{M}} = \underline{\mathbf{D}}\,\underline{\mathbf{D}}^{\mathrm{H}} \tag{1.36}$$

is valid. Then, the values of energy raises η_n, η and $\bar{\eta}$ become equal to the values of the noise raises δ_n, δ and $\bar{\delta}$, respectively. This will be shown for the case of η_n and δ_n. From δ_n of (1.26) and η_n of (1.32) and $\underline{\mathbf{H}}$ of (1.35) follow

$$\delta_n = \left[(\underline{\mathbf{H}}\,\underline{\mathbf{M}})^{\mathrm{H}}\,\underline{\mathbf{H}}\,\underline{\mathbf{M}} \right]_{n,n} \left[\left[(\underline{\mathbf{H}}\,\underline{\mathbf{M}})^{\mathrm{H}}\,\underline{\mathbf{H}}\,\underline{\mathbf{M}} \right]^{-1} \right]_{n,n} = \left[\underline{\mathbf{M}}^{\mathrm{H}}\underline{\mathbf{H}}^{\mathrm{H}}\underline{\mathbf{H}}\,\underline{\mathbf{M}} \right]_{n,n} \left[\left[\underline{\mathbf{M}}^{\mathrm{H}}\underline{\mathbf{H}}^{\mathrm{H}}\underline{\mathbf{H}}\,\underline{\mathbf{M}} \right]^{-1} \right]_{n,n}$$

$$= \left[\underline{\mathbf{M}}^{\mathrm{H}}\underbrace{(\underline{\mathbf{H}}^{\mathrm{H}}\underline{\mathbf{H}})}_{\mathbf{I}^{N \times N}}\underline{\mathbf{M}} \right]_{n,n} \left[\left[\underline{\mathbf{M}}^{\mathrm{H}}\underbrace{(\underline{\mathbf{H}}^{\mathrm{H}}\underline{\mathbf{H}})}_{\mathbf{I}^{N \times N}}\underline{\mathbf{M}} \right]^{-1} \right]_{n,n} = \left[\underline{\mathbf{M}}^{\mathrm{H}}\underline{\mathbf{M}} \right]_{n,n} \left[\left[\underline{\mathbf{M}}^{\mathrm{H}}\underline{\mathbf{M}} \right]^{-1} \right]_{n,n}$$

$$\tag{1.37}$$

and

$$\eta_n = \left[\left[\underline{\mathbf{D}}\,\underline{\mathbf{H}}\,(\underline{\mathbf{D}}\,\underline{\mathbf{H}})^{\mathrm{H}} \right]^{-1} \right]_{n,n} \left[\underline{\mathbf{D}}\,\underline{\mathbf{H}}\,(\underline{\mathbf{D}}\,\underline{\mathbf{H}})^{\mathrm{H}} \right]_{n,n} = \left[\left[\underline{\mathbf{D}}\,\underline{\mathbf{H}}\,\underline{\mathbf{H}}^{\mathrm{H}}\underline{\mathbf{D}}^{\mathrm{H}} \right]^{-1} \right]_{n,n} \left[\underline{\mathbf{D}}\,\underline{\mathbf{H}}\,\underline{\mathbf{H}}^{\mathrm{H}}\underline{\mathbf{D}}^{\mathrm{H}} \right]_{n,n}$$

$$= \left[\left[\underline{\mathbf{D}}\,\underbrace{(\underline{\mathbf{H}}\,\underline{\mathbf{H}}^{\mathrm{H}})}_{\mathbf{I}^{N \times N}}\underline{\mathbf{D}}^{\mathrm{H}} \right]^{-1} \right]_{n,n} \left[\underline{\mathbf{D}}\,\underbrace{(\underline{\mathbf{H}}\,\underline{\mathbf{H}}^{\mathrm{H}})}_{\mathbf{I}^{N \times N}}\underline{\mathbf{D}}^{\mathrm{H}} \right]_{n,n} = \left[\left[\underline{\mathbf{D}}\,\underline{\mathbf{D}}^{\mathrm{H}} \right]^{-1} \right]_{n,n} \left[\underline{\mathbf{D}}\,\underline{\mathbf{D}}^{\mathrm{H}} \right]_{n,n},$$

$$\tag{1.38}$$

respectively. By the comparison of (1.37) and (1.38) we can state that the equality among the values δ_n of (1.26) and η_n of (1.32) can be ensured by the relation of (1.36). Hence, the two ZF schemes are performance wise equivalent. Exemplary, for OFDM, if we abstract the self-obvious FFT or IFFT operations, $\underline{\mathbf{M}}$ of (1.23) to (1.28) in the case of RxZF and $\underline{\mathbf{D}}$ of (1.29) to (1.34) in the case of TxZF could be chosen as identity matrices, and (1.36) would hold for the case of square channel matrices.

The duality stated above is a consequence of the basic requirement for ZF schemes stated by (1.17). However, for general types of channel matrices the duality of the performance criteria is no longer valid for each channel matrix, but rather in a statistical sense, and also depends on the system dimensioning and system loads. The influence of these two aspects of system design on the performance of the rationale TxZF will be considered in Subsection 3.4.3, apart from which only square channel matrices of dimensions 4×4 and full system loads will be considered.

The consideration of duality among the matrices $\underline{\mathbf{M}}$ and $\underline{\mathbf{D}}$ could be extended to more general TO and RO schemes, and can also be derived for more general types of channel

matrices [VT03] and other rationales than ZF as well [BS02], which are all, for the sake of
brevity, omitted here. An information theoretical review on this topic, that is the duality
of multiple access and broadcast channels, can be found in [JVG04].

After the recapitulation of the relative performance criteria noise raise and energy
raise of RxZF and TxZF, respectively, we now introduce a performance criterion which
will be appropriate in the further course of this work. As will be explained in Section
1.5, our goal will be to minimize the required transmit energy of TxZF by proper choice
of $\underline{\mathbf{d}}^{(r)}$. Therefore, the adequate performance criterion would be the magnitude of this
energy depending on $\underline{\mathbf{d}}^{(r)}$.

With $\underline{\mathbf{t}}^{(r)}$ of (1.8) the energy required for the transmission of $\underline{\mathbf{d}}^{(r)}$ becomes [MBQ04,
HMBZ06a]

$$T^{(r)} = \frac{1}{2}\underline{\mathbf{t}}^{(r)\mathrm{H}}\underline{\mathbf{t}}^{(r)} . \tag{1.39}$$

With (1.13) and (1.20), this expression can be rewritten as

$$
\begin{aligned}
T^{(r)} &= \tfrac{1}{2}\mathrm{trace}\left\{\underline{\mathbf{M}}\,\underline{\mathbf{d}}^{(r)}\underline{\mathbf{d}}^{(r)\mathrm{H}}\underline{\mathbf{M}}^{\mathrm{H}}\right\} = \tfrac{1}{2}\left(\underline{\mathbf{M}}\,\underline{\mathbf{d}}^{(r)}\right)^{\mathrm{H}}\underline{\mathbf{M}}\,\underline{\mathbf{d}}^{(r)} \\
&= \tfrac{1}{2}\underline{\mathbf{d}}^{(r)\mathrm{H}}\left[\underline{\mathbf{D}}\,\underline{\mathbf{H}}\,(\underline{\mathbf{D}}\,\underline{\mathbf{H}})^{\mathrm{H}}\right]^{-1}\underline{\mathbf{d}}^{(r)} .
\end{aligned}
\tag{1.40}
$$

From (1.31) and (1.40) follows that in general the inequality

$$\sum_{n=1}^{N} T_n^{(r)} \neq T^{(r)} \tag{1.41}$$

holds. However, if the N components $\underline{\mathbf{d}}_n^{(r)}$ of $\underline{\mathbf{d}}^{(r)}$, $r = 1\ldots R$, of (1.9) are stationary and
independent, then we can obtain from (1.31) and (1.40) the average required transmit
energy

$$
\begin{aligned}
T &= \sum_{n=1}^{N} \underset{r=1\ldots R}{\mathrm{E}}\left\{T_n^{(r)}\right\} \\
&= \tfrac{1}{2}\mathrm{trace}\left\{\underline{\mathbf{M}}\,\underset{r=1\ldots R}{\mathrm{E}}\left\{\underline{\mathbf{d}}^{(r)}\underline{\mathbf{d}}^{(r)\mathrm{H}}\right\}\underline{\mathbf{M}}^{\mathrm{H}}\right\} \\
&= \tfrac{1}{2}\mathrm{trace}\left\{\underline{\mathbf{M}}\,\underline{\mathbf{M}}^{\mathrm{H}}\underset{r=1\ldots R}{\mathrm{E}}\left\{\underline{\mathbf{d}}^{(r)}\underline{\mathbf{d}}^{(r)\mathrm{H}}\right\}\right\} \\
&= \tfrac{1}{2}\mathrm{trace}\left\{\left[\underline{\mathbf{D}}\,\underline{\mathbf{H}}\,(\underline{\mathbf{D}}\,\underline{\mathbf{H}})^{\mathrm{H}}\right]^{-1}\underset{r=1\ldots R}{\mathrm{E}}\left\{\underline{\mathbf{d}}^{(r)}\underline{\mathbf{d}}^{(r)\mathrm{H}}\right\}\right\} \\
&= \underset{r=1\ldots R}{\mathrm{E}}\left\{T^{(r)}\right\} .
\end{aligned}
\tag{1.42}
$$

If

$$\underline{\mathbf{R}}_{\mathrm{d}} = \underset{r=1\ldots R}{\mathrm{E}}\left\{\underline{\mathbf{d}}^{(r)}\underline{\mathbf{d}}^{(r)\mathrm{H}}\right\} = \sigma_{\mathrm{d}}^2 \cdot \mathbf{I}^{N\times N} \tag{1.43}$$

holds for the covariance matrix of $\underline{\mathbf{d}}^{(r)}$ of (1.9), then the average required transmit energy

$$T = \frac{1}{2}\sigma_{\mathrm{d}}^2 \operatorname{trace} \left\{ \left[\underline{\mathbf{D}}\,\underline{\mathbf{H}}\,(\underline{\mathbf{D}}\,\underline{\mathbf{H}})^{\mathrm{H}} \right]^{-1} \right\} \tag{1.44}$$

follows from (1.42), where, as already stated earlier in this subsection, $\underline{\mathbf{D}}$ and $\underline{\mathbf{H}}$ are assumed fixed and only the time variance of the data $\mathbf{a}$ is considered when determining the average T. The resulting T strongly depends on the realization of $\underline{\mathbf{H}}$, which may be well or ill conditioned, resulting in a small or large value T, correspondingly. In Subsection 3.4.3 the required transmit energy will be reconsidered.

1.5 State-of-the-art and open questions

The idea of taking into account CSI on the transmitter side has a long history, see for instance [Sha58, GP80, Cos83]. However, to the author's knowledge, its concretization in the sense of RO transmission as treated in this thesis has been first published in 1993 by Nakagawa and Esmailzadeh in their paper on the Pre-Rake for spread spectrum communications [EN93]. The application of RO specifically in MIMO multi-user mobile radio DLs has only lately found some interest [EN93, TC94, MSN97, VJ98, MGS98, BF99, KSS99, MBW+00, KM00, BPD00] and recently started being studied more intensively [CLM01, INBF01, UY01, GC02a, HvHJ+, WM03, IRF03, HSB03, CM04, MBQ04, WFH04, QMBW04, WMZ04, HPS05a, HPS05b, HRF06, HMBZ06a, HMBZ06b, HIRF05, KB07b, KB07a, KE07, KHB07, FWLH02b, FWLH02a]. In the meantime RO is even considered in the standardization activities [Yan05].

In the structure of Fig. 1.4 each realization $\mathbf{a}^{(r)}$ is uniquely represented by a vector $\underline{\mathbf{d}}^{(r)}$. Such a scheme of unique data representation goes along with a strong constraint on the formation of the transmit vector $\underline{\mathbf{t}}^{(r)}$, and also on other system characteristics as for instance the required transmit power. Therefore, once the assignment procedure $\mathbf{a}^{(r)} \to \underline{\mathbf{d}}^{(r)}$, $r = 1 \ldots R$, is decided and $\underline{\mathbf{D}}$ and $\underline{\mathbf{H}}$ are given, which by virtue of (1.20) implies a given $\underline{\mathbf{M}}$ as well, there is virtually no free design space left for influencing system characteristics as for instance the required transmit power or the amplitude dynamics of the received signals.

Alternatives to RO transmission schemes with unique data representation as illustrated in Fig. 1.4 would be RO schemes with selectable data representation. Such a scheme is shown in Fig. 1.5. In contrast to the structure shown in Fig. 1.4, now each realization $\mathbf{a}^{(r)}$, $r = 1 \ldots R$, of $\mathbf{a}$ can be alternatively represented by any vector $\underline{\mathbf{d}}^{(r)}$ taken from a selection

$$\underline{\mathbf{d}}^{(r)} \in \left\{ \underline{\mathbf{d}}^{(r,1)} \cdots \underline{\mathbf{d}}^{(r,L)} \right\}, \ \underline{\mathbf{d}}^{(r,l)} = \left(\underline{d}_1^{(r,l)} \cdots \underline{d}_N^{(r,l)} \right)^{\mathrm{T}}, \tag{1.45}$$
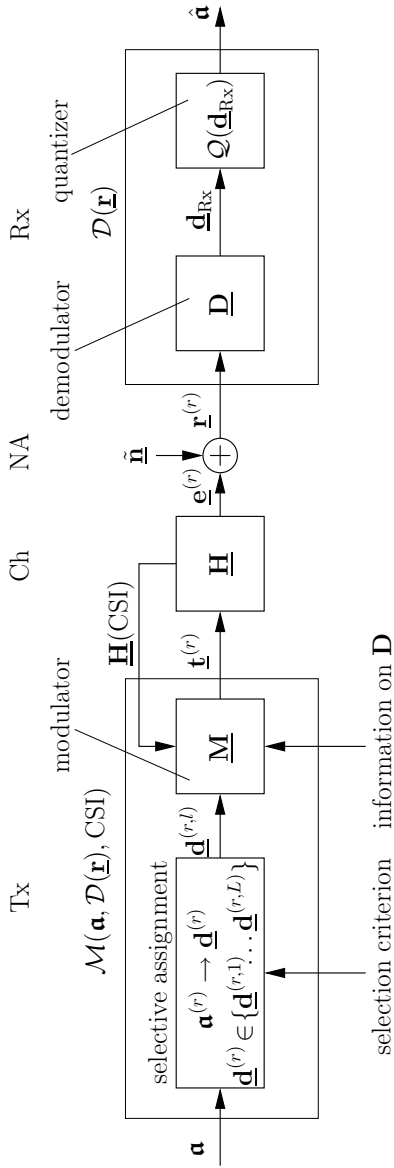
Fig. 1.5. RO transmission with selectable data representation

of L representative vectors $\underline{\mathbf{d}}^{(r,l)}$, each of them representing $\boldsymbol{\mathfrak{a}}^{(r)}$. Again, sometimes in this thesis the components $\underline{d}_n^{(r,l)}$ of $\underline{\mathbf{d}}^{(r,l)}$ are denoted as landing points. As indicated in Fig. 1.5, the selection procedure is performed under the control of a selection criterion. This criterion may concern for instance the required transmit power, the amplitude dynamics of the receive signals etc.. In contrast to unique data representation, see Figs. 1.3 and 1.4, selectable data representation, see Fig. 1.5, introduces new degrees of freedom, when designing and parameterizing the system under consideration of said criteria.

Both in the case of unique and selective data representation, see Figs. 1.4 and 1.5, respectively, the R realizations $\boldsymbol{\mathfrak{a}}^{(r)}$ of $\boldsymbol{\mathfrak{a}}$ of (1.7) could be mapped on a complex column vector $\underline{\mathbf{a}}^{(r)}$ each, and these vectors could be arranged in a matrix

$$\underline{\boldsymbol{\mathfrak{A}}} = \left(\underline{\mathbf{a}}^{(1)} \ldots \underline{\mathbf{a}}^{(R)} \right) . \tag{1.46}$$

Correspondingly, in the case of unique data representation, the R representative vectors $\underline{\mathbf{d}}^{(r)}$ of (1.9) could be compiled in a matrix

$$\underline{\boldsymbol{\mathfrak{D}}} = \left(\underline{\mathbf{d}}^{(1)} \ldots \underline{\mathbf{d}}^{(R)} \right) . \tag{1.47}$$

Now, by suitably choosing the R vectors $\underline{\mathbf{a}}^{(r)}$ in (1.46), a linear relation between the matrices $\underline{\boldsymbol{\mathfrak{A}}}$ of (1.46) and $\underline{\boldsymbol{\mathfrak{D}}}$ of (1.47) could be achieved. In this sense the scheme of unique data representation could be considered linear on the transmit side. In the case of selective data representation, a multitude of matrices $\underline{\boldsymbol{\mathfrak{D}}}$ of (1.47) correspond to $\underline{\boldsymbol{\mathfrak{A}}}$ of (1.46), from which one has to be chosen. This necessity of choice makes the generation of $\underline{\boldsymbol{\mathfrak{D}}}$ from $\underline{\boldsymbol{\mathfrak{A}}}$ a non-linear procedure. In this sense, the schemes with selective data representation can be considered non-linear on the transmit side.

Some publications exist in which the two possibilities of data representation in RO transmission, which the author gives the attributes 'unique' or 'selectable', have been already touched implicitly [IRF03, PHS03, WMS03, MWQ04, HPS05a, HPS05b, QMBW04, HMBZ06a, KHB07, KB07b, KE07, KB07a], even if these attributes are not used and the crux of the two possibilities is not - as in the present thesis - boiled down to the question of data representation. In some publications also a transmit power reduction enabled by selectable data representation is insinuated [MWQ04, QMBW04, HPS05b, HMBZ06a, KHB07, KB07b, KE07, KB07a]. However, this aspect has not yet been elaborated in detail, particularly not for the MIMO multi-user mobile radio DLs being of interest in the present thesis. As another point, the issue of the amplitude dynamics of the receive signals has not yet been addressed at all. In Table 1.1 some typical recent publications on RO transmission, both - as the author puts it - with unique and selectable data representation, are listed and briefly commented. Concerning the conceptions 'simply connected',

'multiply connected' and 'decision regions' occurring in Table 1.1 as well as the figures mentioned, defined clarifications will follow in Chapter 2.

Even though the potential of transmit energy reduction by selectable data representation in RO transmission is basically recognized [MWQ04, HPS05b, HMBZ06a, KB07b], for a deeper understanding the illustration of how such a reduction is accomplished would be helpful, especially for engineers engaged in system design and development. In addition, a concise and consistent mathematical formulation of RO transmission with selectable data representation would foster its application.

To the author's knowledge virtually all RO transmission concepts with selectable data representation published up to now rely on Tomlinson-Harashima Precoding

decision regions	data representation	references	comments
simply connected	unique, see Fig. 2.1	[EN93, ESN93] [KSS99, Fis02] [VJ98, MBW$^+$00] [MBQ04, HPS05b]	choice of the modulator matrix TxMF/TxZF/TxMMSE/ max. SNIR
	selectable, continuous valued representatives, see Fig. 2.2 a	[WM03][WMS03] [IHRF03][IRF03]	minimization of BER/SER with transmit power constraints
		[KHB07][KB07b]	transmit energy minimization with BER/SER constraints
multiply connected	selectable, discrete valued representatives, see Fig. 2.2 b	[FWLH02a] [HIRF05][HPS05b] [HMBZ06a] [PJU06]	discussion of possible lattice search techniques
		[GC02b][FWLH02b] [MWQ04][QMBW04] [WFH04][WMZ04]	stepwise approaches based on ordered THP
	selectable, continuous valued representatives, see Fig. 2.2 c	[Cos83][CS03] [ESZ00] [ESZ05]	information theoretical considerations

Table 1.1. Important contributions on Receiver Orientation

(THP) [Tom71, HM72, Fis02, PHS03, MWQ04, QMBW04, HPS05b, HIRF05, KB07a, FWLH02b], which is characterized by working with infinitely extended lattice reducing quantization schemes in the receive operator $\mathcal{D}(\underline{\mathbf{r}})$. The question, if or to which extent other RO transmission concepts with selectable data representation - relying either on modifications of THP or differing from THP altogether - may have the one or other advantage over the THP-based concepts has not yet been seriously asked.

As already explained, in RO transmission systems, see Fig. 1.2 c, CSI is required at the transmitter. This information has to be gained by channel estimation procedures. The obvious place to obtain a channel estimate would be on the receiver side, that is in the case of mobile radio DLs considered in this thesis in the MTs and not in the access point (AP), where it is needed. If the applied duplexing scheme is Time Division Duplexing (TDD), then, due to the reciprocity of the UL and DL channels, the UL CSI acquired in the AP may serve as CSI for RO DL transmission as well [SB93]. However, in the case of the duplexing scheme Frequency Division Duplexing (FDD) this possibility does not exist, and then the question how to provide DL CSI to the AP arises. An advantageous way to tackle this problem has for instance been elaborated in [HMBZ06b, JBM+02]. Nevertheless, both in the case of TDD and FDD the provision of DL CSI to the AP is prone to inaccuracies due to channel estimation errors, and a frequently asked question in discussions on RO transmission, especially with selectable data representation, concerns the impact of such inaccuracies of the DL CSI available in the AP.

All cellular mobile radio systems including the lately rolled out third generation (3G) systems are single carrier systems. An alternative to this approach would be multi-carrier techniques, preferably of the type Orthogonal Frequency Division Duplexing (OFDM) [Sal67, WE71, Bin90, RG96, vNP00], and in the present standardization activities towards fourth generation (4G) mobile radio systems OFDM plays a major role [BBT02, RG02, Yan05]. In non-cellular mobile radio systems as for instance Wireless Local Area Networks (WLAN) OFDM is already in successful operation [IEE05, IEE, IEE99]. Due to its obvious importance, OFDM would deserve particular attention when considering RO transmission with selectable data representation.

1.6 Goals and contents of the thesis

In consideration of the state-of-the-art and the open questions formulated in Section 1.5, the present thesis has the following goals:

- Development of a concise, general mathematical model for RO transmission suitable for being personalized to system versions with linear inner section for the cases of both unique and selectable data representation.

- Personalization of the general model to RO transmission with selectable data representation based on THP, introduction of advantageous modifications of THP, and visualization of the system operation and performance.

- Personalization of the general model to a - to the author's knowledge - new version of RO transmission with selectable data representation based on continuous valued representatives, which will be termed Minimum Energy Soft Precoding (MESP) for reasons to become evident later, and visualization of the system operation and performance.

- Consideration of MIMO multi-user mobile radio DLs in the framework of the elaborated system modelling.

- Inclusion of OFDM in the system considerations.

- Derivation of a method for evaluating the impact of imperfect CSI on the performance of RO transmission with selectable data representation.

The considerations will be corroborated by numerical results whenever appropriate, with the focus lying on the required transmit energy and on the amplitude dynamics of the received signals.

Chapter 2
Fundamentals of RO transmission with selectable data representation

2.1 Data representation

As explained in Section 1.5, the vector $\underline{\mathbf{d}}^{(r)}$ representing the realization $\mathbf{a}^{(r)}$ of $\mathbf{a}$ has N components $\underline{d}_n^{(r)}$, $n = 1 \ldots N$. In this thesis we will assume that, irrespective of which realization $\mathbf{a}^{(r)}$ is concerned, each one of these components results from accessing invariably the same complex set

$$\mathbb{V} = \{\mathbb{V}_1 \ldots \mathbb{V}_M\}. \tag{2.1}$$

$\mathbb{V}$ of (2.1) consists of M sub-sets

$$\mathbb{V}_m \in \mathbb{C}, \; m = 1 \ldots M, \tag{2.2}$$

which are assumed to be disjoint, that is

$$\mathbb{V}_{m'} \cap \mathbb{V}_m = \emptyset, \text{if } m' \neq m. \tag{2.3}$$

$\mathbb{V}$ as characterized by (2.1) to (2.3) is a generalization of $\mathbb{V}$ of (1.10). This generalization, as already mentioned in Section 1.5, introduces additional degrees of freedom in system design and parametrization. $\mathbb{V}$ is again termed representative set of $\mathbf{a}$, and the subsets $\mathbb{V}_m$ of $\mathbb{V}$ are termed partial representative sets. As a further generalization, which, however, would be beyond the scope of this thesis, different representative sets could be conceived for different components of the representative vectors $\underline{\mathbf{d}}^{(r)}$ and/or for different realizations $\mathbf{a}^{(r)}$ of $\mathbf{a}$.

In the context of system design, to each of the R realizations $\mathbf{a}^{(r)}$ of $\mathbf{a}$ a representative vector $\underline{\mathbf{d}}^{(r)}$ has to be assigned, either in a unique or a selectable manner, see (1.9) or (1.45), respectively. This assignment shall be performed by deciding for each component $\underline{d}_n^{(r)}$ of $\underline{\mathbf{d}}^{(r)}$ which discrete value $\underline{v}_m$ it assumes in the case of a unique assignment, see (1.9), or from which partial representative set $\mathbb{V}_m$ of (2.1) to (2.3) it stems in the case of a selectable assignment. The taken decisions can be expressed by integers $m_n^{(r)}$, $r = 1 \ldots R$, $n = 1 \ldots N$, which have the following meaning: The component $\underline{d}_n^{(r)}$ of the vector $\underline{\mathbf{d}}^{(r)}$ representing $\mathbf{a}^{(r)}$ shall be taken from the partial representative set $\mathbb{V}_m$ with subscript m equal to $m_n^{(r)}$, that is from the partial representative set $\mathbb{V}_{m_n^{(r)}}$:

$$\underline{d}_n^{(r)} \in \mathbb{V}_{m_n^{(r)}}. \tag{2.4}$$

In this way, to each realization $\mathbf{a}^{(r)}$ of $\mathbf{a}$ a vector

$$\mathbf{m}^{(r)} = \left(m_1^{(r)} \ldots m_N^{(r)} \right)^{\mathrm{T}} \tag{2.5}$$

termed integer representative vector of $\mathbf{a}^{(r)}$ is attributed.

An important step in system design is the concrete formation of $\mathbb{V}$ of (1.10) or of (2.1) to (2.3). As mentioned in Section 1.3, in the case of unique data representation $\mathbb{V}$ consists of M discrete valued representatives $\underline{v}_1 \ldots \underline{v}_M$. In Fig. 2.1 this case is illustrated by an example in which the cardinality M is equal to four. In the case of selectable data representation being of interest in this thesis, see Fig. 1.4, various options concerning the basic structure and parametrization of $\mathbb{V}$ exist, three of which are illustrated in Figs. 2.2 a to c, again for the case M equal to four. These three options will be characterized in what follows. Each $\mathbb{V}_m$, $m = 1 \ldots M$, is constituted by

- a set of P discrete valued complex representatives, that is

$$\mathbb{V}_m = \left\{ \underline{v}_{m,1} \ldots \underline{v}_{m,P} \right\} \tag{2.6}$$

in the case of Fig. 2.2 a, where we choose P equal to four as an example. We term the quantities $\underline{v}_{m,p}$ selectable representative values and designate this kind of selectable data representation as Approach I.

- a simply connected continuous valued complex domain $\mathbb{D}_m$, that is

$$\mathbb{V}_m = \mathbb{D}_m \tag{2.7}$$

in the case of Fig. 2.2 b. We term the domains $\mathbb{D}_m$ representative domains and designate this kind of selectable data representation as Approach II.

- a P-fold connected continuous valued complex domain $\mathbb{D}_m$ consisting of P disjoint partial domains $\mathbb{D}_{m,1} \ldots \mathbb{D}_{m,P}$, that is

$$\mathbb{V}_m = \mathbb{D}_m = \{\mathbb{D}_{m,1} \ldots \mathbb{D}_{m,P}\} \tag{2.8}$$

in the case of Fig. 2.2 c, where as an example we again choose P equal to four. We term the domains $\mathbb{D}_m$ again representative domains and the domains $\mathbb{D}_{m,p}$ partial representative domains, and designate this kind of selectable data representation as Approach III.
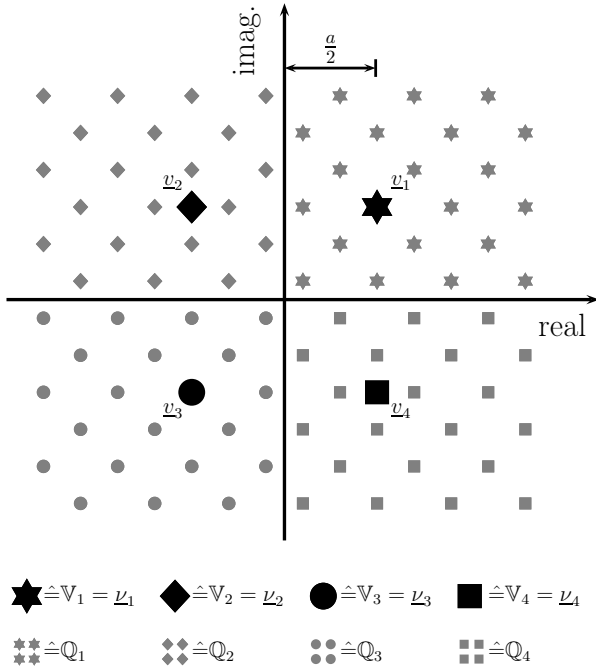
Fig. 2.1. Unique data representation
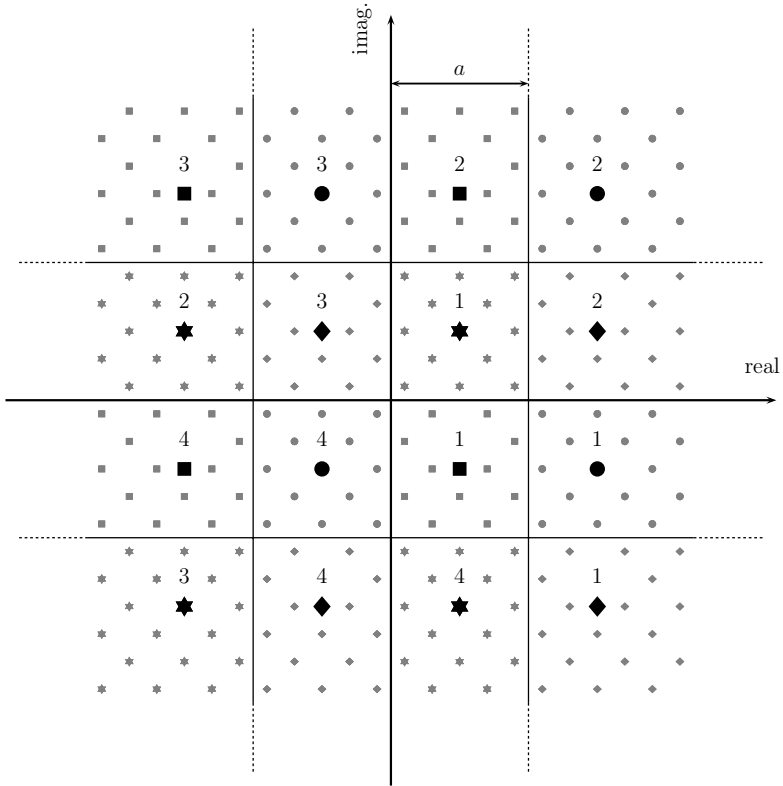
a) Approach I: $\mathbb{V}_m$ constituted by P discrete valued representatives

$\underline{v}_{m,p},\ m = 1\ldots M,\ p = 1\ldots P,\ M = P = 4$

★ $\hat{=}\mathbb{V}_1 \in \{\underline{\nu}_{1,1}\ldots\underline{\nu}_{1,4}\}$ ◆ $\hat{=}\mathbb{V}_2 \in \{\underline{\nu}_{2,1}\ldots\underline{\nu}_{2,4}\}$

● $\hat{=}\mathbb{V}_3 \in \{\underline{\nu}_{3,1}\ldots\underline{\nu}_{3,4}\}$ ■ $\hat{=}\mathbb{V}_4 \in \{\underline{\nu}_{4,1}\ldots\underline{\nu}_{4,4}\}$

⁑ $\hat{=}\mathbb{Q}_1$ ⁑ $\hat{=}\mathbb{Q}_2$ ⁑ $\hat{=}\mathbb{Q}_3$ ⁑ $\hat{=}\mathbb{Q}_4$

the numbers in the figure are the values $p = 1\ldots P$
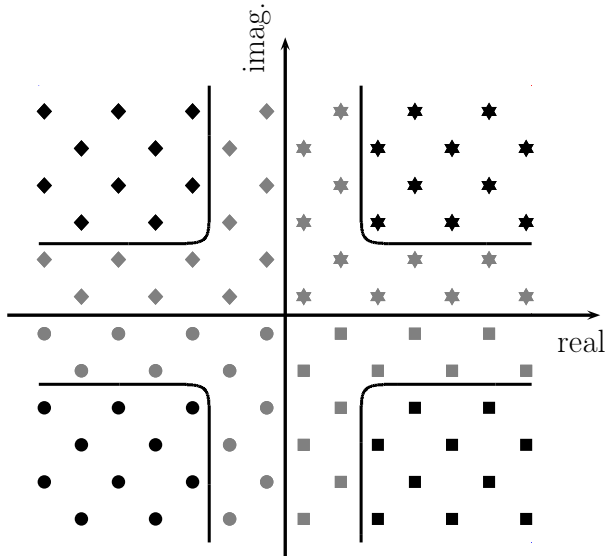
b) Approach II: $\mathbb{V}_m$ constituted by simple connected domains
$\mathbb{D}_m, \ m = 1 \ldots M, \ M = 4$

$\hat{=} \mathbb{V}_1 = \mathbb{D}_1 \qquad \hat{=} \mathbb{V}_2 = \mathbb{D}_2 \qquad \hat{=} \mathbb{V}_3 = \mathbb{D}_3 \qquad \hat{=} \mathbb{V}_4 = \mathbb{D}_4$

$\hat{=} \mathbb{Q}_1 \qquad\qquad \hat{=} \mathbb{Q}_2 \qquad\qquad \hat{=} \mathbb{Q}_3 \qquad\qquad \hat{=} \mathbb{Q}_4$
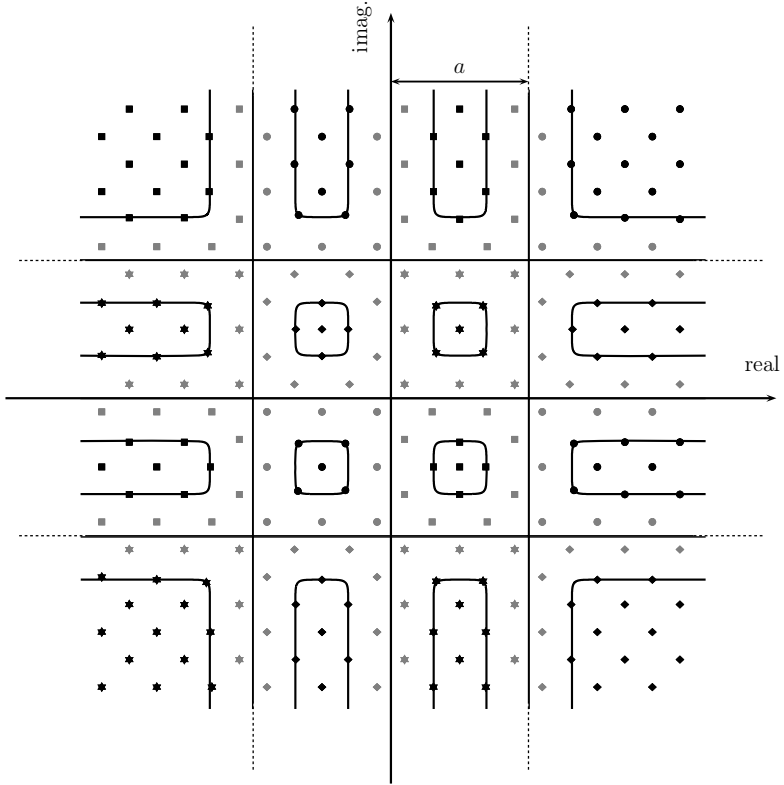
c) Approach III: $\mathbb{V}_m$ constituted by P-fold connected domains

$$\mathbb{D}_{m,p},\ m = 1 \ldots M,\ p = 1 \ldots P,\ M = P = 4$$

$\blacksquare\ \hat{=}\mathbb{V}_1$ $\blacklozenge\ \hat{=}\mathbb{V}_2$ $\bullet\ \hat{=}\mathbb{V}_3$ $\blacksquare\ \hat{=}\mathbb{V}_4$

$\hat{=}\mathbb{Q}_1$ $\hat{=}\mathbb{Q}_2$ $\hat{=}\mathbb{Q}_3$ $\hat{=}\mathbb{Q}_4$

Fig. 2.2. Selectable data representation

Approach I is related to known Tomlinson-Harashima Precoding (THP) [Tom71, HM72, QMBW04, FWLH02b] even though in literature the choice of $P < \infty$ has not been considered in greater detail up to now. Approaches II and III are, to the author's knowledge, new, and, therefore, form part of the original work of this thesis. In the case of Approach I,

$$L = P^N \tag{2.9}$$

holds for the integer L in (1.45), whereas in the Approaches II and III formally

$$L \to \infty \tag{2.10}$$

would be valid. In this thesis the options according to (2.6) and (2.7), that is Approaches I and II will be considered, and the grid parameter a introduced in Fig. 2.2 a and c is usually chosen equal to one.

By means of the integer representative vectors $\mathbf{m}^{(r)}$ of (2.5) we can assign to each realization $\mathfrak{a}^{(r)}$ of $\mathfrak{a}$ a data specific representative set

$$\mathbb{G}_{\mathfrak{a}^{(r)}} = \left\{ \mathbb{V}_{m_1^{(r)}} \ldots \mathbb{V}_{m_N^{(r)}} \right\} \in \mathbb{C}^N . \tag{2.11}$$

With these sets holds for the representative vector of $\mathfrak{a}^{(r)}$

$$\underline{\mathbf{d}}^{(r)} \in \mathbb{G}_{\mathfrak{a}^{(r)}} . \tag{2.12}$$

The constellation in Fig. 2.1 can be considered a basis of the constellations in Figs. 2.2 a to c in the sense that these originate from the constellation in Fig. 2.1 by certain systematic extensions or generalizations. Therefore, we say that the schemes of Fig. 2.1 and Figs. 2.2 a to c belong to one family of data representation, the root of which is the constellation in Fig. 2.1.

We conclude this section by an illustration of Approach I. We consider the scheme of Fig. 2.2 a and set N equal to four. We further assume for the considered data realization $\mathfrak{a}^{(r)}$

$$m_1^{(r)} = 1, \quad m_2^{(r)} = 4, \quad m_3^{(r)} = 2, \quad m_4^{(r)} = 3. \tag{2.13}$$

Then,

$$L = P^N = 4^4 = 256 \tag{2.14}$$

holds for the superscript L introduced in (1.45), and the 256 representative vectors $\underline{\mathbf{d}}^{(r,l)}$

of $\mathfrak{a}^{(r)}$ are

$$
\begin{aligned}
\underline{\mathbf{d}}^{(r,1)} &= \left(\begin{array}{cccc} \underline{v}_{1,1} & \underline{v}_{4,1} & \underline{v}_{2,1} & \underline{v}_{3,1} \end{array} \right)^{\mathrm{T}}, \\
&\ \vdots \qquad\qquad\qquad \vdots \\
\underline{\mathbf{d}}^{(r,L)} &= \left(\begin{array}{cccc} \underline{v}_{1,4} & \underline{v}_{4,4} & \underline{v}_{2,4} & \underline{v}_{3,4} \end{array} \right)^{\mathrm{T}}.
\end{aligned}
\tag{2.15}
$$

To each superscript l corresponds a different combination of four values $p = 1 \ldots 4$. With the symbols introduced in Figs 2.1 and 2.2 we can represent the data given by (2.13) in a symbolic way as

$$
\mathfrak{a}^{(r)} = (\; \bigstar \; \blacksquare \; \blacklozenge \; \bullet \;).
\tag{2.16}
$$

2.2   Quantisation in the receiver

We consider the quantizer contained in the structures of Figs. 1.3 or 1.5. This quantizer allocates to each partial representative set $\mathbb{V}_m$ of (2.1) to (2.3) a decision region [Pro95]

$$
\mathbb{Q}_m \in \mathbb{C},
\tag{2.17}
$$

where we can also include the case (1.9) of unique data representation by setting $\mathbb{V}_m$ equal to $\underline{v}_m$. The allocation shall be done in such a way that

- $\mathbb{V}_m$ becomes a subset of $\mathbb{Q}_m$, that is

$$
\mathbb{V}_m \subseteq \mathbb{Q}_m,
\tag{2.18}
$$

- the M decision regions completely tile the complex plane, that is

$$
\mathbb{Q}_1 \cup \mathbb{Q}_2 \ldots \cup \mathbb{Q}_M = \mathbb{C},
\tag{2.19}
$$

and that

- the decision regions are disjoint, that is

$$
\mathbb{Q}_{m'} \cap \mathbb{Q}_m = \emptyset, \text{if } m^{'} \neq m.
\tag{2.20}
$$

In Figs. 2.1 and 2.2 exemplary decision regions are included.

The quantizer has the task to determine from $\underline{\mathbf{d}}_{\mathrm{Rx}}$ of (1.16) an estimate $\hat{\mathfrak{a}}$ of the transmitted data realization of $\mathfrak{a}^{(r)}$. With the quantizer operator $\mathcal{Q}(.)$ the function of the quantizer can be expressed as

$$
\hat{\mathfrak{a}} = \mathcal{Q}(\underline{\mathbf{d}}_{\mathrm{Rx}}).
\tag{2.21}
$$

It is assumed that the quantizer works in a component wise fashion as follows: For each of the N components $\underline{d}_{\mathrm{Rx},n}$ of $\underline{\mathbf{d}}_{\mathrm{Rx}}$ of (1.16) an integer estimate $\hat{m}_n$ of $m_n^{(r)}$ of (2.5) is calculated according to

$$\hat{m}_n : \text{ if } \underline{d}_{\mathrm{Rx},n} \in \mathbb{Q}_{m'}, \text{ then } \hat{m}_n = m' . \tag{2.22}$$

With the values $\hat{m}_n$ the estimate

$$\hat{\mathbf{m}} = (\hat{m}_1 \ldots \hat{m}_N)^{\mathrm{T}} \tag{2.23}$$

of the integer representative vector $\mathbf{m}^{(r)}$ of (2.5) of the sent data realization $\mathbf{a}^{(r)}$ is formed. Due to (1.11), where we presuppose the sign of equality, $\hat{\mathbf{m}}$ of (2.23) becomes always equal to one of the R integer representative vectors $\mathbf{m}^{(r)}$, $r = 1 \ldots R$, of (2.5). Now, with these vectors and $\hat{\mathbf{m}}$ of (2.23) the estimate

$$\hat{r} : \text{ if } \hat{m} = m^{(r')}, \text{ then } \hat{r} = r' \tag{2.24}$$

of the superscript r of the sent data realization $\mathbf{a}^{(r)}$ is determined. Then, finally, it is decided that the realization $\mathbf{a}^{(\hat{r})}$ of $\mathbf{a}$ has been transmitted, that is

$$\hat{\mathbf{a}} = \mathbf{a}^{(\hat{r})} . \tag{2.25}$$

This decision is erroneous if the estimate $\hat{\mathbf{m}}$ of (2.23) differs in at least one of its N components from the true integer representative vector $\mathbf{m}^{(r)}$. The occurrence of such errors is due to the received noise vector $\underline{\tilde{\mathbf{n}}}$, which may have the effect that one or more components of the vector $\underline{\mathbf{d}}_{\mathrm{Rx}}$ of (1.16) land outside of their correct decision regions $\mathbb{Q}_m$, see (2.17) to (2.20). With $\hat{\mathbf{m}}$ of (2.23) the error probability, see (1.1), can be written as

$$P_{\mathrm{e}} = \mathrm{Prob}\left(\hat{\mathbf{a}} \neq \mathbf{a}\right) = \mathop{\mathrm{E}}_{r=1\ldots R}\{\mathrm{Prob}(\hat{\mathbf{m}} \neq \mathbf{m}^{(r)})\} . \tag{2.26}$$

In the previous Section 2.1 and in the present Section 2.2 we give the impression that the quasi natural order when establishing the representative set $\mathbb{V}$ of (2.1) and the decision regions $\mathbb{Q}_m$ of (2.17) to (2.20) would be to determine $\mathbb{V}$ in a first step and then set the decision regions $\mathbb{Q}_m$, $m = 1 \ldots M$. However, $\mathbb{V}$ and the decision regions $\mathbb{Q}_m$ should be rather determined in a joint manner. In Subsection 2.3.2 we will make certain assumptions for the statistics of the noise vector $\underline{\mathbf{n}}$ at the demodulator output. Under these assumptions, in the cases (1.9) or (2.6) of discrete valued representatives the decision regions $\mathbb{Q}_m$ should be the Voronoi regions (VR) [CS99] of these representatives. In the cases (2.7) and (2.8) of continuous valued representatives the situation is somewhat more

complicated. In these cases we propose to set out from the decision regions $\mathbb{Q}_m$ of the cases (1.9) or (2.6), and then choose within these regions continuous valued complex domains which are bounded by Contours of Constant Symbol Error Probability (CCSP). CCSPs were first introduced by the author in [KHB07] and will be explained in Chapter 4.

2.3   Process of system design

2.3.1   Followed rationale

Due to the complexity of the task, trying to find - in an ad hoc manner - RO transmission systems performing optimum or at least close to optimum with respect to the criteria of required transmit power and amplitude dynamics of the received signals would be futile. Therefore, the author proposes a not absolutely optimum, but viable alternative of system design which leads to reasonably attractive system concepts, and which consists of the three following steps:

1. First, a root system, that is a RO transmission system with unique data representation, see Sections 1.3 and 2.1, is chosen. This choice includes the determination of
   - the system parameters R, M and N, which are related by (1.11),
   - the constellation of the M unique representative values $\underline{v}_1 \ldots \underline{v}_M$, see (1.10), and
   - the demodulator matrix $\underline{\mathbf{D}}$.

2. Then, the root system is extended in the sense of Approaches I and II, see Section 2.1, where in Approach I also the parameter P plays a role, and the performance of the originating systems is analysed. Typical of these systems are their R data specific representative sets $\mathbb{G}_{\mathfrak{a}^{(r)}}$ of (2.11). In the system analysis we investigate to which degree the required transmit power decreases due to said extensions, and what their impact on the amplitude dynamics of the received signals would be.

3. Finally, the performances of the considered root system and the extended RO transmission systems obtained by Approaches I and II are compared with a view to identify the performance-wise most attractive one of them.

The outlined rationale could be designated as 'system optimization by directed analysis'.

2.3.2   Basic system characteristics and parametrizations

In order to confine the scope of the investigations in a reasonable way, without restricting the general validity of our findings, with a few exceptions we choose in the thesis a root

system with the constellation of Fig. 2.1, the cardinality M of which is four. We further assume that the received noise vector $\underline{\tilde{\mathbf{n}}}$ is stationary and white with the variance σ^2 of its real and imaginary parts, that is $\underline{\tilde{\mathbf{n}}}$ has the covariance matrix

$$\underline{\mathbf{R}}_{\tilde{\mathbf{n}}} = \mathrm{E}\left\{\underline{\tilde{\mathbf{n}}}\,\underline{\tilde{\mathbf{n}}}^{\mathrm{H}}\right\} = 2\sigma^2 \cdot \mathbf{I}. \tag{2.27}$$

Concerning the demodulator matrix $\underline{\mathbf{D}}$, it shall be assumed that its rows are orthonormal, that is

$$\underline{\mathbf{D}}\,\underline{\mathbf{D}}^{\mathrm{H}} = \mathbf{I} \tag{2.28}$$

shall hold for the Gram matrix $\underline{\mathbf{D}}\,\underline{\mathbf{D}}^{\mathrm{H}}$. Then, also the noise vector $\underline{\mathbf{n}}$ at the input of the quantizer in the structures of Figs. 1.3 and 1.4 is white with the same covariance matrix as $\underline{\tilde{\mathbf{n}}}$, see (2.27), that is

$$\underline{\mathbf{R}}_{\mathbf{n}} = \mathrm{E}\left\{\underline{\mathbf{n}}\,\underline{\mathbf{n}}^{\mathrm{H}}\right\} = 2\sigma^2 \cdot \mathbf{I}. \tag{2.29}$$

When studying the system performance, we assume that from channel access to channel access

- the data $\boldsymbol{\alpha}$ randomly and independently take on their realizations $\boldsymbol{\alpha}^{(r)}$, and that

- the channel matrix $\underline{\mathbf{H}}$ varies independently in a stationary manner as elaborated in more detail below.

We term a single channel access constituted by a realization $\boldsymbol{\alpha}^{(r)}$ of $\boldsymbol{\alpha}$ and a realization of the channel matrix $\underline{\mathbf{H}}$ a snapshot.

Two versions of a stationary time variant channel are considered throughout this thesis, namely a fair channel, and an unfair channel, see also [HMBZ06a]. In both cases the realizations of the channel matrices are assumed to have independent bivariate Gaussian entries, which independently vary from channel snapshot to channel snapshot. In the case of the fair channel, all elements of $\underline{\mathbf{H}}$ have unit variances σ_{h}^2 of their real and imaginary parts. In the case of the unfair channel, the variances of the first $Z/2$ rows of $\underline{\mathbf{H}}$ are all equal and 10 dB below the variances of the second $Z/2$ rows, which are also all equal. The unfair channel matrix is normalized in such a way that its Euclidian norm becomes equal to the Euclidian norm of the fair channel matrix, that is

$$\|\mathbf{H}_{\mathrm{fair}}\|_2^2 = \|\mathbf{H}_{\mathrm{unfair}}\|_2^2 \tag{2.30}$$

In the case of the fair channel all Z channel outputs experience the same mean channel attenuation - hence the attribute fair -, whereas in the case of the unfair channel the first $Z/2$ channel outputs are subject to mean channel attenuations which are on the average 10 dB higher than those of the second $Z/2$ channel outputs. The motivation of introducing

an unfair channel consists in the fact that later in this thesis we consider mobile radio communications; due to fast and slow fading, attenuation-wise unfairness is typical of real world mobile radio scenarios [3GP03, SDS+05]. For the sake of distinction we sometimes use the symbols $\underline{\mathbf{H}}_{\mathrm{fair}}$ and $\underline{\mathbf{H}}_{\mathrm{unfair}}$ instead of $\underline{\mathbf{H}}$ for the fair and unfair channels, respectively. For the case of Z and Q equal to four an example of a pair of fair and unfair channel matrices as defined above would be

$$
\underline{\mathbf{H}}_{\mathrm{fair}} = \begin{pmatrix} -0.48+\mathrm{j}0.40 & -0.42-\mathrm{j}0.18 & 0.37-\mathrm{j}0.98 & 1.94+\mathrm{j}0.86 \\ -0.50-\mathrm{j}0.86 & 0.16+\mathrm{j}0.11 & -0.64-\mathrm{j}0.91 & 0.09+\mathrm{j}1.18 \\ -1.21+\mathrm{j}0.17 & -0.80-\mathrm{j}0.12 & -0.10+\mathrm{j}0.28 & 0.59+\mathrm{j}0.50 \\ 0.71-\mathrm{j}0.23 & -1.38-\mathrm{j}0.44 & -0.56-\mathrm{j}1.14 & -0.12-\mathrm{j}0.01 \end{pmatrix}
\tag{2.31}
$$

and

$$
\underline{\mathbf{H}}_{\mathrm{unfair}} = \begin{pmatrix} -0.07+\mathrm{j}0.06 & -0.06-\mathrm{j}0.03 & 0.06-\mathrm{j}0.15 & 0.30+\mathrm{j}0.13 \\ -0.08-\mathrm{j}0.13 & 0.02+\mathrm{j}0.02 & -0.10-\mathrm{j}0.14 & 0.01+\mathrm{j}0.18 \\ -1.85+\mathrm{j}0.26 & -1.23-\mathrm{j}0.18 & -0.15+\mathrm{j}0.43 & 0.91+\mathrm{j}0.77 \\ 1.09-\mathrm{j}0.35 & -2.12-\mathrm{j}0.68 & -0.85-\mathrm{j}1.75 & -0.19-\mathrm{j}0.02 \end{pmatrix}.
\tag{2.32}
$$

The rows of $\underline{\mathbf{H}}_{\mathrm{unfair}}$ differ from the rows of $\underline{\mathbf{H}}_{\mathrm{fair}}$ by real factors.

The above introduced channel matrices are adequate for modelling multi-carrier transmission, which, in the form of OFDM, will be a focus later in this thesis. Therefore, the entries of said matrices $\underline{\mathbf{H}}$ represent transfer function values, see also Section 1.1. In the case of single-carrier transmission, $\underline{\mathbf{H}}$ would be a convolution matrix featuring Toeplitz-like structures with numerous zero entries [Trö03].

2.3.3   Closer look at the considered performance criteria

In each snapshot we obtain a certain transmit vector $\underline{\mathbf{t}}$ of (1.2), and the transmission of this vector requires the radiated energy [MBQ04]

$$
T_{\mathrm{S}} = \frac{1}{2}\underline{\mathbf{t}}^{\mathrm{H}}\underline{\mathbf{t}}
\tag{2.33}
$$

In what follows, instead of resorting to the radiated power, we rather consider the radiated energy T_{S} of (2.33) and its mean

$$
T = \mathop{\mathrm{E}}_{\mathbf{a},\underline{\mathbf{H}}}\{T_{\mathrm{S}}\} = \frac{1}{2}\cdot\mathop{\mathrm{E}}_{\mathbf{a},\underline{\mathbf{H}}}\{\underline{\mathbf{t}}^{\mathrm{H}}\underline{\mathbf{t}}\}
\tag{2.34}
$$

obtained by averaging T of (2.33) over sufficiently many snapshots. If the considered transmission system would be a single carrier system, then with the dimension Q of $\underline{\mathbf{t}}$,

the radiated power would result from (2.34) according to

$$P_{\mathrm{r}} = \frac{1}{2Q} \cdot \underline{t}^{\mathrm{H}} \underline{t}. \qquad (2.35)$$

If the considered transmission system would be a multi-carrier system, then the relation

$$P_{\mathrm{r}} = \frac{1}{2} \cdot \underline{t}^{\mathrm{H}} \underline{t} \qquad (2.36)$$

holds between T and the radiated power P.

A measure of the noise impact in the receiver is the variance σ^2 of $\underline{\tilde{n}}$ of (1.4). As shown in [MBQ04], the appropriate measure for characterizing the system performance is the ratio of the average transmit energy T of (2.34) and σ^2 of (2.29). This ratio

$$\gamma = \frac{T}{\sigma^2} \qquad (2.37)$$

is termed pseudo SNR. Power- or energy-wise a certain RO transmission system is superior to another one, if, in order not to exceed a given error probability P_{e} of (1.1), the required pseudo SNR γ of the first system is below the pseudo SNR of the other one.

Concerning the amplitude dynamics of the received signals, we consider the variance of the useful received vector $\underline{e}$ of (1.4), either component-wise, that is

$$\sigma_{\mathrm{e},z}^2 = \frac{1}{2} \underset{\underline{a}, \underline{H}}{\mathrm{E}} \left\{ \underline{e}_z \underline{e}_z^* \right\}, \; z = 1 \ldots Z, \qquad (2.38)$$

or over the entire vector $\underline{e}$, that is

$$\sigma_{\mathrm{e}}^2 = \frac{1}{Z} \cdot \sum_{z=1}^{Z} \sigma_{\mathrm{e},z}^2 \qquad (2.39)$$

the adequate measure.

2.4 System analysis and optimization in view of transmit energy minimization

The characteristics of an RO transmission system structured as shown in Fig. 1.4 can be concisely described by

- its demodulator matrix $\underline{D}$,

- the statistics [Bel63] of the channel matrix $\underline{H}$, and

- its R data specific representative sets $\mathbb{G}_{\underline{a}^{(r)}}$ of (2.11).

Let us first consider a single snapshot constituted by a realization of the channel matrix $\underline{\mathbf{H}}$ generated in accordance with the valid channel statistics and a realization $\boldsymbol{\mathfrak{a}}^{(r)}$ of the data $\boldsymbol{\mathfrak{a}}$. Then, by (2.11) the set of representative vectors $\underline{\mathbf{d}}^{(r)}$ allowed for the considered snapshot is circumscribed. By virtue of (1.12) and (1.13) each of these vectors $\underline{\mathbf{d}}^{(r)}$ leads to a transmit vector

$$\underline{\mathbf{t}}^{(r)} = \underline{\mathbf{M}}\,\underline{\mathbf{d}}^{(r)} = (\underline{\mathbf{D}}\,\underline{\mathbf{H}})^{\mathrm{H}}\left[(\underline{\mathbf{D}}\,\underline{\mathbf{H}})\,(\underline{\mathbf{D}}\,\underline{\mathbf{H}})^{\mathrm{H}}\right]^{-1}\underline{\mathbf{d}}^{(r)} \tag{2.40}$$

and to the transmit energy $T^{(r)}$ as expressed by (1.40). Now, we are interested in the specific $\underline{\mathbf{d}}^{(r)}$ from the set $\mathbb{G}_{\boldsymbol{\mathfrak{a}}^{(r)}}$ yielding the minimum transmit energy $T^{(r)}$ of (1.40). We designate this representative vector of $\boldsymbol{\mathfrak{a}}^{(r)}$ as $\underline{\mathbf{d}}^{(r)}_{\mathrm{opt}}$, and with (2.33) its determination reads mathematically

$$\underline{\mathbf{d}}^{(r)}_{\mathrm{opt}} = \arg\left\{\min_{\underline{\mathbf{d}}^{(r)'}\in\mathbb{G}_{\boldsymbol{\mathfrak{a}}^{(r)}}}\left[\frac{1}{2}\cdot\underline{\mathbf{d}}^{(r)'\mathrm{H}}\left[(\underline{\mathbf{D}}\,\underline{\mathbf{H}})\,(\underline{\mathbf{D}}\,\underline{\mathbf{H}})^{\mathrm{H}}\right]^{-1}\underline{\mathbf{d}}^{(r)'}\right]\right\}. \tag{2.41}$$

$\underline{\mathbf{d}}^{(r)}_{\mathrm{opt}}$ of (2.41) gives the transmit vector

$$\underline{\mathbf{t}}^{(r)}_{\mathrm{opt}} = \underline{\mathbf{M}}\,\underline{\mathbf{d}}^{(r)}_{\mathrm{opt}} \tag{2.42}$$

and the transmit energy

$$T^{(r)}_{\mathrm{min}} = \frac{1}{2}\cdot\underline{\mathbf{d}}^{(r)\mathrm{H}}_{\mathrm{opt}}\left[(\underline{\mathbf{D}}\,\underline{\mathbf{H}})\,(\underline{\mathbf{D}}\,\underline{\mathbf{H}})^{\mathrm{H}}\right]^{-1}\underline{\mathbf{d}}^{(r)}_{\mathrm{opt}}. \tag{2.43}$$

Finally, by averaging over sufficiently many snapshots, each constituted by a realization of the channel matrix $\underline{\mathbf{H}}$ and the data $\boldsymbol{\mathfrak{a}}$, we obtain the minimum average required transmit energy

$$T_{\mathrm{min}} = \mathop{\mathrm{E}}_{\boldsymbol{\mathfrak{a}},\underline{\mathbf{H}}}\left\{T^{(r)}_{\mathrm{min}}\right\} \tag{2.44}$$

of the considered RO transmission system.

2.5   Résumé

Instead of representing the data to be transmitted by unique discrete valued representatives in the complex plane, which is the conventional approach, a possibility of choice can be introduced in data representation by resorting to by selectable discrete valued or continuous valued representatives. By doing so, freedom is gained when designing the transmit signals. This freedom can be exploited to arrive at transmit signals with minimum power.

Chapter 3
RxZF and TxZF in the light of the SVD of the channel matrix

3.1 Preliminary remarks

In this chapter, based on a mathematical procedure the channel is decomposed into parallel subchannels characterized by a single parameter, namely their associated singular values. Based on this criterion and its statistical properties, RxZF and TxZF will be analysed and compared quite generally in terms of system dimensioning and performance, as a pre-stage to the precoding schemes to be introduced in Chapter 4. Although in this chapter, we only consider the conventional schemes RxZF and TxZF, that employ unique data representation, the findings of this chapter can easily be extended to the case of schemes that employ selectable data representation, as the channel equalization is identical with respect to the linear inner section, and the selective assignment can be considered as additional preprocessing, see Fig. 1.5.

3.2 SVD of the channel matrix

By performing SVD [Lue96], the channel matrix $\underline{\mathbf{H}}$ of (1.3) can be expressed by two unitary matrices

$$\underline{\mathbf{U}} = (\underline{\mathbf{u}}_1 \ldots \underline{\mathbf{u}}_Z) \in \mathbb{C}^{Z \times Z} \tag{3.1}$$

and

$$\underline{\mathbf{V}} = (\underline{\mathbf{v}}_1 \ldots \underline{\mathbf{v}}_Q) \in \mathbb{C}^{Q \times Q} \tag{3.2}$$

and a $Z \times Q$ matrix $\boldsymbol{\Lambda}$ as

$$\underline{\mathbf{H}} = \underline{\mathbf{U}} \boldsymbol{\Lambda} \underline{\mathbf{V}}^{\mathrm{H}}. \tag{3.3}$$

The Z columns $\underline{\mathbf{u}}_z$, $z = 1 \ldots Z$, of $\underline{\mathbf{U}}$ of (3.1) and the Q columns $\underline{\mathbf{v}}_q$, $q = 1 \ldots Q$, of $\underline{\mathbf{V}}$ of (3.2) are termed left or right side singular vectors of $\underline{\mathbf{H}}$, respectively. $\boldsymbol{\Lambda}$ in (3.3) has the form

$$\boldsymbol{\Lambda} = \begin{pmatrix} \lambda_1 & \cdots & 0 \\ \vdots & \ddots & \vdots \\ 0 & \cdots & \lambda_Q \\ \vdots & \ddots & \vdots \\ 0 & \cdots & 0 \end{pmatrix} \in \mathbb{R}_{\geq 0}^{Z \times Q} \tag{3.4}$$

in the case $Z > Q$ (high matrix $\underline{\mathbf{H}}$), and the form

$$\mathbf{\Lambda} = \begin{pmatrix} \lambda_1 & \cdots & 0 & \cdots & 0 \\ \vdots & \ddots & \vdots & \ddots & \vdots \\ 0 & \cdots & \lambda_Z & \cdots & 0 \end{pmatrix} \in \mathbb{R}_{\geq 0}^{Z \times Q} \tag{3.5}$$

in the case $Z < Q$ (wide matrix $\underline{\mathbf{H}}$). In case of $Z = Q$ (square matrix $\underline{\mathbf{H}}$), $\mathbf{\Lambda}$ in (3.3) is a diagonal matrix. The elements λ_q of (3.4) and λ_z of (3.5) are non-negative real values which are termed singular values [Lue96] of the channel matrix $\underline{\mathbf{H}}$. In general,

$$G = \min(Q, Z) \tag{3.6}$$

singular values exist. Let us assume that these are sorted in decreasing order:

$$\lambda_1 \geq \lambda_2 \geq \ldots \geq \lambda_G \geq 0. \tag{3.7}$$

Then, λ_1 is termed principal singular value of $\underline{\mathbf{H}}$. The singular vectors $\underline{\mathbf{u}}_1$ of (3.1) and $\underline{\mathbf{v}}_1$ of (3.2) belonging to λ_1 are termed principal singular vectors of $\underline{\mathbf{H}}$. The rank of $\underline{\mathbf{H}}$ is equal to the number of its non-zero singular values λ_g, $g = 1 \ldots G$, that is with G of (3.6)

$$\text{rank}(\underline{\mathbf{H}}) \leq G \tag{3.8}$$

holds. The minimum rank of a non-zero channel matrix $\underline{\mathbf{H}}$ is one. We term $\mathbf{\Lambda}$ of (3.4) or (3.5) core channel matrix.

The Gram matrices $\underline{\mathbf{H}}^{\text{H}}\underline{\mathbf{H}}$ and $\underline{\mathbf{H}}\,\underline{\mathbf{H}}^{\text{H}}$ of $\underline{\mathbf{H}}$ are hermitian. Their SVDs degenerate to eigenvalue decompositions (EVD) [Lue96]. With $\underline{\mathbf{U}}$ of (3.1), $\underline{\mathbf{V}}$ of (3.2) and $\mathbf{\Lambda}$ of (3.4) or (3.5) follow from (3.3) the relations

$$\underline{\mathbf{H}}^{\text{H}}\underline{\mathbf{H}} = \underline{\mathbf{V}}\mathbf{\Lambda}^{\text{T}}\mathbf{\Lambda}\underline{\mathbf{V}}^{\text{H}} \tag{3.9}$$

and

$$\underline{\mathbf{H}}\,\underline{\mathbf{H}}^{\text{H}} = \underline{\mathbf{U}}\mathbf{\Lambda}\mathbf{\Lambda}^{\text{T}}\underline{\mathbf{U}}^{\text{H}}. \tag{3.10}$$

If $\underline{\mathbf{H}}$ is time variant, then for each realization (snapshot) of $\underline{\mathbf{H}}$ a different set of matrices $\underline{\mathbf{U}}, \mathbf{\Lambda}, \underline{\mathbf{V}}$ has to be expected.

By means of examples we are now going to illustrate the SVD of $\underline{\mathbf{H}}$ to gain some insight into the performance of SVD particularly in the case of the fair and unfair channels introduced in Subsection 2.3.2. To this purpose we first perform the SVD of the two

channel matrices $\underline{\mathbf{H}}_{\text{fair}}$ and $\underline{\mathbf{H}}_{\text{unfair}}$ of (2.31) and (2.32), respectively. For $\underline{\mathbf{H}}_{\text{fair}}$ we obtain

$$
\underline{\mathbf{U}}_{\text{fair}} = \begin{pmatrix} -0.73 + \text{j}0.18 & -0.25 - \text{j}0.25 & 0.36 - \text{j}0.02 & 0.23 - \text{j}0.36 \\ -0.38 - \text{j}0.31 & -0.05 + \text{j}0.39 & 0.29 - \text{j}0.42 & -0.40 + \text{j}0.43 \\ -0.43 + \text{j}0.06 & 0.23 + \text{j}0.03 & -0.44 + \text{j}0.46 & -0.58 - \text{j}0.12 \\ -0.09 - \text{j}0.01 & -0.73 + \text{j}0.36 & -0.31 + \text{j}0.32 & 0.24 + \text{j}0.25 \end{pmatrix}, \tag{3.11}
$$

$$
\underline{\mathbf{V}}_{\text{fair}} = \begin{pmatrix} 0.44 & -0.49 & 0.26 & 0.71 \\ 0.21 - \text{j}0.11 & 0.36 - \text{j}0.29 & 0.33 - \text{j}0.77 & 0.01 + \text{j}0.16 \\ 0.07 - \text{j}0.26 & -0.08 - \text{j}0.73 & 0.25 + \text{j}0.31 & -019 - \text{j}0.44 \\ -0.62 + \text{j}0.54 & -0.01 - \text{j}0.14 & 0.16 - \text{j}0.21 & 0.33 - \text{j}0.36 \end{pmatrix} \tag{3.12}
$$

and

$$
\boldsymbol{\Lambda}_{\text{fair}} = \begin{pmatrix} 3.04 & 0 & 0 & 0 \\ 0 & 2.39 & 0 & 0 \\ 0 & 0 & 1.33 & 0 \\ 0 & 0 & 0 & 0.52 \end{pmatrix}. \tag{3.13}
$$

SVD of $\underline{\mathbf{H}}_{\text{unfair}}$ of (2.32) yields

$$
\underline{\mathbf{U}}_{\text{unfair}} = \begin{pmatrix} 0.01 - \text{j}0.00 & -0.08 + \text{j}0.07 & -0.47 + \text{j}0.66 & -0.36 + \text{j}0.44 \\ 0.00 - \text{j}0.05 & -0.03 - \text{j}0.05 & -0.44 + \text{j}0.38 & 0.66 - \text{j}0.48 \\ -0.29 - \text{j}0.22 & -0.86 + \text{j}0.35 & 0.05 - \text{j}0.08 & 0.06 - \text{j}0.03 \\ 0.65 - \text{j}0.66 & 0.09 + \text{j}0.35 & -0.00 - \text{j}0.03 & -0.03 - \text{j}0.04 \end{pmatrix}, \tag{3.14}
$$

$$
\underline{\mathbf{V}}_{\text{unfair}} = \begin{pmatrix} 0.44 & 0.67 & -0.14 & -0.58 \\ -0.16 - \text{j}0.63 & 0.22 - \text{j}0.52 & -0.06 + \text{j}0.43 & 0.15 - \text{j}0.23 \\ 0.17 + \text{j}0.57 & -0.17 + \text{j}0.07 & -0.38 - \text{j}0.35 & 0.02 + \text{j}0.59 \\ -0.17 + \text{j}0.05 & -0.23 + \text{j}0.38 & -0.03 + \text{j}0.73 & -0.38 + \text{j}0.31 \end{pmatrix} \tag{3.15}
$$

and

$$
\boldsymbol{\Lambda}_{\text{unfair}} = \begin{pmatrix} 3.28 & 0 & 0 & 0 \\ 0 & 2.48 & 0 & 0 \\ 0 & 0 & 0.32 & 0 \\ 0 & 0 & 0 & 0.11 \end{pmatrix}. \tag{3.16}
$$

From (3.13) and (3.16) follow

$$
\text{trace}\left(\boldsymbol{\Lambda}_{\text{fair}}\boldsymbol{\Lambda}_{\text{fair}}^{\text{H}}\right) = 17.00 \tag{3.17}
$$

and

$$
\text{trace}\left(\boldsymbol{\Lambda}_{\text{unfair}}\boldsymbol{\Lambda}_{\text{unfair}}^{\text{H}}\right) = 17.00, \tag{3.18}
$$

respectively, that is both traces are equal. This equality results from the specific relation between $\underline{\mathbf{H}}_{\mathrm{fair}}$ and $\underline{\mathbf{H}}_{\mathrm{unfair}}$ introduced in Subsection 2.3.2, see (2.30).

We now consider a large stationary ensemble of fair and unfair channel matrices $\underline{\mathbf{H}}_{\mathrm{fair}}$ and $\underline{\mathbf{H}}_{\mathrm{unfair}}$, respectively, again with the dimensions 4×4 so that G of (3.6) becomes equal to four. In Figs. 3.1 a and b we depict the probability density functions (PDF) of the G singular values λ_g, $g = 1 \ldots G$, of said two ensembles of channel matrices. The PDFs of the G singular values λ_g, $g = 1 \ldots G$, in the case of the ensemble of matrices of the type $\underline{\mathbf{H}}_{\mathrm{fair}}$ can be expressed in closed form as follows:

$$
\begin{aligned}
p_{\lambda_1}(\lambda_1) = e^{-\lambda_1^2} \Big[& 4(2 - 6e^{-\lambda_1^2} + 6e^{-2\lambda_1^2} - e^{-3\lambda_1^2})\lambda_1 - 24(1 - 2e^{-\lambda_1^2} + e^{-2\lambda_1^2})\lambda_1^3 \\
& + (\frac{108}{3} - 48e^{-\lambda_1^2} + 12e^{-2\lambda_1^2})\lambda_1^5 - (\frac{68}{3} - \frac{16}{3}e^{-\lambda_1^2} - \frac{28}{3}e^{-2\lambda_1^2})\lambda_1^7 \\
& + (\frac{21}{3} - \frac{8}{3}e^{-\lambda_1^2} + \frac{23}{3}e^{-2\lambda_1^2})\lambda_1^9 - (1 - \frac{8}{3}e^{-\lambda_1^2} - \frac{5}{3}e^{-2\lambda_1^2})\lambda_1^{11} \\
& + (\frac{1}{18} + \frac{8}{9}e^{-\lambda_1^2} + \frac{1}{6}e^{-2\lambda_1^2})\lambda_1^{13} + \frac{1}{9}e^{-\lambda_1^2}\lambda_1^{15} - \frac{1}{36}e^{-\lambda_1^2}\lambda_1^{17} \Big],
\end{aligned}
\tag{3.19}
$$

$$
\begin{aligned}
p_{\lambda_2}(\lambda_2) = e^{-2 \cdot \lambda_2^2} \Big[& 24(1 - 2e^{-\lambda_2^2} + 1e^{-2\lambda_2^2})\lambda_2 - 48(1 - e^{-\lambda_2^2})\lambda_2^3 \\
& - 24(2 - e^{-\lambda_2^2})\lambda_2^5 - (\frac{16}{3} + \frac{56}{3}e^{-\lambda_2^2})\lambda_2^7 + (\frac{8}{3} - \frac{46}{3}e^{-\lambda_2^2})\lambda_2^9 \\
& - (\frac{8}{3} + \frac{10}{3}e^{-\lambda_2^2})\lambda_2^{11} + (\frac{8}{9} - \frac{1}{3}e^{-\lambda_2^2})\lambda_2^{13} - \frac{1}{9}\lambda_2^{15} + \frac{1}{36}\lambda_2^{17} \Big],
\end{aligned}
\tag{3.20}
$$

$$
p_{\lambda_3}(\lambda_3) = e^{-3 \cdot \lambda_3^2} \Big[24(1 - e^{-\lambda_3^2})\lambda_3 - 24\lambda_3^3 + 12\lambda_3^5 + \frac{28}{3}\lambda_3^7 + \frac{23}{3}\lambda_3^9 + \frac{5}{3}\lambda_3^{11} + \frac{1}{6}\lambda_3^{13} \Big]
\tag{3.21}
$$

and

$$
p_{\lambda_4}(\lambda_4) = 8 \cdot e^{-4 \cdot \lambda_3^2}.
\tag{3.22}
$$

The derivation of these four expressions by means of applying results of random matrix theory [Ede89] is shown in Appendix A.1. However, for the case of the channel matrices of the type $\underline{\mathbf{H}}_{\mathrm{unfair}}$, which result from the matrices $\underline{\mathbf{H}}_{\mathrm{fair}}$ not only by a linear transformation, but by an additional adaptation of the Euclidean norms, see (2.30), the author is not aware of an analytical approach to determining the PDFs of the singular values of the channel matrices. Therefore, for the case of the channel matrices $\underline{\mathbf{H}}_{\mathrm{unfair}}$ only numerically determined PDFs of the singular values are displayed.

a)

b)
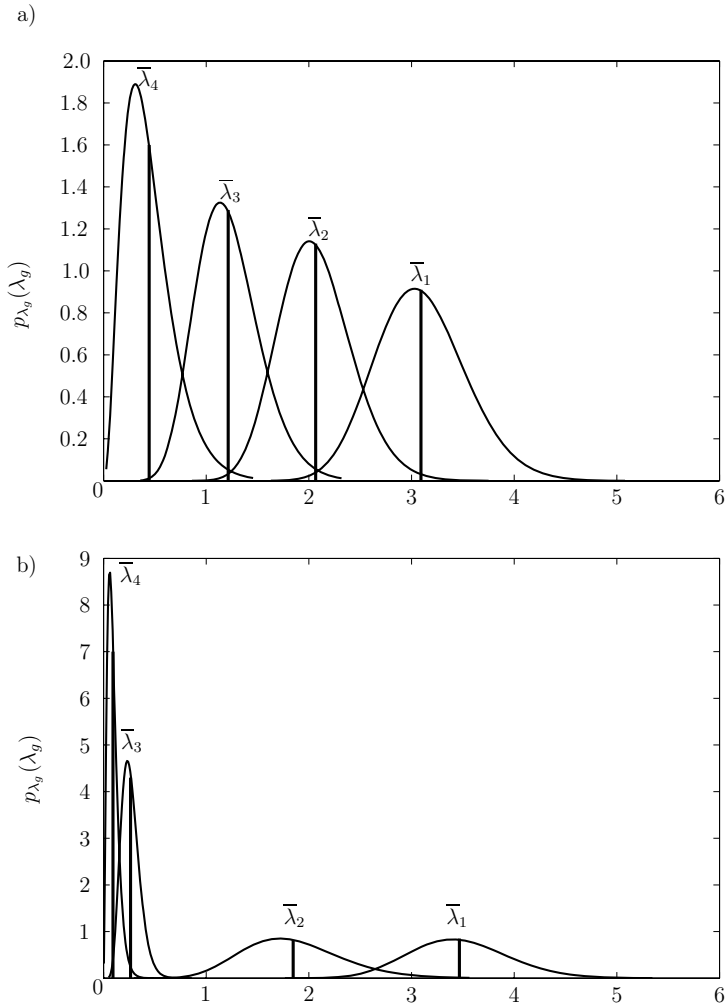
Fig. 3.1. PDFs and averages $\overline{\lambda}_g$ of the singular values
λ_g, $g = 1 \ldots G$, of two large ensembles of 4×4 channel matrices $\underline{\mathbf{H}}$
a) fair channel
b) unfair channel

From Figs. 3.1 a and b one can further conclude that each of the G singular values λ_g, $g = 1 \ldots G$, is more or less concentrated around a distinct average value

$$\overline{\lambda}_g = \mathrm{E}\left\{\lambda_g\right\} = \int_0^\infty \lambda_g \cdot p(\lambda_g) d\lambda_g, \qquad (3.23)$$

with the variance

$$\mathrm{var}\left\{\lambda_g\right\} = \int_0^\infty \left(\lambda_g - \overline{\lambda}_g\right)^2 \cdot p(\lambda_g) d\lambda_g, \qquad (3.24)$$

see Table 3.1. In Fig. 3.1 these average values $\overline{\lambda}_g$ are marked by solid vertical lines. The spectra of the average singular values of the fair and unfair channels can be considered earmarks of these channels. In some of the later considerations, for instance in Subsection 3.4.3, we will assume that the PDFs of the G singular values of a stationary channel matrix $\underline{\mathbf{H}}$ can be approximated by their averages values $\overline{\lambda}_g$. A quantity suitable to rate the quality of this approximation would be the ratio $\overline{\lambda}_g / \sqrt{\mathrm{var}\left\{\lambda_g\right\}}$, which should be sufficiently above unity. For the examples of Figs. 3.1 a and b these ratios are listed in Table 3.1, and we see that said ratios are indeed significantly larger than one. The averages $\overline{\lambda}_g$ can be considered the invariant essence of a stationary time variant channel matrix, whereas the matrices $\underline{\mathbf{U}}$ and $\underline{\mathbf{V}}$ in (3.3) vary from channel snapshot to channel snapshot.

	fair channel			unfair channel		
$g =$	$\overline{\lambda}_g / \sqrt{\mathrm{var}\left\{\lambda_g\right\}}$	$\overline{\lambda}_g$	$\mathrm{var}\left(\lambda_g\right)$	$\overline{\lambda}_g / \sqrt{\mathrm{var}\left\{\lambda_g\right\}}$	$\overline{\lambda}_g$	$\mathrm{var}\left(\lambda_g\right)$
1	7.0367	3.10	0.19	7.1811	3.47	0.23
2	5.8975	2.07	0.12	3.9859	1.85	0.21
3	4.0142	1.22	0.09	2.8625	0.26	0.01
4	1.9435	0.44	0.05	1.7385	0.09	0.00

Table 3.1. Ratios $\overline{\lambda}_g / \sqrt{\mathrm{var}\left\{\lambda_g\right\}}$ for the PDFs of Figs. 3.1 a and b

3.3 Representation of the demodulator matrix and the modulator matrix by the singular vectors of the channel matrix

With $\underline{\mathbf{U}}$ of (3.1) and a matrix

$$\underline{\mathbf{G}} = \begin{pmatrix} \underline{g}_{1,1} & \cdots & \underline{g}_{1,Z} \\ \vdots & \ddots & \vdots \\ \underline{g}_{N,1} & \cdots & \underline{g}_{N,Z} \end{pmatrix} \in \mathbb{C}^{N \times Z} \tag{3.25}$$

we can express the demodulator matrix $\underline{\mathbf{D}}$ of (1.15) as [Lue96]

$$\underline{\mathbf{D}} = \underline{\mathbf{G}}\,\underline{\mathbf{U}}^{\mathrm{H}}. \tag{3.26}$$

From (3.26) follows

$$\underline{\mathbf{G}} = \underline{\mathbf{D}}\,\underline{\mathbf{U}} \in \mathbb{C}^{N \times Z}. \tag{3.27}$$

The element $\underline{g}_{n,z}$ of $\underline{\mathbf{G}}$ of (3.27) is a measure of the degree to which the left side singular vector $\underline{\mathbf{u}}_z$ of $\underline{\mathbf{H}}$ contributes to row n of $\underline{\mathbf{D}}$. If the rows of $\underline{\mathbf{D}}$ would be orthonormal as presupposed in (2.28), then we obtain from (3.27)

$$\underline{\mathbf{G}}\,\underline{\mathbf{G}}^{\mathrm{H}} = \underline{\mathbf{D}}\,\underline{\mathbf{U}}\,(\underline{\mathbf{D}}\,\underline{\mathbf{U}})^{\mathrm{H}} = \mathbf{I}^{N \times N}, \tag{3.28}$$

that is in this case also the rows of $\underline{\mathbf{G}}$ would be orthonormal. We term $\underline{\mathbf{G}}$ of (3.27) the core demodulator matrix of the considered system.

Similarly to (3.26), with $\underline{\mathbf{V}}$ of (3.2) and a matrix

$$\underline{\mathbf{F}} = \begin{pmatrix} \underline{f}_{1,1} & \cdots & \underline{f}_{1,N} \\ \vdots & \ddots & \vdots \\ \underline{f}_{Q,1} & \cdots & \underline{f}_{Q,N} \end{pmatrix} \in \mathbb{C}^{Q \times N} \tag{3.29}$$

the modulator matrix $\underline{\mathbf{M}}$ of (1.12) can be expressed as

$$\underline{\mathbf{M}} = \underline{\mathbf{V}}\,\underline{\mathbf{F}}. \tag{3.30}$$

From (3.30) follows

$$\underline{\mathbf{F}} = \underline{\mathbf{V}}^{\mathrm{H}}\underline{\mathbf{M}} \in \mathbb{C}^{Q \times N}. \tag{3.31}$$

The element $\underline{f}_{q,n}$ of $\underline{\mathbf{F}}$ of (3.31) is a measure of the degree to which the right side singular

vector $\underline{\mathbf{v}}_q$ of $\underline{\mathbf{H}}$ contributes to column n of $\underline{\mathbf{M}}$. If the columns of $\underline{\mathbf{M}}$ would be orthonormal, then

$$\underline{\mathbf{F}}^{\mathrm{H}}\underline{\mathbf{F}} = \left(\underline{\mathbf{V}}^{\mathrm{H}}\underline{\mathbf{M}}\right)^{\mathrm{H}}\underline{\mathbf{V}}^{\mathrm{H}}\underline{\mathbf{M}} = \mathbf{I}^{N\times N} \tag{3.32}$$

would hold, that is also the columns of $\underline{\mathbf{F}}$ would be orthonormal. We designate $\underline{\mathbf{F}}$ of (3.31) as core modulator matrix of the considered system.

3.4 Core of the linear inner section

3.4.1 Definitions

Fig. 3.2 a shows the linear inner section of the transmission systems of Figs. 1.3 and 1.4. At the moment we only postulate some type of zero forcing, that is

$$\underline{\mathbf{D}}\,\underline{\mathbf{H}}\,\underline{\mathbf{M}} = \mathbf{I}^{N\times N} \tag{3.33}$$

shall hold without specifically featuring RxZF or TxZF. Then, with the input vector $\underline{\mathbf{d}}$ and the additive noise vector $\underline{\tilde{\mathbf{n}}}$ we obtain at the output of the system of Fig. 3.2 a the vector $\underline{\mathbf{d}}_{\mathrm{Rx}}$ of (1.16). We now substitute in (3.33) $\underline{\mathbf{D}}$ by (3.26), $\underline{\mathbf{H}}$ by (3.3) and $\underline{\mathbf{M}}$ by (3.30). This yields

$$\underline{\mathbf{D}}\,\underline{\mathbf{H}}\,\underline{\mathbf{M}} = \underline{\mathbf{G}}\,\underline{\mathbf{U}}^{\mathrm{H}}\underline{\mathbf{U}}\boldsymbol{\Lambda}\underline{\mathbf{V}}^{\mathrm{H}}\underline{\mathbf{V}}\,\underline{\mathbf{F}} = \underline{\mathbf{G}}\boldsymbol{\Lambda}\underline{\mathbf{F}} = \mathbf{I}^{N\times N}. \tag{3.34}$$

The noise vector $\underline{\mathbf{D}}\,\underline{\tilde{\mathbf{n}}}$ at the output of the system of Fig. 3.2 a can be written as

$$\underline{\mathbf{D}}\,\underline{\tilde{\mathbf{n}}} = \underline{\mathbf{G}}\,\underline{\mathbf{U}}^{\mathrm{H}}\underline{\tilde{\mathbf{n}}}. \tag{3.35}$$

With $\underline{\mathbf{d}}_{\mathrm{Rx}}$ of (1.16) and with (3.34) the linear inner section shown in Fig. 3.2 a can be equivalently represented by the linear system shown in Fig. 3.2 b, which we term core of the linear inner section.

As already mentioned in Section 1.4, in the case of TO realized for instance by RxZF or RxMF,

- $\underline{\mathbf{M}}$ is a priori set and known also to the receiver,

- CSI in the form of a known channel matrix $\underline{\mathbf{H}}$ is available to the receiver (not, however, to the transmitter), and,

- based on the knowledge of $\underline{\mathbf{M}}$ and $\underline{\mathbf{H}}$, the demodulator matrix $\underline{\mathbf{D}}$ is a posteriori determined in the receiver from (1.19) or (1.23), respectively.

If we resort in investigations of RxZF and RxMF not to the original system of Fig. 3.2 a, but to its equivalent core of Fig. 3.2 b, then (1.19) and (1.23) can be written as

$$\underline{\mathbf{G}} = \left[(\mathbf{\Lambda}\,\underline{\mathbf{F}})^{\mathrm{H}}\,\mathbf{\Lambda}\,\underline{\mathbf{F}}\right]^{-1}(\mathbf{\Lambda}\,\underline{\mathbf{F}})^{\mathrm{H}} \tag{3.36}$$

and

$$\underline{\mathbf{G}}_{\mathrm{RxMF}} = \left(\mathrm{diag}\left[(\mathbf{\Lambda}\,\underline{\mathbf{F}})^{\mathrm{H}}\,\mathbf{\Lambda}\,\underline{\mathbf{F}}\right]\right)^{-1}(\mathbf{\Lambda}\,\underline{\mathbf{F}})^{\mathrm{H}}, \tag{3.37}$$

respectively. However, even though the modulator matrix $\underline{\mathbf{M}}$ is known at the receiver, this is not true for the core modulator matrix $\underline{\mathbf{F}}$ of (3.31). This is due to the fact that in the case of TO $\underline{\mathbf{H}}$ and, therefore, $\underline{\mathbf{V}}$ of (3.2) and (3.3) are unknown at the receiver so that $\underline{\mathbf{F}}$ cannot be gained from $\underline{\mathbf{M}}$ by evaluating (3.31). In addition, if $\underline{\mathbf{M}}$ is kept fix and $\underline{\mathbf{H}}$ is time variant, then for each realization of $\underline{\mathbf{H}}$ a different matrix $\underline{\mathbf{V}}$ of (3.2) and (3.3) has to be expected. To summarize, (3.36) and (3.37) cannot be performed without CSI available at the transmitter.
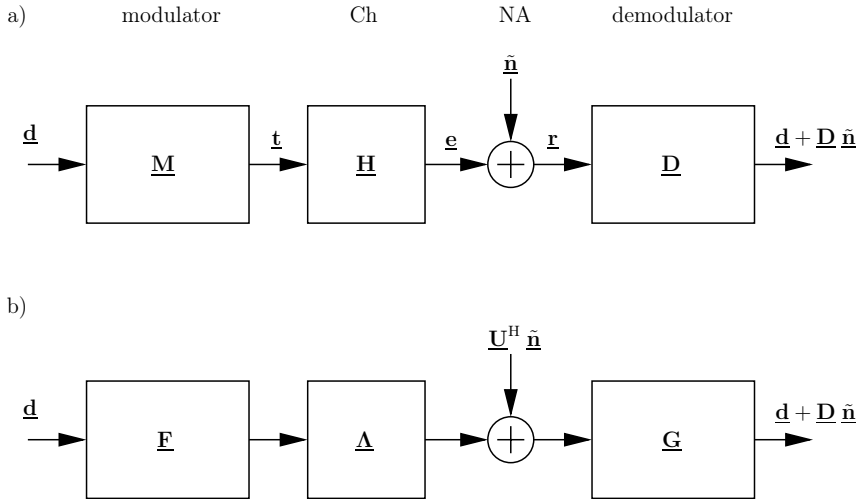

Fig. 3.2. Linear inner section of the transmission system of Figs. 1.3 and 1.4
     a) original system
     b) core system

We again refer to Section 1.4 and consider RO realized by TxZF or TxMF, see Fig. 1.4. In this case

- $\underline{\mathbf{D}}$ is a priori given and known also to the transmitter,

- CSI in the form of a known channel matrix $\underline{\mathbf{H}}$ is available to the transmitter (not, however, to the transmitter), and,

- according to (1.20) or (1.29) the modulator matrix $\underline{\mathbf{M}}$ is obtained from $\underline{\mathbf{H}}$ and $\underline{\mathbf{D}}$.

If we investigate instead of an original TxZF or TxMF system of Fig. 3.2 a its equivalent core of Fig. 3.2 b, then (1.20) and (1.29) can be rewritten as

$$\underline{\mathbf{F}} = (\underline{\mathbf{G}}\,\mathbf{\Lambda})^{\mathrm{H}} \left[\underline{\mathbf{G}}\,\mathbf{\Lambda}\,(\underline{\mathbf{G}}\,\mathbf{\Lambda})^{\mathrm{H}} \right]^{-1} \tag{3.38}$$

and

$$\underline{\mathbf{F}}_{\mathrm{TxMF}} = (\underline{\mathbf{G}}\,\mathbf{\Lambda})^{\mathrm{H}} \left(\mathrm{diag}\left[\underline{\mathbf{G}}\,\mathbf{\Lambda}\,(\underline{\mathbf{G}}\,\mathbf{\Lambda})^{\mathrm{H}} \right] \right)^{-1}, \tag{3.39}$$

respectively. Now, even though the demodulator matrix $\underline{\mathbf{D}}$ is known at the transmitter, this is not the case for the core demodulator matrix written as $\underline{\mathbf{G}}$ of (3.27). This results from the fact that $\underline{\mathbf{H}}$ and, therefore, $\underline{\mathbf{U}}$ of (3.1) and (3.3) are unknown at the receiver so that $\underline{\mathbf{G}}$ cannot be obtained from $\underline{\mathbf{D}}$ by evaluating (3.27). Moreover, if $\underline{\mathbf{D}}$ is kept fix and $\underline{\mathbf{H}}$ is time variant, a different matrix $\underline{\mathbf{U}}$ of (3.1) occurs for each realization of $\underline{\mathbf{H}}$. To summarize, (3.38) and (3.39) cannot be performed without CSI available at the receiver.

In order to illustrate the considerations of this subsection by just one example, we set out from $\underline{\mathbf{H}}_{\mathrm{fair}}$ of (2.31) and its SVD given by (3.11), (3.12) and (3.13) and consider TxZF for the case N equal to two with the demodulator matrix

$$\underline{\mathbf{D}} = \begin{pmatrix} 1 & 0 & 0 & 0 \\ 0 & 0 & 0 & 1 \end{pmatrix} . \tag{3.40}$$

Substituting $\underline{\mathbf{H}}$ equal to $\underline{\mathbf{H}}_{\mathrm{fair}}$ of (2.31) and $\underline{\mathbf{D}}$ of (3.40) in (1.20) we obtain for the original linear inner section, see Fig. 3.2 a, the modulator matrix

$$\underline{\mathbf{M}} = (\underline{\mathbf{D}}\,\underline{\mathbf{H}})^{\mathrm{H}} \left[(\underline{\mathbf{D}}\,\underline{\mathbf{H}})\,(\underline{\mathbf{D}}\,\underline{\mathbf{H}})^{\mathrm{H}} \right]^{-1} = \begin{pmatrix} -0.12 - \mathrm{j}0.05 & 0.18 + \mathrm{j}0.09 \\ -0.04 - \mathrm{j}0.05 & -0.33 + \mathrm{j}0.12 \\ 0.03 + \mathrm{j}0.10 & -0.11 + \mathrm{j}0.24 \\ 0.34 - \mathrm{j}0.16 & -0.14 + \mathrm{j}0.05 \end{pmatrix} . \tag{3.41}$$

From $\underline{\mathbf{D}}$ of (3.40) and $\underline{\mathbf{M}}$ of (3.41) follow by virtue of (3.27) and (3.31), respectively,

$$\underline{\mathbf{G}} = \begin{pmatrix} -0.73 + \mathrm{j}0.18 & -0.25 - \mathrm{j}0.25 & 0.36 - \mathrm{j}0.02 & 0.23 - \mathrm{j}0.36 \\ -0.09 - \mathrm{j}0.01 & -0.73 + \mathrm{j}0.36 & -0.31 + \mathrm{j}0.32 & 0.24 + \mathrm{j}0.26 \end{pmatrix} \tag{3.42}$$

and

$$\underline{\mathbf{F}} = \begin{pmatrix} -0.38 - \mathrm{j}0.11 & -0.01 + \mathrm{j}0.13 \\ -0.00 + \mathrm{j}0.06 & -0.39 + \mathrm{j}0.21 \\ 0.12 + \mathrm{j}0.00 & -0.12 - \mathrm{j}0.13 \\ 0.02 + \mathrm{j}0.04 & 0.04 - \mathrm{j}0.05 \end{pmatrix}. \tag{3.43}$$

Substitution of $\underline{\mathbf{G}}$ of (3.42), $\boldsymbol{\Lambda}_{\mathrm{fair}}$ of (3.13) and $\underline{\mathbf{F}}$ of (3.43) in (3.34) yields

$$\underline{\mathbf{G}}\boldsymbol{\Lambda}\underline{\mathbf{F}} =$$

$$\begin{pmatrix} -0.73 + \mathrm{j}0.18 & -0.25 - \mathrm{j}0.25 & 0.36 - \mathrm{j}0.02 & 0.23 - \mathrm{j}0.36 \\ -0.09 - \mathrm{j}0.01 & -0.73 + \mathrm{j}0.36 & -0.31 + \mathrm{j}0.32 & 0.24 + \mathrm{j}0.26 \end{pmatrix}.$$

$$\begin{pmatrix} 3.04 & 0 & 0 & 0 \\ 0 & 2.39 & 0 & 0 \\ 0 & 0 & 1.33 & 0 \\ 0 & 0 & 0 & 0.52 \end{pmatrix} . \begin{pmatrix} -0.38 - \mathrm{j}0.11 & -0.01 + \mathrm{j}0.13 \\ -0.00 + \mathrm{j}0.06 & -0.39 + \mathrm{j}0.21 \\ 0.12 + \mathrm{j}0.00 & -0.12 - \mathrm{j}0.13 \\ 0.02 + \mathrm{j}0.04 & 0.04 - \mathrm{j}0.05 \end{pmatrix} \tag{3.44}$$

$$= \begin{pmatrix} 1 & 0 \\ 0 & 1 \end{pmatrix}.$$

By the unit matrix $\mathbf{I}^{2\times 2}$ resulting in (3.44) the equivalence of the original and core linear inner sections, see Figs. 3.2 a and b, is proved.

3.4.2   Structural properties of the core modulator and demodulator matrices

We set out from the product $\underline{\mathbf{G}}\,\boldsymbol{\Lambda}\underline{\mathbf{F}}$ in (3.34) and consider first the case $Z > Q$ and $G = Q$ (high channel matrix). Then, this product can be visualized as shown in Fig. 3.3 a for the case

$$N = Q \,(\text{full system load}) \tag{3.45}$$

and in Fig. 3.3 b for the case

$$N < Q \,(\text{partial system load}). \tag{3.46}$$

As shown in Fig. 3.3, the core demodulator matrix $\underline{\mathbf{G}}$ can be subdivided according to

$$\underline{\mathbf{G}} = (\underline{\mathbf{G}}_{\mathrm{rel}}, \underline{\mathbf{G}}_{\mathrm{irrel}}) \tag{3.47}$$

in a left part

$$\underline{\mathbf{G}}_{\mathrm{rel}} \in \mathbb{C}^{N \times Q} \tag{3.48}$$

$$\mathbf{I}^{N\times N} = \underline{\mathbf{F}} \in \mathbb{C}^{N\times N} \cdot \mathbf{\Lambda} \in \mathbb{R}_{\geq 0}^{Z\times Q} \cdot \underline{\mathbf{G}} \in \mathbb{C}^{N\times Z}$$

$\mathbf{\Lambda}_{\text{rel}} \in \mathbb{R}_{\geq 0}^{Q\times Q}$

$\mathbf{\Lambda}_{\text{irrel}} \in \mathbf{0}^{(Z-Q)\times Q}$

$\underline{\mathbf{G}}_{\text{rel}} \in \mathbb{C}^{N\times N}$

$\underline{\mathbf{G}}_{\text{irrel}} \in \mathbb{C}^{N\times(Z-N)}$

a)

Fig. 3.3 Visualization of the product $\underline{\mathbf{G}}\mathbf{\Lambda}\underline{\mathbf{F}}$ of (3.28) for the case of a high channel matrix $\underline{\mathbf{H}}$
a) full system load ($N = Q$)
b) partial system load ($N < Q$)

b)

which we term relevant partial core demodulator matrix, and in a right part

$$\underline{\mathbf{G}}_{\mathrm{irrel}} \in \mathbb{C}^{N \times (Z-Q)}, \tag{3.49}$$

which we term irrelevant partial core demodulator matrix. Also the core channel matrix $\mathbf{\Lambda}$ of (3.4) can be split up into a relevant partial core channel matrix

$$\mathbf{\Lambda}_{\mathrm{rel}} = \begin{pmatrix} \lambda_1 & \cdots & 0 \\ \vdots & \ddots & \vdots \\ 0 & \cdots & \lambda_Q \end{pmatrix} \in \mathbb{C}^{Q \times Q} \tag{3.50}$$

and an irrelevant partial core channel matrix

$$\mathbf{\Lambda}_{\mathrm{irrel}} = \mathbf{0}^{(Z-Q) \times Q} \tag{3.51}$$

according to

$$\mathbf{\Lambda} = \begin{pmatrix} \mathbf{\Lambda}_{\mathrm{rel}} \\ \mathbf{0}^{(Z-Q) \times Q} \end{pmatrix}. \tag{3.52}$$

Only the relevant partial matrices $\underline{\mathbf{G}}_{\mathrm{rel}}$ of (3.48) and $\mathbf{\Lambda}_{\mathrm{rel}}$ of (3.50) contribute to the transmission, whereas the irrelevant partial matrices have no impact. In the case of a high channel matrix $\underline{\mathbf{H}}$ the entire core modulator matrix $\underline{\mathbf{F}}$ can be considered relevant, that is we can write

$$\underline{\mathbf{F}}_{\mathrm{rel}} = \underline{\mathbf{F}}. \tag{3.53}$$

Then, with $\underline{\mathbf{G}}_{\mathrm{rel}}$ of (3.48), $\mathbf{\Lambda}_{\mathrm{rel}}$ of (3.50), and $\underline{\mathbf{F}}_{\mathrm{rel}}$ of (3.53) we obtain

$$\underline{\mathbf{G}} \, \mathbf{\Lambda} \underline{\mathbf{F}} = \underline{\mathbf{G}}_{\mathrm{rel}} \, \mathbf{\Lambda}_{\mathrm{rel}} \underline{\mathbf{F}}_{\mathrm{rel}}. \tag{3.54}$$

We now consider the case $Z < Q$ and $G = Z$ (wide channel matrix). In this case, full and partial system loads are characterized by

$$N = Z \text{ (full system load)} \tag{3.55}$$

and

$$N < Z \text{ (partial system load)}, \tag{3.56}$$

and the product $\underline{\mathbf{G}} \, \mathbf{\Lambda} \underline{\mathbf{F}}$ in (3.34) can be illustrated as shown in Figs. 3.4 a and b. The core modulator matrix $\underline{\mathbf{F}}$ can be subdivided in an upper part

$$\underline{\mathbf{F}}_{\mathrm{rel}} \in \mathbb{C}^{Z \times N} \tag{3.57}$$

$$\mathbf{I}^{N \times N} = \underline{\mathbf{F}} \in \mathbb{C}^{Q \times N} \cdot \boldsymbol{\Lambda} \in \mathbb{R}_{\geq 0}^{Z \times Q} \cdot \underline{\mathbf{G}} \in \mathbb{C}^{N \times Z}$$

$\underline{\mathbf{F}} \in \mathbb{C}^{Q \times N}$

$\underline{\mathbf{F}}_{\text{rel}} \in \mathbb{C}^{Z \times N}$

$\underline{\mathbf{F}}_{\text{irrel}} \in \mathbb{C}^{(Q-Z) \times N}$

$\boldsymbol{\Lambda} \in \mathbb{R}_{\geq 0}^{Z \times Q}$

$\boldsymbol{\Lambda} \in \mathbb{R}_{\geq 0}^{Z \times Z}$

$\boldsymbol{\Lambda}_{\text{irrel}} \in \mathbf{0}^{Z \times (Q-Z)}$

$\underline{\mathbf{G}} \in \mathbb{C}^{N \times Z}$

a)
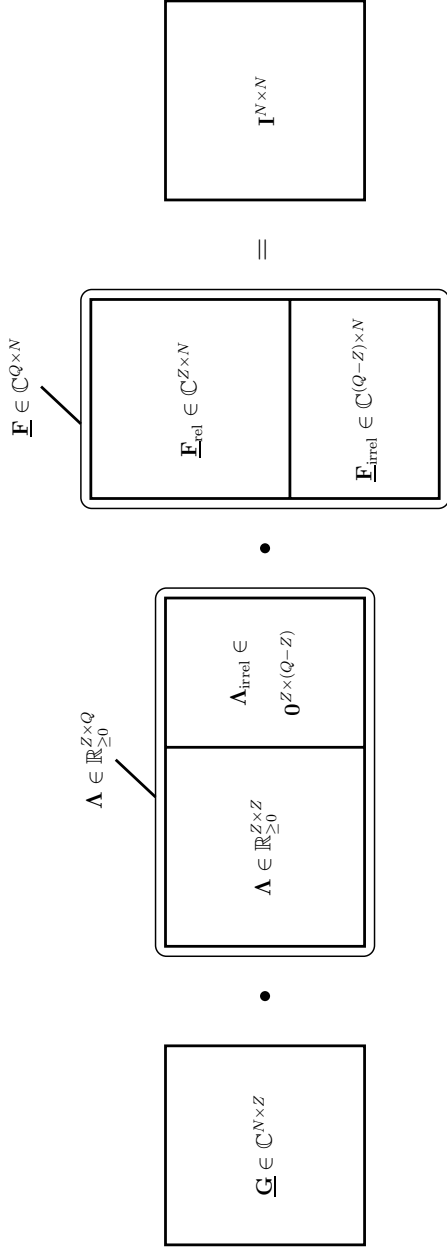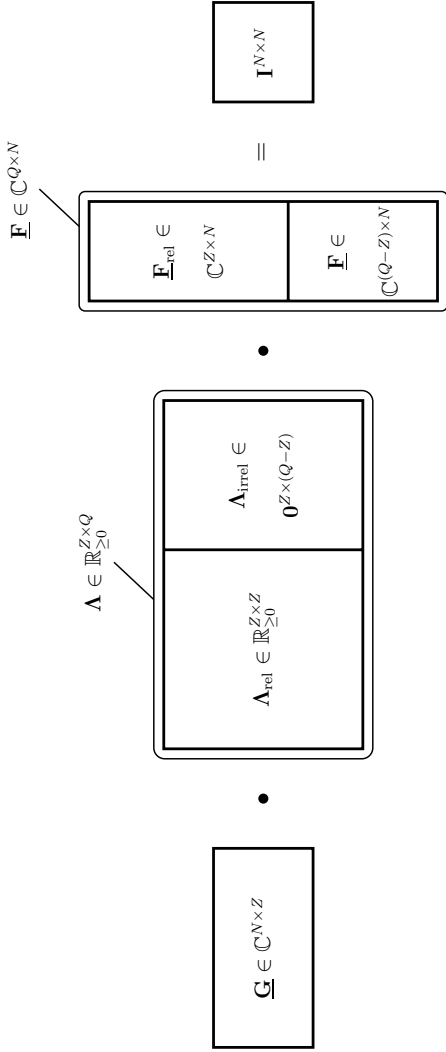
Fig. 3.4. Visualization of the product $\underline{\mathbf{G}}\boldsymbol{\Lambda}\underline{\mathbf{F}}$ of (3.48) for the case of a wide channel matrix $\underline{\mathbf{H}}$
a) full system load ($N = Z$)
b) partial system load ($N < Z$)

and a lower part

$$\underline{\mathbf{F}}_{\mathrm{irrel}} \in \mathbb{C}^{(Q-Z) \times N}, \tag{3.58}$$

which we term relevant and irrelevant partial core modulator matrices, respectively. With these matrices we can write

$$\underline{\mathbf{F}} = \left(\begin{array}{c} \underline{\mathbf{F}}_{\mathrm{rel}} \\ \underline{\mathbf{F}}_{\mathrm{irrel}} \end{array} \right) \in \mathbb{C}^{Q \times N}. \tag{3.59}$$

A corresponding subdivision of $\mathbf{\Lambda}$ yields

$$\mathbf{\Lambda}_{\mathrm{rel}} = \left(\begin{array}{ccc} \lambda_1 & \cdots & 0 \\ \vdots & \ddots & \vdots \\ 0 & \cdots & \lambda_Z \end{array} \right) \in \mathbb{C}^{Z \times Z}, \tag{3.60}$$

$$\mathbf{\Lambda}_{\mathrm{irrel}} = \mathbf{0}^{Z \times (Q-Z)} \tag{3.61}$$

and

$$\mathbf{\Lambda} = (\mathbf{\Lambda}_{\mathrm{rel}}, \mathbf{\Lambda}_{\mathrm{irrel}}) . \tag{3.62}$$

In the case $Z > Q$ of a wide channel matrix $\underline{\mathbf{H}}$ the entire core demodulator matrix can be considered relevant, and we can write

$$\underline{\mathbf{G}}_{\mathrm{rel}} = \underline{\mathbf{G}}. \tag{3.63}$$

Then, by a similar argument as in the case of a high channel matrix, we obtain again (3.54).

3.4.3 Required average transmit energy of TxZF

The numerically determined PDFs $p_{T_s}(T_S)$ of the required transmit energy of TxZF for the case of the ensemble of 4×4 matrices of the type $\underline{\mathbf{H}}_{\mathrm{fair}}$ and $\underline{\mathbf{H}}_{\mathrm{unfair}}$ are given by the Figs. 3.5 a and b, respectively. However, the derivation of a closed form expression of $p_{T_s}(T_S)$ is not applicable, which will be shortly discussed in Appendix A.2. As can be seen by the Fig. 3.5, in both cases, $p_{T_s}(T_S)$ is a long tailed distribution. Hence, the ratio among peak and average energies of T_S tends to infinity, which is not acceptable for realistic applications. As already mentioned in Subsection 1.4.2, the resulting snapshot specific energy T_S strongly depends on the realization of the channel $\underline{\mathbf{H}}$, such that in ill conditioned channels large values of T_S result. The occurrence of such ill conditioned channels was also mentioned in [HPS05a], where as a possible counter measure, regularization was proposed to upper bound T_S, which otherwise could assume infinity. In this thesis, another counter

a)

b)

Fig. 3.5. PDF $p_{T_s}(T_s)$ of T_s of the required transmit energy T_s in the case of TxZF

       a) fair channel

       b) unfair channel

measure will be proposed in Section 3.5, where a criterion for eliminating certain channel realizations from further consideration will be introduced, based on the SVD of the channel matrices $\underline{\mathbf{H}}$, such that ill conditioned channels can be a priori omitted.
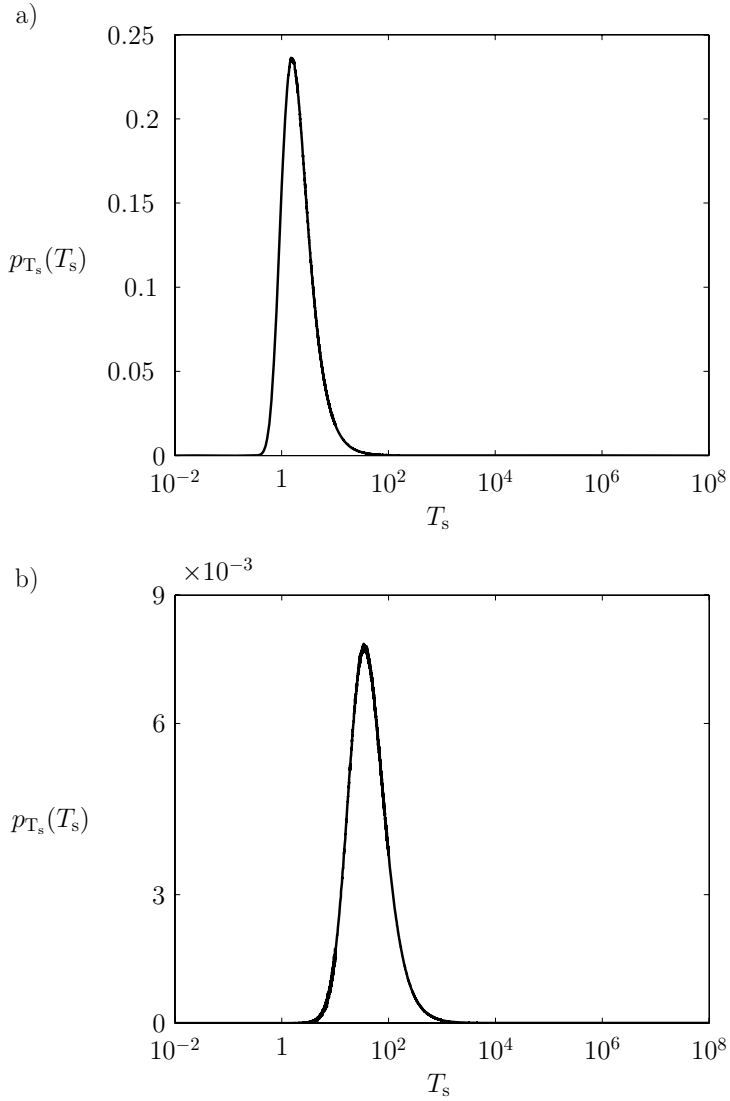
In the remainder of this subsection we will ask and partially answer the question, if statements on the required transmit energy of TxZF can be made based solely on the knowledge of the singular values λ_g, $g = 1 \ldots G$, of the prevailing channel matrix $\underline{\mathbf{H}}$. If in such an analysis we can assume that the singular values λ_g of a stationary channel are approximately invariant so that they can be approximated by their averages $\overline{\lambda}_g$ - see the considerations at the end of Section 3.2 - then the answers to be hopefully obtained in this subsection would apply to the whole ensemble of channel snapshots of a certain stationary channel type as for instance the fair and unfair channels introduced earlier. As a topic of future research, the implications of such an approximation λ_g by $\overline{\lambda}_g$ could be studied in detail.

We assume that (1.43) and (3.27) hold for $\underline{\mathbf{d}}^{(r)}$ and for the matrices $\underline{\mathbf{D}}$ and $\underline{\mathbf{G}}$, respectively. Under consideration of (3.36) and (3.26) the average required transmit energy of (1.44) can be written as

$$
\begin{aligned}
T &= \tfrac{1}{2}\sigma_{\mathrm{d}}^2 \cdot \mathrm{trace}\left\{ \left[\underline{\mathbf{D}}\,\underline{\mathbf{H}}\left(\underline{\mathbf{D}}\,\underline{\mathbf{H}}\right)^{\mathrm{H}}\right]^{-1}\right\} = \tfrac{1}{2}\sigma_{\mathrm{d}}^2 \cdot \mathrm{trace}\left\{ \left[\underline{\mathbf{G}}\,\boldsymbol{\Lambda}\underline{\mathbf{V}}^{\mathrm{H}}\left(\underline{\mathbf{G}}\,\boldsymbol{\Lambda}\underline{\mathbf{V}}^{\mathrm{H}}\right)^{\mathrm{H}}\right]^{-1}\right\} \\
&= \tfrac{1}{2}\sigma_{\mathrm{d}}^2 \cdot \mathrm{trace}\left\{ \left[\underline{\mathbf{G}}\,\boldsymbol{\Lambda}\boldsymbol{\Lambda}^{\mathrm{H}}\underline{\mathbf{G}}^{\mathrm{H}}\right]^{-1}\right\} = \tfrac{1}{2}\sigma_{\mathrm{d}}^2 \cdot \mathrm{trace}\left\{ \left(\underline{\mathbf{G}}^{\mathrm{H}}\right)^{-1}\boldsymbol{\Lambda}\boldsymbol{\Lambda}^{\mathrm{H}}\underline{\mathbf{G}}^{-1}\right\}.
\end{aligned}
\tag{3.64}
$$

We first consider the case of a wide channel matrix $\underline{\mathbf{H}}$, that is $Z < Q$ and $G = Z$. For full system load , see (3.54), $\underline{\mathbf{D}}$ and $\underline{\mathbf{G}}$ are square matrices of dimensions $N \times N$, see Fig. 3.4 a, and we obtain from (3.64)

$$
T = \frac{1}{2}\sigma_{\mathrm{d}}^2 \cdot \mathrm{trace}\left\{ \boldsymbol{\Lambda}\boldsymbol{\Lambda}^{\mathrm{H}}\underbrace{\underline{\mathbf{G}}^{-1}\left(\underline{\mathbf{G}}^{\mathrm{H}}\right)^{-1}}_{\mathbf{I}^{N \times N}}\right\} = \frac{1}{2}\sigma_{\mathrm{d}}^2 \cdot \sum_{g=1}^{G}\frac{1}{\lambda_g^2}.
\tag{3.65}
$$

According to (3.65), for a wide channel matrix $\underline{\mathbf{H}}$, for full system load and a for given σ_{d}^2, T is only determined by the G singular values λ_g, $g = 1 \ldots G$ of $\underline{\mathbf{H}}$, and, in particular, does not depend on the choice of the fixed matrix $\underline{\mathbf{D}}$, and, if $\underline{\mathbf{H}}$ varies under keeping its singular values λ_g, on the variant matrices $\underline{\mathbf{U}}$, $\underline{\mathbf{V}}$ and $\underline{\mathbf{G}}$ of (3.3) and (3.27), respectively. The larger the singular values λ_g, $g = 1 \ldots G$, the smaller T.

We now remain with a wide channel matrix $\underline{\mathbf{H}}$, and consider the case of partial system load, see (3.56). Then, the fixed matrix $\underline{\mathbf{D}}$ and the variant matrix $\underline{\mathbf{G}}$ are no longer square, but wide with the dimensions $N \times Z$. Of the infinitely many appearances the matrix $\underline{\mathbf{G}}$ can take on if $\underline{\mathbf{H}}$ varies, two extreme ones are depicted in Figs. 3.6 a and b, where we

choose the parameters

$$Z = 3, \, Q = 4, \, N = 2 \,. \tag{3.66}$$

In the case of Fig. 3.6 a the N largest singular values, namely λ_n, $n = 1 \ldots N$, are utilized for transmission, and from (3.64) follows the minimum possible average required transmit energy

$$T_1 = \frac{1}{2}\sigma_{\mathrm{d}}^2 \sum_{g=1}^{N} \frac{1}{\lambda_g^2} = \frac{1}{2}\sigma_{\mathrm{d}}^2 \left(\frac{1}{\lambda_1^2} + \frac{1}{\lambda_2^2} \right) \,. \tag{3.67}$$

In the case of Fig. 3.6 b, the N smallest singular values, namely $\lambda_{G-(N-1)} \ldots \lambda_G$, are utilized for transmission, and now the average required transmit energy becomes

$$T_2 = \frac{1}{2}\sigma_{\mathrm{d}}^2 \sum_{g=G-(N-1)}^{G} \frac{1}{\lambda_g^2} = \frac{1}{2}\sigma_{\mathrm{d}}^2 \left(\frac{1}{\lambda_2^2} + \frac{1}{\lambda_3^2} \right) \,. \tag{3.68}$$

If the channel varies in a stationary manner under keeping its singular values λ_g, then the minimum average required transmit energy T of each channel snapshot lies within the limits T_1 of (3.67) and T_2 of (3.68), that is

$$T_1 \leq T \leq T_2. \tag{3.69}$$

We now come to the case of a high channel matrix $\underline{\mathbf{H}}$, that is $Z > Q$ and $G = Q$, and consider first full system load as characterized by (3.45). In this case the two matrices $\underline{\mathbf{D}}$ and $\underline{\mathbf{G}}$ are wide with the dimensions $Z \times N$, and, in contrast to the case of a wide channel matrix $\underline{\mathbf{H}}$ and full system load, the average required transmit energy T depends on the
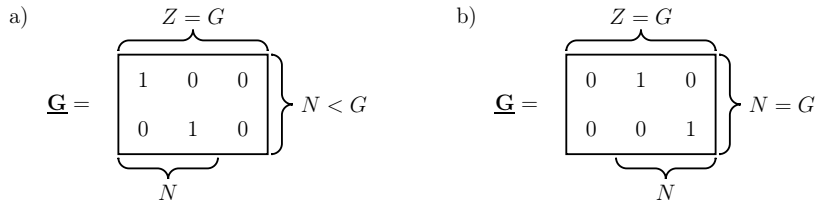
Fig. 3.6. Wide channel matrix $\underline{\mathbf{H}}$. Two extreme appearances of the matrix $\underline{\mathbf{G}}$ for partial system load with $Z = 3$, $Q = 4$, $N = 2$ and $G = 3$ yielding
a) $T = T_1$ of (3.62)
b) $T = T_2$ of (3.63)

appearance of $\underline{\mathbf{G}}$. We consider two extreme cases, see Figs. 3.7 a and b, where we choose

$$Z = 4,\, Q = 3,\, N = 3\,. \tag{3.70}$$

In the case of Fig. 3.7 a all G equal to three singular values are employed for transmission, and the average required transmit energy T attains its minimum possible value

$$T = T_1 = \frac{1}{2}\sigma_{\mathrm{d}}^2 \sum_{g=1}^{G} \frac{1}{\lambda_g^2} = \frac{1}{2}\sigma_{\mathrm{d}}^2 \left(\frac{1}{\lambda_1^2} + \frac{1}{\lambda_2^2} + \frac{1}{\lambda_3^2} \right)\,. \tag{3.71}$$

In the case of Fig. 3.7 b only the singular values λ_2 and λ_3 are utilized for transmission, and the required transmit energy

$$T = T_2 = \frac{1}{2}\sigma_{\mathrm{d}}^2 \left(\frac{1}{\lambda_2^2} + \frac{1}{\lambda_3^2} + \frac{1}{0^2} \right) \to \infty \tag{3.72}$$

grows beyond all limits. In the case of partial system load, see (3.46), the average required transmit energy cannot be below $\frac{1}{2}\sigma_{\mathrm{d}}^2 \sum_{g=1}^{N} \frac{1}{\lambda_g^2}$ and may, depending on the channel snapshot, that is on the appearance of $\underline{\mathbf{G}}$, again grow beyond all limits.

a)

$$\underline{\mathbf{G}} = \begin{matrix} & \overbrace{\qquad\qquad}^{Z > G} & \\ \left[\begin{matrix} 1 & 0 & 0 & 0 \\ 0 & 1 & 0 & 0 \\ 0 & 0 & 1 & 0 \end{matrix}\right] & \left.\vphantom{\begin{matrix}1\\1\\1\end{matrix}}\right\} N = G \\ \underbrace{\qquad\qquad}_{N} & \end{matrix}$$

b)

$$\underline{\mathbf{G}} = \begin{matrix} & \overbrace{\qquad\qquad}^{Z > G} & \\ \left[\begin{matrix} 0 & 1 & 0 & 0 \\ 0 & 0 & 1 & 0 \\ 0 & 0 & 0 & 1 \end{matrix}\right] & \left.\vphantom{\begin{matrix}1\\1\\1\end{matrix}}\right\} N = G \\ \underbrace{\qquad\qquad}_{N} & \end{matrix}$$
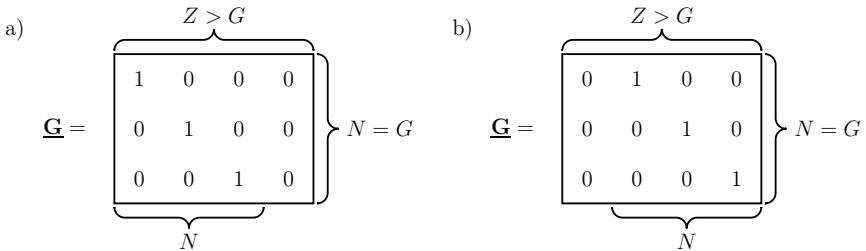
Fig. 3.7. High channel matrix $\underline{\mathbf{H}}$. Two extreme appearances of the matrix $\underline{\mathbf{G}}$ for full system load with $Z = 4$, $Q = 3$, $N = 3$ and $G = 3$ yielding
a) $T = T_1$ of (3.66)
b) $T = T_2 \to \infty$, see (3.67)

To conclude this subsection, we now denominate by means of simulations that the required energy T indeed lies within the limits T_1 and T_2 introduced in (3.67), (3.68), (3.71) and (3.72), respectively. We set σ_{d}^2 equal to 0.5.

We first consider the case of a wide channel matrix $\underline{\mathbf{H}}$ and assume the parameters given in (3.66). Further, we set out from the three singular values

$$\lambda_1 = 3.03, \quad \lambda_2 = 1.67, \quad \lambda_3 = 0.81\,. \tag{3.73}$$

Under these premises we obtain from (3.67) and (3.68) the limits

$$T_1 = 0.117 \tag{3.74}$$

and

$$T_2 = 0.470, \tag{3.75}$$

respectively. We now determine the average required transmit energy T of (3.64) for a large set of randomly chosen core demodulator matrices $\underline{\mathbf{G}}$ and depict the PDF $p_\mathrm{T}(T)$ of T in Fig. 3.8 a. Obviously, all occurring values T lie within the limits T_1 and T_2 of (3.67) and (3.68), respectively.

Next, we consider the case of a high channel matrix $\underline{\mathbf{H}}$ and assume the parameters listed in (3.70). We further choose the three singular values

$$\lambda_1 = 2.42, \quad \lambda_2 = 1.82, \quad \lambda_3 = 1.14\,. \tag{3.76}$$

Then, (3.68) yields the lower limit

$$T_1 = 0.310 \tag{3.77}$$

of T of (3.64). In this case the PDF $p_\mathrm{T}(T)$ of Fig. 3.8 b is obtained, which shows that T is never below T_1 of (3.74) and may assume very large values, what would be in accordance with (3.72).

3.5   Possible criterion for eliminating certain channel realizations from further consideration

In Subsections 2.3.3 and 3.4.3 we spoke about the elimination off ill conditioned channels when performing the averages (2.44) and (2.34). A suitable elimination criterion could be based on the SVD of the realizations of $\underline{\mathbf{H}}$. In order to formulate such a criterion in a way easy to understand, we assume square channel matrices

$$\underline{\mathbf{H}} \in \mathbb{C}^{G \times G} \tag{3.78}$$

and full system load. Then the denominator matrix, which fulfills (2.28). However, the idea behind our criterion could be generalized also to cases where these assumptions are not fulfilled.

Now, in order to judge whether a channel realization characterized by its channel matrix $\underline{\mathbf{H}}$ should be eliminated, we determine the G singular values λ_g, $g = 1 \ldots G$, of

a)

$p_{\mathrm{T_s}}(T_s)$

b)
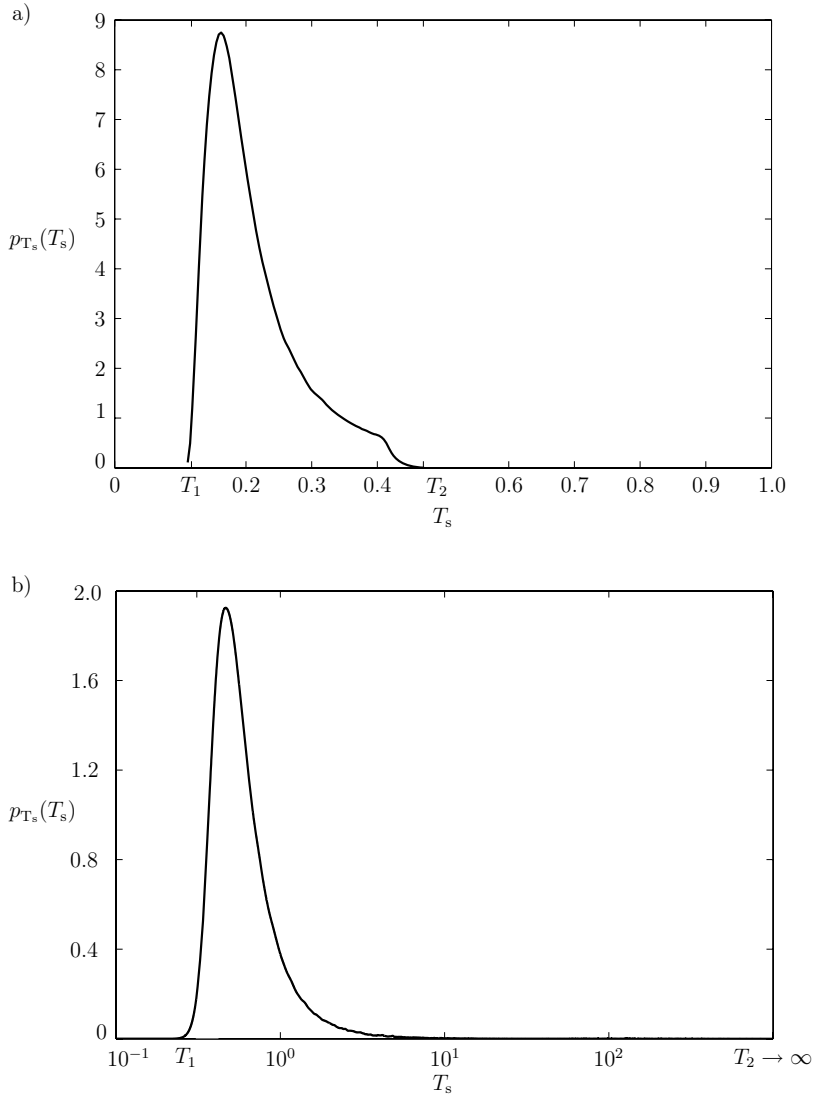
$p_{\mathrm{T_s}}(T_s)$

Fig. 3.8. PDF $p_{\mathrm{T_s}}(T_s)$ of T_s of a core system with

a) wide channel matrix

b) high channel matrix

said channel matrix and, by using (3.65), the required transmit energy

$$T(\underline{\mathbf{H}}) = \frac{1}{2}\sigma_{\mathrm{d}}^2 \sum_{g=1}^{G} \frac{1}{\lambda_g^2}. \tag{3.79}$$

We then compose $T(\underline{\mathbf{H}})$ of (3.79) with the average required transmit energy

$$\overline{T} = \frac{1}{2}\sigma_d^2 \sum_{g=1}^{G} \frac{1}{\overline{\lambda}_g^2}. \tag{3.80}$$

of the whole stationary ensemble of channel realizations which results from (3.65), if we substitute for the singular values λ_g their averages $\overline{\lambda}_g$. For said comparison we form

$$\upsilon = T(\underline{\mathbf{H}})/\overline{T}. \tag{3.81}$$

Whenever υ becomes equal to or larger than a threshold value $\upsilon_{\mathrm{threshold}}$, then the pertaining channel realization is eliminated, that is the elimination criterion reads

$$\text{eleminate realization } \underline{\mathbf{H}} \text{ if } \upsilon \geq \upsilon_{\mathrm{threshold}}. \tag{3.82}$$

$\upsilon_{\mathrm{threshold}}$ in (3.82) is a system parameter which should be set in the framework of system design. The elimination of channel realization leads to system outages, the probability of which is given by

$$P_{\mathrm{out}} = \mathrm{Prob}(\upsilon \geq \upsilon_{\mathrm{threshold}}). \tag{3.83}$$

The larger $\upsilon_{\mathrm{threshold}}$, the larger the peak values of the required transmit energy, and the smaller the outage probability P_{out} of (3.83). In this thesis we set

$$\upsilon_{\mathrm{threshold}} = 10. \tag{3.84}$$

3.6   Résumé

The structure and the quantitative entries of the channel matrix are the decisive factors when it comes to determining the transmission potential of a radio transmission system. This potential is determined by the singular vectors of the channel matrix and their relations to the transmitter and receiver properties, and by the singular values of this matrix. In particular, based on said singular values some useful and generally valid performance limits of RO transmission systems can be formulated.

Chapter 4
Transmit energy minimization by selectable data representation

4.1 Preliminary remarks

The implementation of the concept of transmit energy minimization by selectable data representation as briefly outlined in Section 2.4 comprises the two following steps:

1. Determination of the R data specific representative sets $\mathbb{G}_{\mathfrak{a}^{(r)}}$, $r = 1 \ldots R$, of (2.11), which permit the selectability in question when choosing the vectors $\underline{\mathbf{d}}^{(r)}$ of (1.45).

2. Determination of the optimum representative vectors $\underline{\mathbf{d}}_{\mathrm{opt}}^{(r)}$ of (2.41) which have the effect that the transmit energies $T^{(r)}$ attain their minimum values $T_{\min}^{(r)}$ of (2.43).

In order to arrive at the overall least possible transmit energies $T^{(r)}$, both these steps should be performed in a joint manner. This would mean that the transmit energy minimization should be performed for a comprehensive ensemble of data specific representative sets $\mathbb{G}_{\mathfrak{a}^{(r)}}$, $r = 1 \ldots R$, and then the one set yielding the smallest transmit energies $T^{(r)}$, $r = 1 \ldots R$, should be chosen. However, such a joint approach would be prohibitively complex, not to speak of a still missing theory how one should concretely proceed. Therefore, in this thesis we adopt the following - at the moment - more feasible successive approach: We first choose the R data specific representative sets $\mathbb{G}_{\mathfrak{a}^{(r)}}$, $r = 1 \ldots R$, of (2.11) in a 'reasonable' manner, see Section 2.1, and then, based on the chosen sets, determine the representative vectors $\underline{\mathbf{d}}_{\mathrm{opt}}^{(r)}$ of (2.41). By 'reasonable' we mean in this context that the data specific representative sets, with a view to easy implementation, should show certain regularities and be related to well-established modulation schemes as for instance 4-PSK. Following this rationale, for the choice of the data specific representative sets $\mathbb{G}_{\mathfrak{a}^{(r)}}$, $r = 1 \ldots R$, we proposed in Section 2.1 the Approaches I to III, from which, as mentioned earlier, the former two will be further considered in this work.

Once the first step, namely the choice of the data specific representative sets $\mathbb{G}_{\mathfrak{a}^{(r)}}$, $r = 1 \ldots R$, of (2.11) is done, the remaining problem is how to find for a given realization $\mathfrak{a}^{(r)}$ of $\mathfrak{a}$ the optimum representative vector $\underline{\mathbf{d}}_{\mathrm{opt}}^{(r)}$ of (2.41) and the pertaining transmit vector $\underline{\mathbf{t}}_{\mathrm{opt}}^{(r)}$ of (2.42). With (2.12) and (1.18) this problem can be formulated as [KHB07, KB07a]

$$
\begin{aligned}
\underline{\mathbf{t}}_{\mathrm{opt}}^{(r)} &= \arg \left\{ \min_{\underline{\mathbf{t}}^{(r)} \in \mathbb{C}^{Q \times 1}} \left(\underline{\mathbf{t}}^{(r)\mathrm{H}} \underline{\mathbf{t}}^{(r)} \right) \right\} \\
\text{s.t. } \underline{\mathbf{d}}^{(r)} &= \underline{\mathbf{D}}\,\underline{\mathbf{H}}\,\underline{\mathbf{t}}^{(r)} \in \mathbb{G}_{\mathfrak{a}^{(r)}} \subset \mathbb{C}^N .
\end{aligned}
\tag{4.1}
$$

The determination of $\underline{\mathbf{t}}_{\text{opt}}^{(r)}$ from (4.1) is a non-trivial task. The brute force approach would consist in exhaustively searching (Exhaustive Search, ES) through all transmit vectors $\underline{\mathbf{t}}^{(r)}$ yielding in the receiver a $\underline{\mathbf{d}}^{(r)} \in \mathbb{G}_{\mathbf{a}^{(r)}}$, and then selecting from these transmit vectors the one which yields minimum $T^{(r)}$ of (1.40). However, such an exhaustive and, therefore, non-systematic search would be very expensive, particularly in the case of large values R and of sets $\mathbb{G}_{\mathbf{a}^{(r)}}$, which allow rich selections of $\underline{\mathbf{d}}^{(r)}$. In the case of Approach I, such a rich selection would be enabled if L of (2.9) would be large. In Approach I L is the dimension of the selection space and, therefore, a measure of the complexity of ES. When performing ES, TxZF has to be executed L times.

In the case of Approach I the author is not aware of a systematic approach to exactly determining $\underline{\mathbf{t}}_{\text{opt}}^{(r)}$ by solving (4.1). In the way of such an approach stands the fact that the representative sets $\mathbb{G}_{\mathbf{a}^{(r)}}$ are multiply connected. In what follows we therefore adopt an approximate, but systematic and hence rather low-cost stepwise solution of (4.1), which is based on Transmit Non-linear Zero Forcing (TxNZF) as described in [MWQ04]. We further compare our results generated by TxNZF with those obtained by ES. The attribute non-linear in TxNZF expresses the fact that this scheme is non-linear on the transmit side, see Section 1.5.

In the case of Approach II we develop a systematic solution of (4.1) based on constrained optimization through Sequential Quadratic Programming (SQP) [Sch85, Pow83, Big75]. As already mentioned in Section 1.6, we introduce for this approach the acronym MESP.

4.2   Approach I to selectable data representation

4.2.1   Determination of the optimum transmit vectors

As already stated earlier, in the case of Approach I in total L equal to P^N different vectors $\underline{\mathbf{t}}^{(r)}$ exist for transmitting the realization $\mathbf{a}^{(r)}$ of the data $\mathbf{a}$, see (2.9). As mentioned in Section 4.1, in order to determine $\underline{\mathbf{t}}_{\text{opt}}^{(r)}$ by exactly solving (4.1), each of these vectors should be determined and probed. With the N normalized component-specific transmit vectors $\underline{\mathbf{t}}_{0,n}^{(r)}$ of (1.14), the coefficients $m_n^{(r)}$ of (2.4) and the representatives $\underline{v}_{m,p}$ of (2.6), the problem of solving (4.1) can in the case of Approach I be expressed as

$$\underline{\mathbf{t}}_{\text{opt}}^{(r)} = \sum_{n=1}^{N} \underline{\mathbf{t}}_{0,n}^{(r)} \underline{v}_{m_n^{(r)},p_n}, \text{ where } (p_1 \ldots p_n) = \arg\left\{ \min_{p_1' \ldots p_N' \in \{1 \ldots P\}} \left| \sum_{n=1}^{N} \underline{\mathbf{t}}_{0,n}^{(r)} \underline{v}_{m_n^{(r)},p_n'} \right| \right\}. \quad (4.2)$$

We are now going to describe TxNZF. In doing so we refer the reader also to [WMZ04, QMBW04, MWQ04]. The basics of TxNZF were first published in [MWQ04]. In the

present thesis it will be further elaborated, and later its performance will be illustrated by simulations. In the scheme TxNZF, for the transmission of each of the N components $\underline{d}_n^{(r)}$ of $\underline{\mathbf{d}}^{(r)}$ of (1.45) a component-specific transmit vector $\underline{\mathbf{t}}_n^{(r)}$ is designed in a stepwise manner, where we start with $\underline{\mathbf{t}}_1^{(r)}$ and conclude with $\underline{\mathbf{t}}_N^{(r)}$. The finally transmitted vector is then

$$\underline{\mathbf{t}}^{(r)} = \sum_{n=1}^{N} \underline{\mathbf{t}}_n^{(r)}. \tag{4.3}$$

In contrast to the N component-specific non-interfering transmit-vectors mentioned in Subsection 1.4.1, the N vectors $\underline{\mathbf{t}}_n^{(r)}$ used in TxNZF may cause interference on the elements $\underline{d}_{n'}^{(r)}$, $n' > n$, of $\underline{\mathbf{d}}^{(r)}$. In detail, these vectors are designed by Transmit Partial Zero Forcing (TxPZF) [WMZ04] in such a way that by $\underline{\mathbf{t}}_n^{(r)}$

- no interference is caused in the complex planes of the $n-1$ prior components $\underline{d}_1^{(r)} \ldots \underline{d}_{n-1}^{(r)}$,

- a desired complex value $\underline{\Delta}_n$ to be determined below is caused in the complex plane of the component $\underline{d}_n^{(r)}$ of $\underline{\mathbf{d}}^{(r)}$, and

- interference is generated in the complex planes of the $N-n$ components $\underline{d}_{n+1}^{(r)} \ldots \underline{d}_N^{(r)}$ of $\underline{\mathbf{d}}^{(r)}$.

Concerning the concept TxPZF, we introduce the N selection matrices

$$\mathbf{S}_n = \left(\mathbf{I}^{n \times n}, \ \mathbf{O}^{(Z-n) \times n} \right) = \overbrace{\left(\begin{array}{ccccc} 1 & \cdots & 0 & \cdots & 0 \\ \vdots & \ddots & \vdots & \vdots & \vdots \\ 0 & \cdots & 1 & \cdots & 0 \end{array} \right)}^{Z} \left. \rule{0pt}{20pt} \right\} n, \ n = 1 \ldots N. \tag{4.4}$$

Then, we form with the demodulator matrix $\underline{\mathbf{D}}$ of (1.15) the N partial demodulator matrices

$$\underline{\mathbf{D}}_n = \mathbf{S}_n \underline{\mathbf{D}}, \ n = 1 \ldots N, \tag{4.5}$$

which consist of the first n rows of $\underline{\mathbf{D}}$. In order to perform TxPZF, we construct with the matrices $\underline{\mathbf{D}}_n$ of (4.5) the partial modulator matrices

$$\underline{\mathbf{M}}_n = \left(\underline{\mathbf{D}}_n \underline{\mathbf{H}} \right)^{\mathrm{H}} \left[\underline{\mathbf{D}}_n \underline{\mathbf{H}} \left(\underline{\mathbf{D}}_n \underline{\mathbf{H}} \right)^{\mathrm{H}} \right]^{-1}. \tag{4.6}$$

Then, with column n of $\underline{\mathbf{M}}_n$ of (4.6), which we designate as $[\underline{\mathbf{M}}_n]_{(n)}$, and the complex value $\underline{\Delta}_n$ introduced above the component-specific transmit vector for the nth component

of $\underline{\mathbf{d}}^{(r)}$ becomes

$$\underline{\mathbf{t}}_n^{(r)} = [\underline{\mathbf{M}}_n]_{(n)} \underline{\Delta}_n \,. \tag{4.7}$$

$\underline{\mathbf{t}}_n^{(r)}$ of (4.7) causes in the complex planes of the components $\underline{d}_{n+1}^{(r)} \ldots \underline{d}_N^{(r)}$ of $\underline{\mathbf{d}}^{(r)}$ the interference values $\underline{i}_{n+1}^{(r)} \ldots \underline{i}_N^{(r)}$. With $[\underline{\mathbf{D}}]^{(n')}$ designating the row n' of the matrix $\underline{\mathbf{D}}$, and with $\underline{\mathbf{t}}_n^{(r)}$ of (4.7) we obtain

$$\underline{i}_{n'}^{(r)} = [\underline{\mathbf{D}}]^{(n')} \underline{\mathbf{H}} \underline{\mathbf{t}}_n^{(r)}, \, n' = n + 1 \ldots N \,. \tag{4.8}$$

Up to now nothing was said about how the complex values $\underline{\Delta}_n$ introduced above should be chosen. This issue will be considered now. We choose $\underline{\Delta}_n$ in such a way that the total interference value

$$\underline{i}_n = \sum_{n'=1}^{n-1} \underline{i}_{n'}^{(r)} = [\underline{\mathbf{D}}]^{(n)} \underline{\mathbf{H}} \sum_{n'=1}^{n-1} \underline{\mathbf{t}}_{n'}^{(r)} \tag{4.9}$$

occurring in the complex plane of the nth component of $\underline{\mathbf{d}}^{(r)}$ and resulting from the interferences determined by (4.8) is compensated by $\underline{\Delta}_n$ in the sense that the next allowed representative value $\underline{v}_{m_{n,p}^{(r)}}$ is reached. With (2.4) this procedure can be formulated as follows [WMZ04]:

$$\underline{d}_n^{(r)} = \underline{v}_{m_{n,p}^{(r)}} \in \mathbb{V}_{m_n^{(r)}}, \, \underline{\Delta}_n = \underline{v}_{m_{n,p}^{(r)}} - \underline{i}_n, \, p = \arg\left\{ \min_{p'=1\ldots P} \left| \underline{v}_{m_{n,p'}^{(r)}} - \underline{i}_n \right| \right\}. \tag{4.10}$$

TxNZF as displayed above can be visualized by the Nassi-Shneiderman diagram of Fig. 4.1.

In the case of ES, TxZF has to be performed P^N times. In the case of TxNZF, we have to execute TxPZF only N times. This shows the dramatic complexity reduction of TxNZF as compared to ES.

As explained above, when considering the nth component $\underline{d}_n^{(r)}$ of $\underline{\mathbf{d}}^{(r)}$ in TxNZF, this is done in such a way that no interference is caused in the complex planes of the previous components $\underline{d}_1^{(r)} \ldots \underline{d}_{n-1}^{(r)}$, but arbitrary interferences are admitted in the complex planes of the components $\underline{d}_{n+1}^{(r)} \ldots \underline{d}_N^{(r)}$. As the crux of TxNZF, the occurring interferences $\underline{i}_n$ of (4.9) are not combated as in conventional TxZF. Rather, they are exploited as useful and constructive contributions. This allows a significant reduction of the required transmit energy.

In TxNZF as described above, see also Fig. 4.1, the stepwise generation of the transmit vector $\underline{\mathbf{t}}^{(r)}$ of (4.3) follows the 'natural order' $n = 1 \ldots N$ of the N components $\underline{d}_n^{(r)}$ of $\underline{\mathbf{d}}^{(r)}$. However, there are indications [HMBZ06a, MWQ04, QMBW04, WMZ04] that the adopted order may have a strong impact on the reached minimum of the required transmit energy $T^{(r)}$, and that in particular said 'natural' order may be quite disadvanta-

$$\begin{array}{|l|}
\hline
\text{for } n = 1 \ldots N \\
\hline
\end{array}$$

for $n = 1 \ldots N$

Y	$n = 1$	N
$\underline{i}_n = 0$	$\underline{i}_n = [\underline{\mathbf{D}}]^{(n)}\underline{\mathbf{H}} \sum\limits_{n'=1}^{n-1} \underline{\mathbf{t}}_{n'}^{(r)}$	

calculation of $\underline{\Delta}_n$ depending on $\underline{i}_n$, see (4.9)

calculation of $\underline{\mathbf{t}}_n^{(r)}$ depending on $\underline{\Delta}_n$, see (4.6)

$$\underline{\mathbf{t}}^{(r)} = \sum_{n=1}^{N} \underline{\mathbf{t}}_n^{(r)}$$
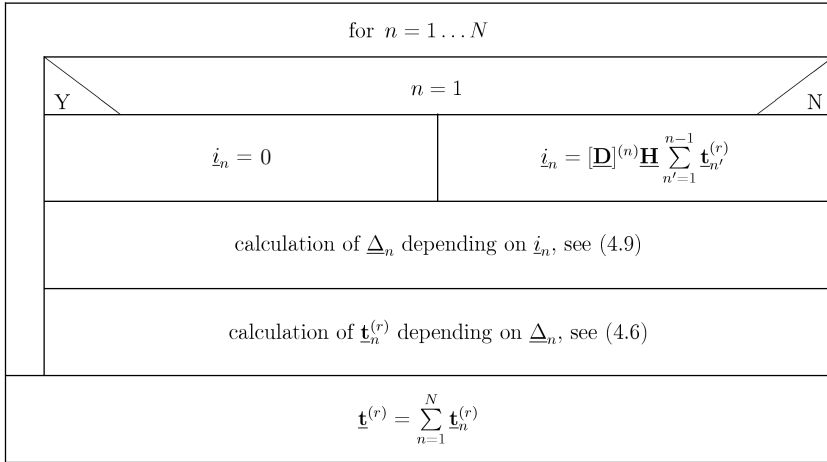
Fig. 4.1. Nassi-Shneiderman diagram describing TxNZF

geous. Following an argument on this issue in [MWQ04], it may be beneficial to order the components of $\underline{\mathbf{d}}^{(r)}$, when performing TxNZF, according to a measure which in some way represents the attenuation between the corresponding transmitter outputs and receiver outputs, where the components suffering the highest attenuation should be treated first. In this context in [HMBZ06a] channel attenuations resulting from the elements of the channel matrix $\underline{\mathbf{H}}$ were introduced. However, these channel attenuations are only suitable attenuation measures if the demodulator matrix $\underline{\mathbf{D}}$ has a diagonal or block diagonal structure. The author proposes to extend and generalize the concept of attenuations by treating the components of $\underline{\mathbf{d}}^{(r)}$ in the order of increasing values $\left|[\underline{\mathbf{D}}\,\underline{\mathbf{H}}]_{(n)}\right|$. By doing so, the impact of both the channel and the demodulator on the attenuations is taken into account.

4.2.2 Illustration of TxNZF and Exhaustive Search (ES) by means of a single snapshot

In order to give an impression of TxNZF and ES we consider an example snapshot characterized as follows:

- Unfair channel matrix $\underline{\mathbf{H}}_{\text{unfair}}$ of (2.32) with the dimensions 4×4,

- unitary demodulator matrix

$$\underline{\mathbf{D}} = \mathbf{I}^{4 \times 4}, \tag{4.11}$$

- realization

$$m_1^{(r)} = 3,\ m_2^{(r)} = 1,\ m_3^{(r)} = 4,\ m_4^{(r)} = 2 \tag{4.12}$$

of the integer representative vector $\mathbf{m}^{(r)}$ of (2.5), from which, with the symbolism introduced in Section 2.1, results

$$\mathfrak{a}^{(r)} = (\ \bullet\ \text{✸}\ \blacksquare\ \blacklozenge\ ),\ \text{and} \tag{4.13}$$

- P equal to nine.

Concerning the attenuation criterion to be observed when performing TxNZF, see the last paragraph in Subsection 4.2.1, the order in which the elements of $\mathfrak{a}$ of (4.13) should be stepwise considered is $n = 2, 1, 3, 4$.

For said example snapshot we list for the two cases TxNZF and ES the obtained transmit vectors $\underline{\mathbf{t}}^{(r)}$ and the required transmit energies $T^{(r)}$ resulting from these vectors in Tables 4.1 and 4.2, respectively. For comparison we also include in these two tables results for conventional TxZF, to which Approach I degenerates if we set P in (2.6) equal to one. According to Table 4.1, the transmit vectors $\underline{\mathbf{t}}^{(r)}$ of the three schemes TxZF, TxNZF and ES clearly differ from each other. As listed in Table 4.2, the required transmit energies $T^{(r)}$ resulting from the transmit vectors $\underline{\mathbf{t}}^{(r)}$ of Table 4.1 decrease, if we go from TxZF over TxNZF to ES. The required transmit energies $T^{(r)}$ of TxNZF and ES are rather closely together, whereas both these energies differ significantly from the transmit energy required by TxZF. This is a manifestation of the benefit offered by selectable data representation.

$\underline{\mathbf{t}}^{(r)}$	TxZF ($P = 1$)	TxNZF ($P = 9$)	ES ($P = 9$)
$\underline{t}_1^{(r)}$	$-0.09 + \mathrm{j}5.89$	$1.19 + \mathrm{j}3.59$	$-2.11 + \mathrm{j}0.57$
$\underline{t}_2^{(r)}$	$-2.03 + \mathrm{j}1.11$	$-1.61 - \mathrm{j}0.83$	$-1.28 + \mathrm{j}0.49$
$\underline{t}_3^{(r)}$	$5.33 + \mathrm{j}0.51$	$4.12 + \mathrm{j}0.06$	$-0.01 + \mathrm{j}0.20$
$\underline{t}_4^{(r)}$	$3.53 + \mathrm{j}3.95$	$2.87 + \mathrm{j}2.79$	$-4.09 + \mathrm{j}3.79$

Table 4.1. Transmit vectors $\underline{\mathbf{t}}^{(r)}$ obtained for TxZF, TxNZF and ES

For the above example snapshot we now further illustrate the mechanism of TxNZF and ES. To this purpose we first show in Fig. 4.2 in the four complex planes of the four components of $\underline{\mathbf{d}}^{(r)}$, see (4.10), on which points these components land in the cases of TxNZF and ES. Then, we demonstrate in Fig. 4.3 how said landing points are made for in the stepwise procedure of TxNZF.

	TxZF $(P = 1)$	TxNZF $(P = 9)$	ES $(P = 9)$
$T^{(r)}$ $T^{(r)}/\,\mathrm{dB}$	48.44 16.9	25.30 14.0	18.92 12.8

Table 4.2. Transmit energies $T^{(r)}$ required for TxZF, TxNZF and ES

In Fig. 4.2 the landing points of TxNZF and ES, which comply with $\mathbf{a}^{(r)}$ of (4.13), are marked by squares or circles, respectively. From Fig. 4.2 we can conclude the following general tendency:

- The landing points of TxNZF and ES differ from each other.

- The distances of the landing points from the origin increase with increasing attenuation in the cases of TxNZF and ES.

We now consider Fig. 4.3. We again depict the landing points of TxNZF as already shown in Fig. 4.2 and additionally include the interference values $\underline{i}_n$, $n = 1 \ldots 4$, of (4.9) as well as the compensation values $\underline{\Delta}_n$, $n = 1 \ldots 4$, of (4.10). Fig. 4.3 shows how in each step of TxNZF the interference is componentwise exploited in such a way that the compensation energy $|\underline{\Delta}_n|^2$ is minimized. Hence, as a reasonable expectation, also the total required transmit energy should become quite low. However, in general such a componentwise minimization is inferior to the overall minimization behind ES; this explains the higher required transmit energy of TxNZF as compared to that of ES, see Table 4.2.

4.2.3   Statistical evaluation of TxZF, TxNZF and ES

After having illustrated TxNZF and ES in Subsection 4.2.2 by an example snapshot, we now aspire to evaluate the overall performance of TxNZF and ES. To this purpose we consider a large number of snapshots, each one characterized by a realization of the channel matrix $\underline{\mathbf{H}}$ and of the data $\mathbf{a}$. Concerning the channel matrix, we assume stationarity as
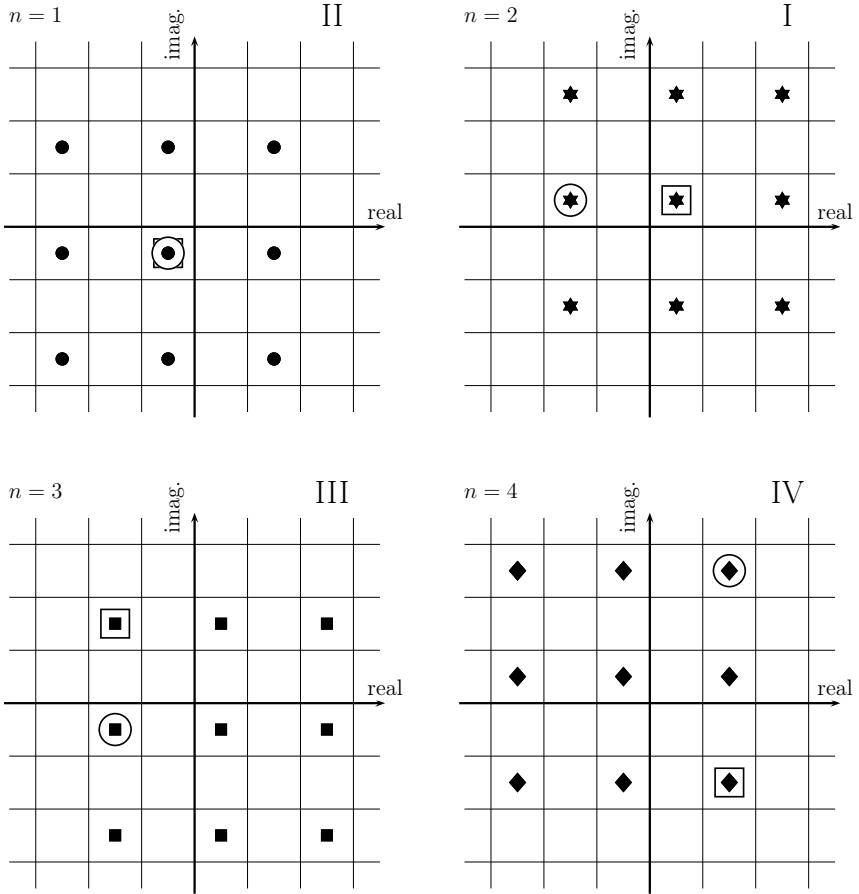
Fig. 4.2. Components $\underline{d}_n^{(r,l)}$ of $\underline{\mathbf{d}}^{(r,l)}$ of (1.45) obtained by performing TxNZF ($\square$) and ES ($\bigcirc$), $P = 9$;
the Roman numbers indicate the step numbers when performing TxNZF

$n = 1$

II

$\underline{d}_2^{(r,l)} = 0.5 + \mathrm{j}0.5$

$\underline{i}_2 = -0.48 + \mathrm{j}0.02$

imag.

real

$\underline{\Delta}_2$

$n = 2$

I

j

$\underline{i}_1 = 0$

imag.

real

1

$\underline{d}_1^{(r,l)} = -0.5 + \mathrm{j}0.5$

$\underline{\Delta}_1$

$n = 3$

III

$\underline{i}_3 = -3.11 + \mathrm{j}5.42$

imag.

$\underline{\Delta}_3$

$\underline{d}_3^{(r,l)} = -1.5 + \mathrm{j}1.5$

real

$n = 4$

IV

imag.

real

$\underline{d}_4^{(r,l)} = 1.5 - \mathrm{j}1.5$

$\underline{\Delta}_4$

$\underline{i}_4 = 8.40 - \mathrm{j}8.22$

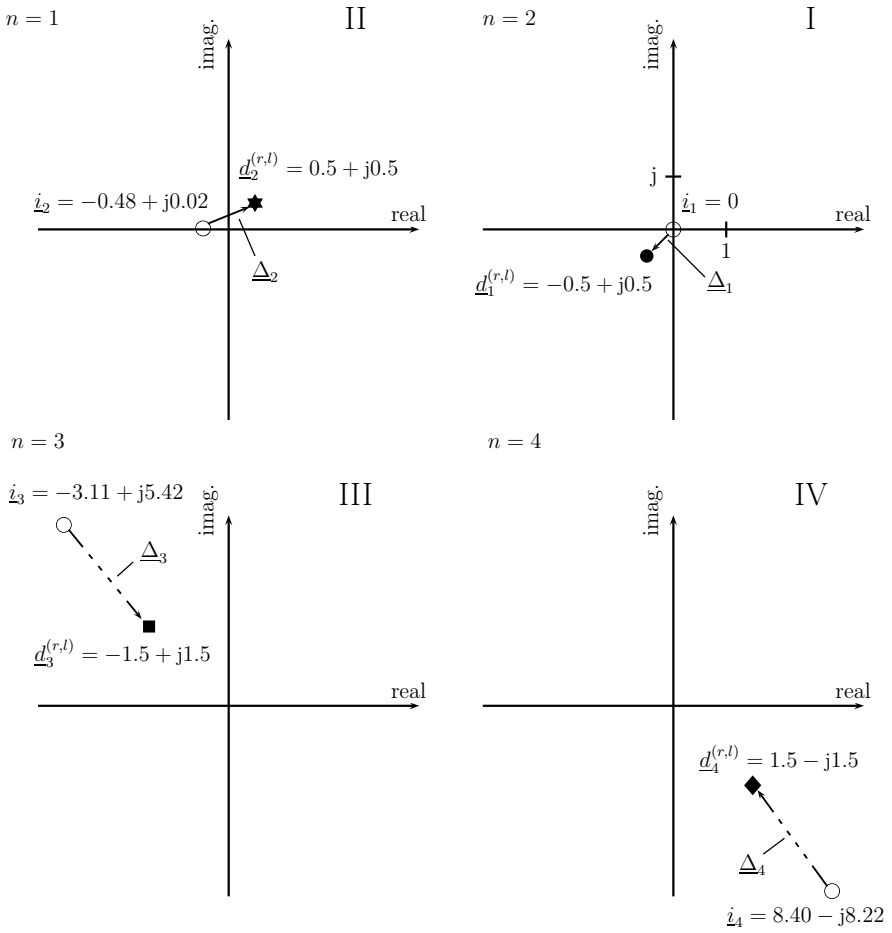Fig. 4.3.   Stepwise determination of the components $\underline{d}_n^{(r,l)}$ of $\underline{\mathbf{d}}^{(r,l)}$ by TxNZF, same example as behind Fig. 4.2; the Roman numbers indicate the step numbers when performing TxNZF

explained in Section 2.3 and choose the dimensions 4×4. The data $\mathfrak{a}$ are taken randomly and with equal probability from the R equal to 256, see (1.11), possible realizations $\mathfrak{a}^{(r)}$, $r = 1 \ldots R$. We take into account the two cases of fair and unfair channels, see Subsection 2.3.2, and the values

$$P = 1,\ 4,\ 9,\ 16,\ 25,\ 36, \tag{4.14}$$

where P equal to one, as already mentioned, corresponds to conventional TxZF. Values of P larger than 36 could not be considered for ES due to limitations of our computing facilities. Table 4.3 shows for the cases of TxZF, TxNZF and ES and for the fair and unfair channels

- the average required transmit energies T, see (2.34). In the case of ES these energies are equal to the minimum average required transmit energies $T_{\min}$ of (2.44).

- The normalized standard derivations $\sqrt{\mathrm{var}(T_{\mathrm{S}})}/T$ of the snapshot specific transmit energies T_{S} of (2.33).

The quantity $\sqrt{\mathrm{var}(T_{\mathrm{S}})}/T$ is a measure of the amplitude dynamics of the transmit signals and should be considered, if it comes to the specification of the required linearity of the transmit amplifiers.

In the case of the fair channel we can draw the following conclusions from the values listed in Table 4.3:

- The average required transmit energy T for P equal to or larger than nine is in the case of TxNZF about 5.5 dB lower than in the case of TxZF. Another transmit energy decrease of about 2.6 dB can be achieved by using ES instead of TxNZF.

- If P is increased beyond nine, no significant further transmit energy reduction can be achieved. This means that, in order to totally exhaust the potential of selective data representation, it is sufficient to choose P equal to nine.

- In order to obtain the smallest possible value $\sqrt{\mathrm{var}(T_{\mathrm{S}})}/T$, it is virtually sufficient to choose P equal to nine in the case of TxNZF, and P equal to 16 in the case of ES. As compared to TxZF, said normalized variance is lower by about 1.6 dB in the case of TxNZF and by about 7.5 dB in the case of ES.

In the case of the unfair channel, the values listed in Table 4.3 teach us the following:

- The sequence of the values T suggests the conjecture that T could be further decreased by choosing P larger than 36, which, however, is not possible due to the already mentioned computational limitations.

- For P equal to 36, TxZF is energywise outperformed by about 6.7 dB by TxNZF and by about 9.7 dB by ES

- With respect to $\sqrt{\text{var}(T_S)}/T$, TxNZF exhibits a minor disadvantage as compared to TxZF, whereas ES in the case of P equal to 36 outperforms TxZF by about 4.2 dB.

As already mentioned in Sections 1.5 and 2.1, selectable data representation introduces additional degrees of freedom in system design and parametrization. In the case of Approach I with its two possible implementations TxNZF and ES, this freedom is manifested by the fact that in the complex plane not only unique landing points close to the origin, see Fig. 2.1, but a multitude of alternative landing points are permitted, see Fig. 2.2 a. An interesting question would be to which degree the schemes TxNZF and ES make use of this freedom. In order to answer this question, we reconsider the complex plane of Fig.

		fair channel		unfair channel	
	P	T	$\dfrac{\sqrt{\text{var}\{T_S\}}}{T}$	T	$\dfrac{\sqrt{\text{var}\{T_S\}}}{T}$
TxZF	1	5.46	3.92	150	4.26
TxNZF	4	1.87	3.23	99.3	4.38
	9	1.57	2.74	72.5	4.57
	16	1.54	2.69	54.0	4.72
	25	1.53	2.68	40.9	4.74
	36	1.53	2.67	32.0	4.65
	∞	1.53	2.67	12.7	0.83
ES	4	1.08	7.77	85.4	29.65
	9	0.86	1.31	34.5	12.17
	16	0.84	0.71	23.4	3.27
	25	0.84	0.68	19.1	1.94
	36	0.84	0.66	16.7	1.61

Table 4.3. Statistical evaluation of TxZF, TxNZF and ES: Average required transmit renergy T and normalized standard derivation $\sqrt{\text{var}(T_S)}/T$

2.2 a in Fig. 4.4 and depict the landing points $\underline{v}_{1,1} \ldots \underline{v}_{1,P}$, which are, as before, marked with the symbol ✦. With the even integers μ and ω the possible distances of these landing points from the origin are given by

$$d_{\mu,\omega} = \sqrt{(0,5 + \mu)^2 + (0,5 + \omega)^2}, \quad \mu, \omega = -\sqrt{P}, -\left(\sqrt{P} + 2\right) \ldots 0, 2 \ldots \left(\sqrt{P} - 2\right). \tag{4.15}$$

If the potential offered by selectable data representation in combination with TxNZF or ES, respectively, would not be exploited, then only $d_{0,0}$ equal to $1/\sqrt{2}$ would be observed. The more values $d_{\mu,\nu}$ unequal $d_{0,0}$ would occur, and the more these values would deviate from $d_{0,0}$, the more extensive said potential would be used. This idea will be elaborated and illustrated in what follows.
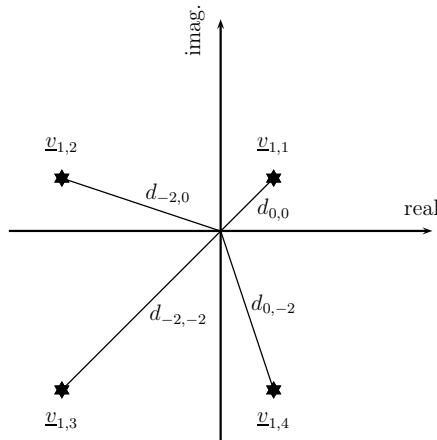
Fig. 4.4. Landing points $\underline{v}_{1,p}$, $p = 1 \ldots P$, $P = 4$, and their distances $d_{\mu,\omega}$ from the origin

In the leftmost columns of Tables 4.4 and 4.5 we list the quantities $2 \cdot d_{\mu,\omega}^2$ as convenient measure of the possible distances $d_{\mu,\omega}$ of (4.15). Depending on P, only certain values are applicable. In the other columns of the tables we list the probabilities with which said values $d_{\mu,\omega}$ are assumed for the values P of (4.14). Tables 4.4 a and b hold for TxNZF and ES, respectively, in the case of the fair channel. Tables 4.5 a and b present corresponding results for the unfair channel. From the occurrence probabilities in Tables 4.4 and 4.5 we can draw the following conclusions:

- The occurring distances $d_{\mu,\omega}$ are spread over the entire range given by (4.15), which means that the freedom offered by selectable data representation is indeed utilized.

a)

$2d^2_{\mu,\omega}$	$P = 4$	$P = 9$	$P = 16$	$P = 25$	$P = 36$
1	0.7656	0.7486	0.7486	0.7486	0.7486
5	0.2049	0.1976	0.1963	0.1963	0.1963
9	0.0295	0.0294	0.0287	0.0287	0.0287
13	x	0.0163	0.0163	0.0162	0.0162
17	x	0.0073	0.0070	0.0069	0.0069
25	x	0.0008	0.0021	0.0020	0.0019
29	x	x	0.0007	0.0007	0.0007
37	x	x	0.0003	0.0003	0.0003
41	x	x	x	0.0002	0.0002
45	x	x	x	0.0001	0.0001
49	x	x	0.0001	0.0001	0
53	x	x	x	0	0.0001
61	x	x	x	x	0
65	x	x	x	0	0
73	x	x	x	x	0
81	x	x	x	0	0
85	x	x	x	x	0
101	x	x	x	x	0
121	x	x	x	x	0

b)

$2d^2_{\mu,\omega}$	$P = 4$	$P = 9$	$P = 16$	$P = 25$	$P = 36$
1	0.6570	0.6428	0.6421	0.6420	0.6420
5	0.2973	0.2788	0.2776	0.2776	0.2775
9	0.0458	0.0394	0.0389	0.0389	0.0389
13	x	0.0266	0.0257	0.0256	0.0256
17	x	0.0110	0.0103	0.0102	0.0102
25	x	0.0014	0.0035	0.0034	0.0034
29	x	x	0.0013	0.0012	0.0012
37	x	x	0.0005	0.0004	0.0004
41	x	x	x	0.0003	0.0003
45	x	x	x	0.0002	0.0002
49	x	x	0.0001	0.0001	0.0001
53	x	x	x	0.0001	0.0001
61	x	x	x	x	0
65	x	x	x	0	0.0001
73	x	x	x	x	0
81	x	x	x	0	0
85	x	x	x	x	0
101	x	x	x	x	0
121	x	x	x	x	0

Table 4.4. Occurence probabilities of the distances $d_{\mu,\omega}$ of (4.15), fair channel
a) TxNZF   b) ES   x $\hat{=}$ not applicable

a)

$2d^2_{\mu,\omega}$	$P = 4$	$P = 9$	$P = 16$	$P = 25$	$P = 36$
1	0.2974	0.0362	0.0369	0.0373	0.0373
5	0.4952	0.1613	0.0671	0.0679	0.0682
9	0.2074	0.2065	0.0311	0.0314	0.0316
13	x	0.1265	0.1280	0.0583	0.0586
17	x	0.3337	0.1203	0.0542	0.0547
25	x	0.1358	0.2306	0.1205	0.0708
29	x	x	0.0912	0.0916	0.0444
37	x	x	0.2111	0.0817	0.0390
41	x	x	x	0.0707	0.0708
45	x	x	x	0.0669	0.0672
49	x	x	0.0836	0.0824	0.0159
53	x	x	x	0.0601	0.0603
61	x	x	x	x	0.0502
65	x	x	x	0.1273	0.0990
73	x	x	x	x	0.0430
81	x	x	x	0.0498	0.0489
85	x	x	x	x	0.0373
101	x	x	x	x	0.0744
121	x	x	x	x	0.0285

b)

$2d^2_{\mu,\omega}$	$P = 4$	$P = 9$	$P = 16$	$P = 25$	$P = 36$
1	0.2798	0.0403	0.0385	0.0372	0.0369
5	0.4970	0.1651	0.0717	0.0698	0.0685
9	0.2232	0.1888	0.0335	0.0328	0.0318
13	x	0.1388	0.1275	0.0607	0.0598
17	x	0.3251	0.1203	0.0575	0.0559
25	x	0.1419	0.2236	0.1195	0.0736
29	x	x	0.0967	0.0906	0.0460
37	x	x	0.2025	0.0818	0.0414
41	x	x	x	0.0725	0.0683
45	x	x	x	0.0699	0.0652
49	x	x	0.0857	0.0742	0.0174
53	x	x	x	0.0638	0.0599
61	x	x	x	x	0.0505
65	x	x	x	0.1202	0.1000
73	x	x	x	x	0.0449
81	x	x	x	0.0496	0.0433
85	x	x	x	x	0.0392
101	x	x	x	x	0.0693
121	x	x	x	x	0.0282

Table 4.5. Occurence probabilities of the distances $d_{\mu,\omega}$ of (4.15), unfair channel
a) TxNZF   b) ES   x $\hat{=}$ not applicable

- In the case of the fair channel the occurrence of the smallest distance, that is of $d_{0,0}$ equal to $1/\sqrt{2}$, clearly prevails with probabilities between about 0.65 and 0.77, whereas in the case of the unfair channel distances $d_{\mu,\omega}$ larger than $1/\sqrt{2}$ are the most probable ones. In the latter case, the occurring distances $d_{\mu,\omega}$ are more evenly distributed over the range given by (4.15).

- Basically, the degree, to which TxNZF and ES exploit the freedom offered by selectable data representation, is similar.

4.2.4   Error probabilities

In Section 2.2 the question of the error probability P_{e} has been already touched. In the present subsection we will resume this issue for the case of Approach I to selectable data representation, which, according to (2.6), features discrete valued multiple complex representatives. For each m, see (2.6), we have P possible landings points $v_{m,p}$, $p = 1 \ldots P$, in the N complex planes of the components $\underline{\mathbf{d}}_n^{(r)}$ of the vector $\underline{\mathbf{d}}^{(r)}$ of (1.45), which are aimed at with certain probabilities $P_1 \ldots P_P$. For the example considered in Subsection 4.2.3, these probabilities can be found in Tables 4.4 and 4.5. In the following we assume for simplicity that all these probabilities are equal to $1/P$.

We further assume at the receiver input the noise vector $\underline{\mathbf{n}}$ of (1.18) and first consider as reference the case P equal to one, that is TxZF. For this case the probability that a component $\underline{\mathbf{d}}_{\mathrm{Rx},n}$ of the vector $\underline{\mathbf{d}}_{\mathrm{Rx}}$ of (1.18) lands in the wrong decision region becomes with σ^2 of (1.22)

$$P_0 = \mathrm{erfc}\left(\frac{a}{2\sigma\sqrt{2}}\right)\left[1 - \frac{1}{4}\mathrm{erfc}\left(\frac{a}{2\sigma\sqrt{2}}\right)\right] \tag{4.16}$$

[Pro95]. For the cases of P larger than one, where we take for P only square numbers into account, see also (4.14), we have for each m, $m = 1 \ldots M$, see Fig. 2.2 a [HMBZ06a]

- 1 corner decision region,

- $2(\sqrt{P} - 1)$ strip decision regions, and

- $(\sqrt{P} - 1)^2$ square decision regions.

For the corner decision regions the error probabilities equal P_0 of (4.16). For the strip and square decision regions the error probabilities can be approximated by $1.5 \cdot P_0$ and $2 \cdot P_0$, respectively [HMBZ06a]. Then, the error probability corresponding to each component $d_{\mathrm{Rx},n}$ of the vector $\underline{\mathbf{d}}_{\mathrm{Rx}}$ of (1.18) can be approximated as

$$P_{\mathrm{s}} = \frac{P_0}{P}\left[1 - 1.5 \cdot 2(\sqrt{P} - 1) + 2 \cdot (\sqrt{P} - 1)^2\right] = P_0\left(2 - \frac{1}{\sqrt{P}}\right). \tag{4.17}$$

For sufficiently large values of P, P_s can be further approximated as

$$P_s \approx 2 \cdot P_0 \,. \tag{4.18}$$

From P_s of (4.17) and (4.18) follows for the error probability introduced in (1.1)

$$P_e = 1 - \sum_{n=1}^{N} P_s^n \cdot P_s^{N-n} \,. \tag{4.19}$$

4.3　Approach II to selectable data representation

4.3.1　Introduction

In this section we consider the solution of (4.1) for the case of Approach II introduced in Section 2.1. Before such a solution can be undertaken, we have first to define the data specific representative sets $\mathbb{G}_{\mathfrak{a}^{(r)}}$ to be utilized in Approach II. This task will be addressed in Subsection 4.3.2, where we introduce data specific representative sets $\mathbb{G}_{\mathfrak{a}^{(r)}}$ based on the conception of CCSPs. Once the data specific representative sets $\mathbb{G}_{\mathfrak{a}^{(r)}}$ are introduced, the solution of (4.1) can be attacked. As already mentioned in Section 4.1, we will develop a systematic solution based on constrained optimization through SQP [NW99, Big75, Pow83, Sch85]. This solution, for which we, as already stated, choose the designation MESP, will be described in Subsection 4.3.3. By the attribute 'soft' in this designation we want to express that, instead of the 'hard' spot landings on discrete valued representative values $\underline{v}_m$ or $\underline{v}_{m,p}$ in the complex plane typical of Approach I, we now aspire landings somewhere within continuous valued representative domains $\mathbb{D}_m$, which means that the constraint on $\underline{\mathbf{d}}^{(r)}$ is softened.

4.3.2　Definition of data specific representative sets based on CCSPs

The CCSPs are curves in the complex planes pertaining to the components $\underline{d}_n^{(r)}$ of the representative vector $\underline{\mathbf{d}}^{(r)}$ of $\mathfrak{a}^{(r)}$. Each CCSP is characterized by two parameters, namely an error probability $P_{\max}$ and the value σ^2 of the noise variance of (2.29). Now, in the case of a landing on a certain CCSP with the parameters $P_{\max}$ and σ^2, the error probability assumes the value $P_{\max}$, if the prevailing noise variance equals σ^2. Figs. 4.5 a and b show CCSPs for the case M equal to four already considered in Fig. 2.2 b. Fig. 4.5 a shows CCSPs for $P_{\max}$ equal to 10^{-3} with σ^2 as the curve parameter. Fig. 4.5 b shows CCSPs for σ^2 equal to 0.01 with $P_{\max}$ as the curve parameter.

In our definition of the representative domains $\mathbb{D}_m$ of (2.7) we set out from given values
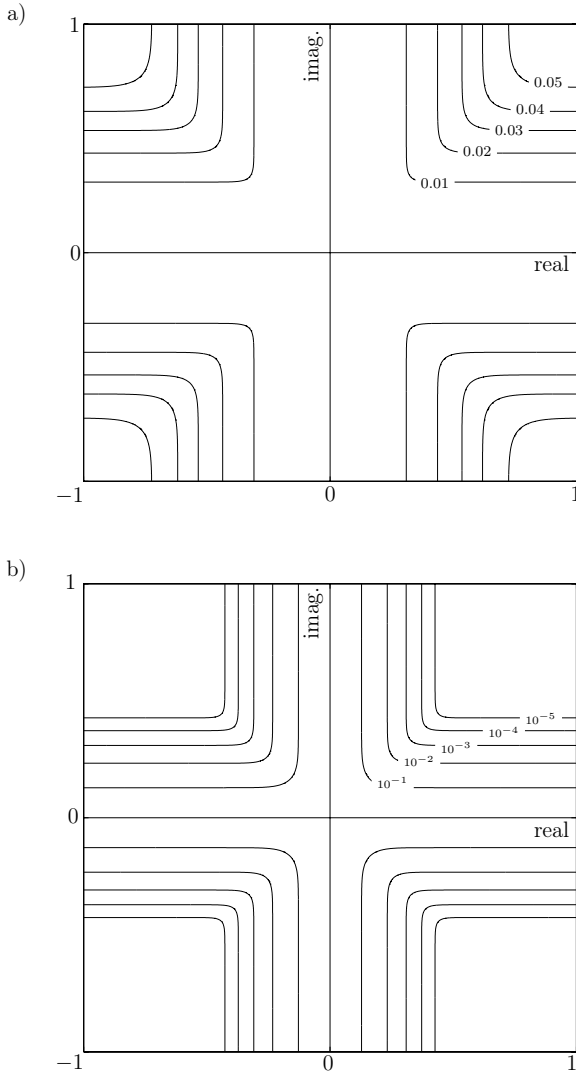
Fig. 4.5. CCSPs for

a) $P_{max} = 10^{-3}$ with σ^2 as the curve parameter

b) $\sigma^2 = 0.01$ with P_{max} as the curve parameter

of $P_{\max}$ and σ^2. Then, the representative domains are the areas on the concave side of the CCSPs. In retrospective, the curves in Fig. 2.2 b were chosen in such a way that they are CCSPs for the parameter values $P_{\max}$ equal to 10^{-3} and σ^2 equal to 0.01. Therefore, Fig. 2.2 b clarifies the just given definition of the representative domains $\mathbb{D}_m$ which will be utilized in what follows. A landing somewhere on a CCSP, that is on a border of $\mathbb{D}_m$, yields the error probability $P_{\max}$, whereas in the case of landings somewhere inside the representative domain $\mathbb{D}_m$ the error probability is equal to or smaller than $P_{\max}$.

By means of the just given definition of the representative domains $\mathbb{D}_m$, analogously to the case of Approach I, see (2.11), we can assign to each realization $\mathbf{a}^{(r)}$ of $\mathbf{a}$ a data specific representative set $\mathbb{G}_{\mathbf{a}^{(r)}}$ such that (2.12) holds for the representative vector $\underline{\mathbf{d}}^{(r)}$ of $\mathbf{a}^{(r)}$. Depending on the realization $\mathbf{a}^{(r)}$ of $\mathbf{a}$, to each component $\underline{d}_n^{(r)}$, $n = 1 \ldots N$, of the representative vector $\underline{\mathbf{d}}^{(r)}$ of $\mathbf{a}^{(r)}$, one of the M representative domains $\mathbb{D}_m$, $m = 1 \ldots M$, is assigned. Again, see Section 2.1, the component $\underline{d}_n^{(r)}$ of the vector $\underline{\mathbf{d}}^{(r)}$ representing $\mathbf{a}^{(r)}$ shall be taken from the partial representative set $\mathbb{V}_m$ with subscript m equal to $m_n^{(r)}$, that is from the partial representative set $\mathbb{V}_{m_n^{(r)}}$:

$$\underline{d}_n^{(r)} \in \mathbb{V}_{m_n^{(r)}} = \mathbb{D}_{m_n^{(r)}} \,, \tag{4.20}$$

see (2.4) and (2.7).

With the integer representative vector $\mathbf{m}^{(r)}$ of (2.5), the feasible region for the representative data vector $\underline{\mathbf{d}}^{(r)}$, that is its specific representative set $\mathbb{G}_{\mathbf{a}^{(r)}}$, can be written as

$$\mathbb{G}_{\mathbf{a}^{(r)}} = \begin{pmatrix} \mathbb{D}_{m_1^{(r)}} \\ \vdots \\ \mathbb{D}_{m_N^{(r)}} \end{pmatrix} . \tag{4.21}$$

Now, in the case of Approach II, we

- first set the values $P_{\max}$ and σ^2,

- then determine the representative domains $\mathbb{D}_m$ as explained above,

- assign the representative domains $\mathbb{D}_m$ to the data specific representative sets $\mathbb{G}_{\mathbf{a}^{(r)}}$ via the integer representative vector $\mathbf{m}^{(r)}$, and

- finally determine the transmit vector $\underline{\mathbf{t}}^{(r)}$ for the considered data realization with a view to arrive at minimum transmit energy $T^{(r)}$ under observation of $\mathbb{G}_{\mathbf{a}^{(r)}}$.

4.3.3 Determination of the optimum transmit vectors

In this subsection, MESP and more specifically its transmit vector design by means of appropriate state-of-the-art optimization algorithms [Big75, Pow83, Sch85] will be discussed. In general, (4.1) constitutes a problem of Nonlinear Programming (NLP) [Pap96, NW99]. In the case of MESP, as stated earlier, the 'hard' landings on discrete points are replaced by 'soft' landings within the data specific representative sets $\mathbb{G}_{\mathbf{a}^{(r)}}$. Hence, optimization can be performed within the infinite set of continuous values in the representative domains $\mathbb{D}_m$ constituting $\mathbb{G}_{\mathbf{a}^{(r)}}$, which will also be termed feasible regions in what follows to accord with the terminology used in [NW99]. Fortunately, in the case of Approach II with its simply connected representatives domains $\mathbb{D}_m$, see Subsection 4.3.2, not only the objective function of (4.1), but also the data specific representative sets $\mathbb{G}_{\mathbf{a}^{(r)}}$ representing the constraint function are convex so that there is a well-defined unique solution. Moreover, as both first and second order derivatives, that is the Gradient and the Hessian, of these convex functions exist, SQP methods can be applied without any loss of generality [NW99].

SQP is an iterative procedure which successively replaces an original NLP by local approximations in the form of Quadratic Programming (QP) subproblems, whose solutions are used to construct new iteration values that will finally converge to a local minimum as the number of iterations increase [Big75]. If a NLP is convex, then a local minimum is always also a global minimum. In this sense, SQP resembles iterative Newton methods, with the distinction that it may involve nonlinear constraints, such as in the case of (4.1). In most cases, SQP provides a significant reduction of computational complexity and has superlinear convergence [NW99]. Another advantage of SQP can be that the iteration values need not be points within the feasible regions of $\mathbb{G}_{\mathbf{a}^{(r)}}$, since the observation of this characteristic in the case of nonlinear constraint functions can be of similar complexity as the original problem [Sch85].

In the following, the SQP method will be discussed as it is integrated in the numerical mathematical and engineering software that was utilized by the author [Mat06]. For the sake of simplicity, strict mathematical conditions are omitted and the reader is referred to the literature, e.g. [NW99]. However, numerical methods usually require real-valued formulations of the problems considered [Mat06]. Therefore, (4.1) is solved considering the real valued equivalent isomorphic form of the complex signals [Wha71, ZF86]. The real valued equivalent isomorphic form of a complex vector $(\underline{\cdot})$ is obtained by stacking its real and imaginary parts separately into a double sized vector yielding

$$(\cdot) = \left[\operatorname{Re} \{(\underline{\cdot})\}^{\mathrm{T}}, \, \operatorname{Im} \{(\underline{\cdot})\}^{\mathrm{T}} \right]^{\mathrm{T}}. \qquad (4.22)$$

Correspondingly, the real valued equivalent isomorphic form of a complex matrix $[\underline{\cdot}]$ is given by

$$[\cdot] = \begin{bmatrix} \text{Re}\{[\underline{\cdot}]\} & -\text{Im}\{[\underline{\cdot}]\} \\ \text{Im}\{[\underline{\cdot}]\} & \text{Re}\{[\underline{\cdot}]\} \end{bmatrix}. \tag{4.23}$$

The real valued solution is then transferred back to its complex representation by the inverse operations. With (4.22) and (4.23) the equivalent real-valued representation of (4.1) reads

$$\mathbf{t}_{\text{opt}}^{(r)} = \arg\left\{ \min_{\mathbf{t}^{(r)} \in \mathbb{C}^{2Q \times 1}} \left(\mathbf{t}^{(r)\text{T}} \mathbf{t}^{(r)} \right) \right\} \\ \text{s.t. } \mathbf{d}^{(r)} = \mathbf{D}\,\mathbf{H}\,\mathbf{t}^{(r)} \in \mathbb{G}_{\mathbf{a}^{(r)}}^{\mathbb{R}} \subset \mathbb{R}^{2N \times 1}, \tag{4.24}$$

which we refer to in this subsection. The extension to complex valued signals is straightforward with the procedure explained above.

In (4.24), the matrices $\mathbf{D}$ and $\mathbf{H}$ are assumed to remain constant for the duration of each snapshot. Thus, only modifications of the values of the components $\mathbf{d}_n^{(r)}$, $n = 1 \ldots N$, of $\mathbf{d}^{(r)}$ may influence the value of the objective function $F\left(\mathbf{t}^{(r)}\right)$, namely twice the transmit energy of $\mathbf{t}^{(r)}$

$$F\left(\mathbf{t}^{(r)}\right) = \mathbf{t}^{(r)\text{T}} \mathbf{t}^{(r)} = 2T, \tag{4.25}$$

see (1.39). With (4.24), (4.25) can be expressed as

$$F\left(\mathbf{t}^{(r)}\right) = \left((\mathbf{D}\,\mathbf{H})^{-1}\, \mathbf{d}^{(r)} \right)^{\text{T}} (\mathbf{D}\,\mathbf{H})^{-1}\, \mathbf{d}^{(r)} = \mathbf{d}^{(r)\text{T}} \left[(\mathbf{D}\,\mathbf{H}) (\mathbf{D}\,\mathbf{H})^{\text{T}} \right]^{-1} \mathbf{d}^{(r)}, \tag{4.26}$$

yielding the Gradient

$$\nabla_{\mathbf{d}^{(r)}} F\left(\mathbf{t}^{(r)}\right) = \frac{\partial F\left(\mathbf{t}^{(r)}\right)}{\partial \mathbf{d}^{(r)}} = \begin{pmatrix} \dfrac{\partial F\left(\mathbf{t}^{(r)}\right)}{\partial d_1^{(r)}} \\ \vdots \\ \dfrac{\partial F\left(\mathbf{t}^{(r)}\right)}{\partial d_{2N}^{(r)}} \end{pmatrix} = 2 \left[(\mathbf{D}\,\mathbf{H}) (\mathbf{D}\,\mathbf{H})^{\text{T}} \right]^{-1} \mathbf{d}^{(r)} \in \mathbb{R}^{2N} \tag{4.27}$$

and the Hessian

$$\nabla_{\mathbf{d}^{(r)}}^2 F\left(\mathbf{t}^{(r)}\right) = \begin{pmatrix} \dfrac{\partial^2 F\left(\mathbf{t}^{(r)}\right)}{\partial d_1^{(r)} \partial d_1^{(r)}} & \cdots & \dfrac{\partial^2 F\left(\mathbf{t}^{(r)}\right)}{\partial d_1^{(r)} \partial d_{2N}^{(r)}} \\ \vdots & \ddots & \vdots \\ \dfrac{\partial^2 F\left(\mathbf{t}^{(r)}\right)}{\partial d_1^{(r)} \partial d_{2N}^{(r)}} & \cdots & \dfrac{\delta^2 F\left(\mathbf{t}^{(r)}\right)}{\partial d_{2N}^{(r)} \partial d_{2N}^{(r)}} \end{pmatrix} \tag{4.28}$$

$$= 2 \left[(\mathbf{D}\,\mathbf{H}) (\mathbf{D}\,\mathbf{H})^{\text{T}} \right]^{-1} \in \mathbb{R}^{2N \times 2N},$$

which will be used to determine the search direction in order to find $\mathbf{d}_{\mathrm{opt}}^{(r)}$ pertaining to $\mathbf{t}_{\mathrm{opt}}^{(r)}$ of (4.24).

The procedure explained above can be mathematically formulated in a recursive manner, starting with an initial vector $\mathbf{d}_0^{(r)}$. A reasonable initial vector $\mathbf{d}_0^{(r)}$ would be the real valued equivalent isomorphic form of the TxZF solution of (1.20) for the case of unique discrete valued representatives $\{\underline{v}_1 \ldots \underline{v}_M\}$, see (1.10). Given a search direction $\mathbf{g}_k^{(r)}$ and the step length $\alpha_k^{(r)}$, starting from the vector $\underline{\mathbf{d}}_k^{(r)}$ resulting by the actual iteration, further iteration values of the components $d_{k,n}^{(r)}$, $n = 1 \ldots N$, of $\mathbf{d}_k^{(r)}$ are derived by the simple update rule

$$\mathbf{d}_{k+1}^{(r)} = \mathbf{d}_k^{(r)} + \alpha_k^{(r)} \cdot \mathbf{g}_k^{(r)} , \qquad (4.29)$$

finally converging to the optimum solution

$$\mathbf{d}_k^{(r)} \underset{k \to \infty}{\to} \mathbf{d}_{\mathrm{opt}}^{(r)} . \qquad (4.30)$$

In general, with the transmit energy

$$T_k^{(r)} = \frac{1}{2} \cdot \mathbf{d}^{(r)\mathrm{T}} \left[(\mathbf{D}\,\mathbf{H}) (\mathbf{D}\,\mathbf{H})^{\mathrm{T}} \right]^{-1} \mathbf{d}^{(r)} \qquad (4.31)$$

of transmit vector $\mathbf{t}_k^{(r)}$ pertaining to the representative vector $\mathbf{d}_k^{(r)}$ resulting from the kth iteration, a stopping criterion

$$\varepsilon \geq T_{k-1}^{(r)} - T_k^{(r)} \qquad (4.32)$$

is defined by the decrease of the objective function, and the SQP procedure ends if the decrease of the transmit energy is smaller than ε. Thus, by choosing ε sufficiently small, arbitrarily close approximations $\mathbf{d}_{\mathrm{opt}}^{(r)}$ and $\mathbf{t}_{\mathrm{opt}}^{(r)}$ of (4.24) can be obtained. The determination of $\mathbf{d}_{\mathrm{opt}}^{(r)}$ pertaining to $\mathbf{t}_{\mathrm{opt}}^{(r)}$ of (4.24) is summarized by the Nassi-Shneiderman diagram of Fig. 4.6. In the following we shortly discuss how appropriate search directions $\mathbf{g}_k^{(r)}$ and step lengths $\alpha_k^{(r)}$ can be determined.

Concerning the search direction $\mathbf{g}_k^{(r)}$, the basic requirement is that it should be a descent direction, enabling reductions of the value of the objective function, in our case the transmit energy, along $\mathbf{g}_k^{(r)}$. To guarantee that $\mathbf{g}_k^{(r)}$ is a descent direction, the angle ϕ_k between $\mathbf{g}_k^{(r)}$ and the Gradient $\nabla_{\mathbf{d}^{(r)}} F \left(\mathbf{t}^{(r)} \right)$ has to fulfill

$$\mathbf{g}_k^{(r)\mathrm{T}} \nabla_{\mathbf{d}^{(r)}} F \left(\mathbf{t}^{(r)} \right) = \left\| \mathbf{g}_k^{(r)} \right\| \left\| \nabla_{\mathbf{d}^{(r)}} F \left(\mathbf{t}^{(r)} \right) \right\| \cos(\phi_k) < 0 . \qquad (4.33)$$

Hence, the most obvious choice is the direction of the steepest descent, that is the direction

of the negative Gradient

$$\mathbf{g}_k^{(r)} = -\frac{\partial F\left(\mathbf{t}^{(r)}\right)}{\partial \mathbf{d}_k^{(r)}} = -2\left[(\mathbf{D}\,\mathbf{H})\,(\mathbf{D}\,\mathbf{H})^{\mathrm{T}}\right]^{-1}\mathbf{d}_k^{(r)}, \tag{4.34}$$

see (4.27). However, the steepest descent direction may suffer from slow convergence, and there exist search directions with faster convergence, the most prominent of which is the Conjugate Gradient Search (CGS) [Pap96, NW99]. For the CGS, the objective function is substituted by its second-order Taylor-series

$$F\left(\mathbf{t}^{(r)}\right)_{\mathbf{d}_k^{(r)}+\mathbf{g}_k^{(r)}} \approx F\left(\mathbf{t}^{(r)}\right)_{\mathbf{d}_k^{(r)}} + \mathbf{g}_k^{(r)\mathrm{T}}\nabla_{\mathbf{d}^{(r)}} F\left(\mathbf{t}^{(r)}\right)_{\mathbf{d}_k^{(r)}} + \frac{1}{2}\mathbf{g}_k^{(r)\mathrm{T}}\nabla_{\mathbf{d}^{(r)}}^2 F\left(\mathbf{t}^{(r)}\right)_{\mathbf{d}_k^{(r)}}\mathbf{g}_k^{(r)}. \tag{4.35}$$

Then, in order to find the best search direction $\mathbf{g}_k^{(r)}$ for the current $\mathbf{d}_k^{(r)}$, the second and

set initial vector $\mathbf{d}_0^{(r)}$
$T_0^{(r)} = \frac{1}{2}\cdot\mathbf{d}_0^{(r)\mathrm{T}}\left[\mathbf{DH}\,(\mathbf{DH})^{\mathrm{T}}\right]^{-1}\mathbf{d}_0^{(r)}$

	calculation of $\mathbf{g}_k^{(r)}$ according to (4.35)
	determination of $\alpha_k^{(r)} \in [0,1]$
	$\mathbf{d}_{k+1}^{(r)} = \mathbf{d}_k^{(r)} + \alpha_k^{(r)}\cdot\mathbf{g}_k^{(r)}$
	$T_{k+1}^{(r)} = \frac{1}{2}\cdot\mathbf{d}_{k+1}^{(r)\mathrm{T}}\left[\mathbf{DH}\,(\mathbf{DH})^{\mathrm{T}}\right]^{-1}\mathbf{d}_{k+1}^{(r)}$

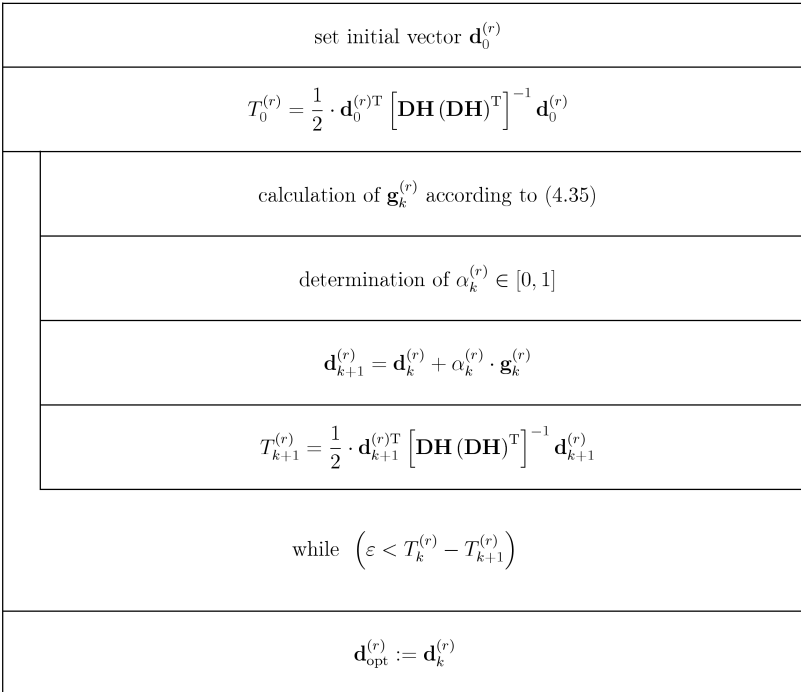| while $\left(\varepsilon < T_k^{(r)} - T_{k+1}^{(r)}\right)$ |
|---|
| $\mathbf{d}_{\mathrm{opt}}^{(r)} := \mathbf{d}_k^{(r)}$ |

Fig. 4.6. Nassi-Shneiderman diagram describing the determination of the optimum data representative vector pertaining to of (4.24) by MESP

last terms on the right hand side of (4.35) have to be minimized with respect to the constraints, that is the subproblem

$$
\begin{aligned}
\mathbf{g}_{k,\text{opt}}^{(r)} = \arg\min_{\mathbf{g_k}^{(r)}} &\left\{ \mathbf{g}_k^{(r)\text{T}}\nabla_{\mathbf{d}^{(r)}}F\left(\mathbf{t}^{(r)}\right)_{\mathbf{d}_k^{(r)}} + \tfrac{1}{2}\mathbf{g}_k^{(r)\text{T}}\nabla_{\mathbf{d}^{(r)}}^2 F\left(\mathbf{t}^{(r)}\right)_{\mathbf{d}_k^{(r)}}\mathbf{g}_k^{(r)} \right\} \\
&\text{s.t. } \mathbf{d}^{(r)} + \mathbf{g}_k^{(r)} \in \mathbb{G}_{\mathfrak{a}^{(r)}}^{\mathbb{R}} \subset \mathbb{R}^{2N\times 1}
\end{aligned}
\tag{4.36}
$$

has to be solved in each iteration. The constraints in (4.36) are usually incorporated into the objective function by augmenting additional penalty functions such that (4.36) can be replaced by an equivalent unconstrained subproblem [Big75, Pow83, NW99].

Once the search direction $\mathbf{g}_k^{(r)}$ is found, the step length $\alpha_k^{(r)}$ is determined via the Line Search (LS) strategy [Flo95, Fle70]. Starting from the current iteration vector $\mathbf{d}_k^{(r)}$, the LS strategy is to find the optimum step length $\alpha_k^{(r)}$ along the direction $\mathbf{g}_k^{(r)}$ that minimizes the objective function of (4.24). However, in most cases, boundary values to $\alpha_k^{(r)}$ are given a priori, e.g. $\alpha_k^{(r)} \in [0,1]$, as the search direction $\mathbf{g}_k^{(r)}$ is in most cases obtained by solving only a local approximation of the original NLP stated by (4.24) [Flo95]. For the determination of the step length $\alpha_k^{(r)}$, the most simple strategy would be an exhaustive search, and of course, there exist approximate strategies of reduced complexity, forcing $\alpha_k^{(r)}$ to attain a discrete value close to the optimum [NW99], e.g. cubic interpolation. In the strategy employed by the numerical software used by the author [Mat06], a compromise is made between a minimum sufficient decrease of the objective function in order to choose $\alpha_k^{(r)} > 0$, and the minimum value of the slope of the decrease to further increase $\alpha_k^{(r)}$. Further details considering the mathematical procedure of SQP can be found in [NW99].

The transmit signal generation of MESP is further illustrated in Figs. 4.7 a to c by exemplary trajectories of the iterative SQP optimization procedure, in which the complex valued solutions are displayed, which were transferred back to from the real valued representation of (4.24) by the inverse operations to (4.22) and (4.23). The trajectories displayed start from the initial components $\underline{d}_{0,n}^{(r)}$, $n = 1\ldots N$, of $\underline{\mathbf{d}}_0^{(r)}$ of (1.20) and converge to the components $\underline{d}_{\text{opt},n}^{(r)}$, $n = 1\ldots N$, of $\underline{\mathbf{d}}_{\text{opt}}^{(r)}$ of (4.1). The symbolic representations of the data $\mathfrak{a}^{(r)}$ are additionally highlighted by squares and circles around the initial components $\underline{d}_{0,n}^{(r)}$ and $\underline{d}_{\text{opt},n}^{(r)}$, respectively. As can be seen by the trajectories, the SQP solutions $\underline{\mathbf{d}}_{\text{opt}}^{(r)}$ remain within the data specific representative sets $\mathbb{G}_{\mathfrak{a}^{(r)}}$, even though in some cases certain iteration values $\underline{d}_{k,n}^{(r)}$ are not situated within $\mathbb{G}_{\mathfrak{a}^{(r)}}$. This observation confirms the robustness and convergence of the SQP method. The convergence behaviour is illustrated by Fig. 4.8, in which the exemplary trajectory of Fig. 4.7 c is displayed once again, but in a more detailed fashion, as only the relevant sections of the quadrants corresponding to the first and last two components of the vectors $\underline{\mathbf{d}}_k^{(r)}$ are shown in Fig. 4.8 a and b, respectively. In Fig. 4.8, the white circles corresponding to the values $\underline{d}_{k,n}^{(r)}$ of the components of $\underline{\mathbf{d}}_k^{(r)}$ are separated by five iterations each.

a)

$n = 1$

$n = 2$

$n = 3$

$n = 4$
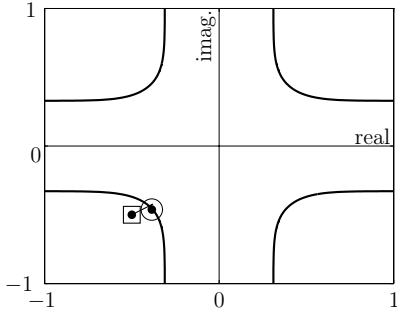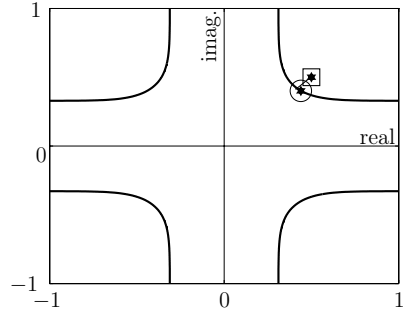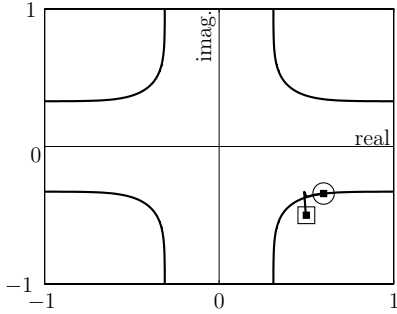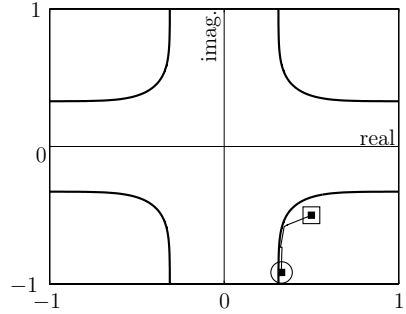
($\square$) initial components $\underline{d}_{0,n}^{(r)}$ ($\bigcirc$) final components $\underline{d}_{\text{opt,n}}^{(r)}$

b)

$n = 1$

$n = 2$

$n = 3$

$n = 4$

($\square$) initial components $\underline{d}_{0,n}^{(r)}$ ($\bigcirc$) final components $\underline{d}_{\mathrm{opt,n}}^{(r)}$

c)

$n = 1$

$n = 2$

$n = 3$

$n = 4$
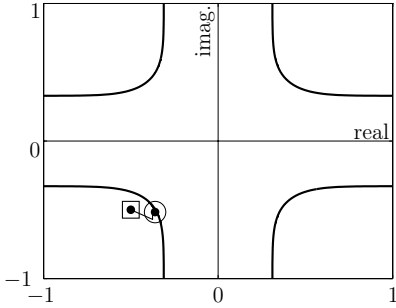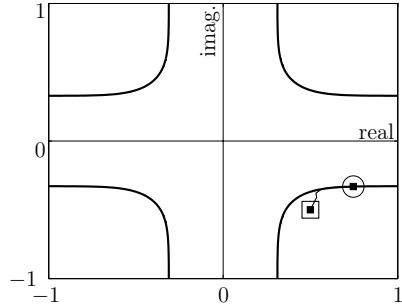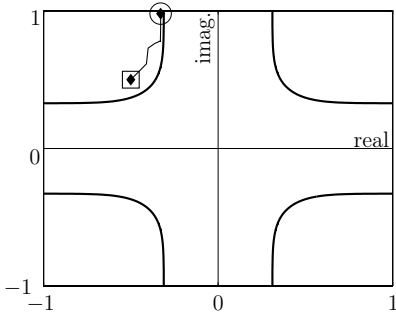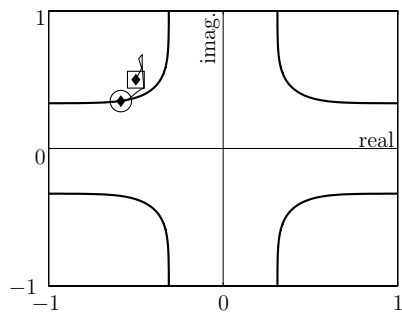
($\square$) initial components $\underline{d}_{0,n}^{(r)}$ ($\bigcirc$) final components $\underline{d}_{\text{opt,n}}^{(r)}$
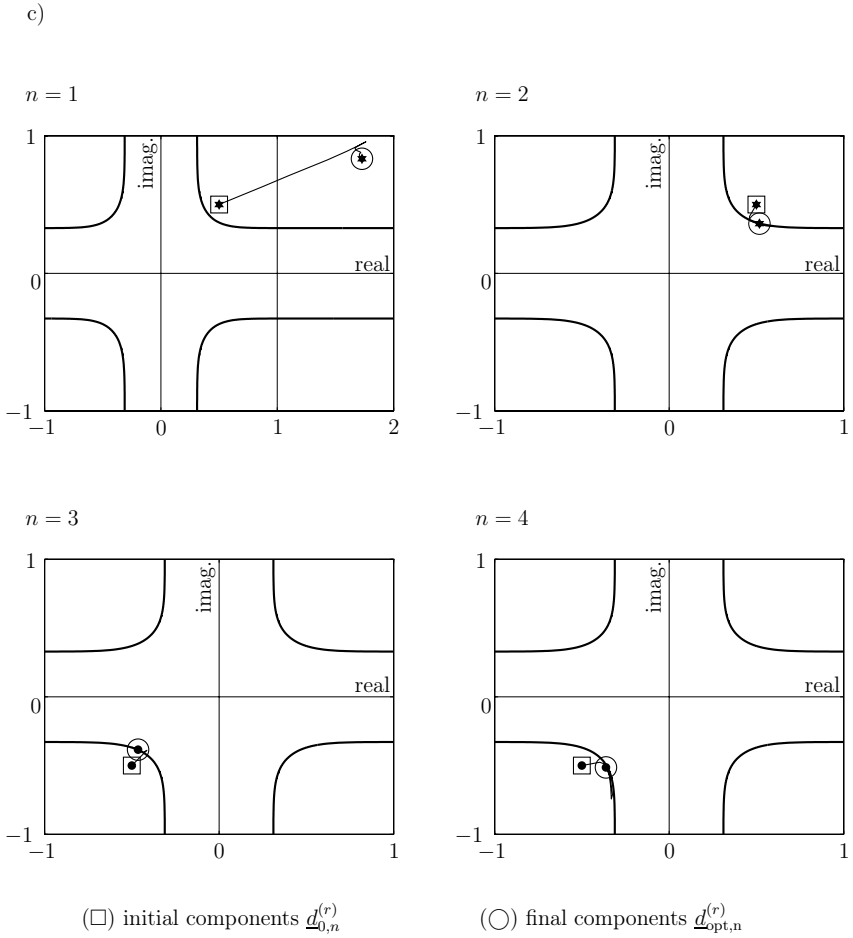
Fig. 4.7. Exemplary trajectories of $\underline{\mathbf{d}}_k^{(r)}$

a) $\mathfrak{a}^{(r)} = (\, \bigstar \ \blacksquare \ \bullet \ \blacksquare \,)$

b) $\mathfrak{a}^{(r)} = (\, \bullet \ \blacklozenge \ \blacksquare \ \blacklozenge \,)$

c) $\mathfrak{a}^{(r)} = (\, \bullet \ \bullet \ \bigstar \ \bigstar \,)$

a)

b)

($\square$) initial values and ($\bigcirc$) final values of $\underline{d}_{k,n}^{(r)}$

Fig. 4.8. Iteration values $d_{k,n}^{(r)}$ for the example of Fig. 4.7 c for

a) $n = 1, 2$

b) $n = 3, 4$

The overall distribution of the landings points of $\underline{\mathbf{d}}_{\text{opt}}^{(r)}$ within the data specific representative sets $\mathbb{G}_{\mathbf{a}^{(r)}}$ are displayed in Fig. 4.9 a and b for the cases of fair and unfair channel matrices, respectively. As can be seen, not all landings points pertaining to the components of the data representative vectors $\underline{\mathbf{d}}_{\text{opt}}^{(r)}$ lie on the boundaries given by the CC-SPs, which in all figures of this subsection are associated with $P_{\max} = 10^{-3}$ and $\sigma^2 = 0.01$. However, it should be noted that at least on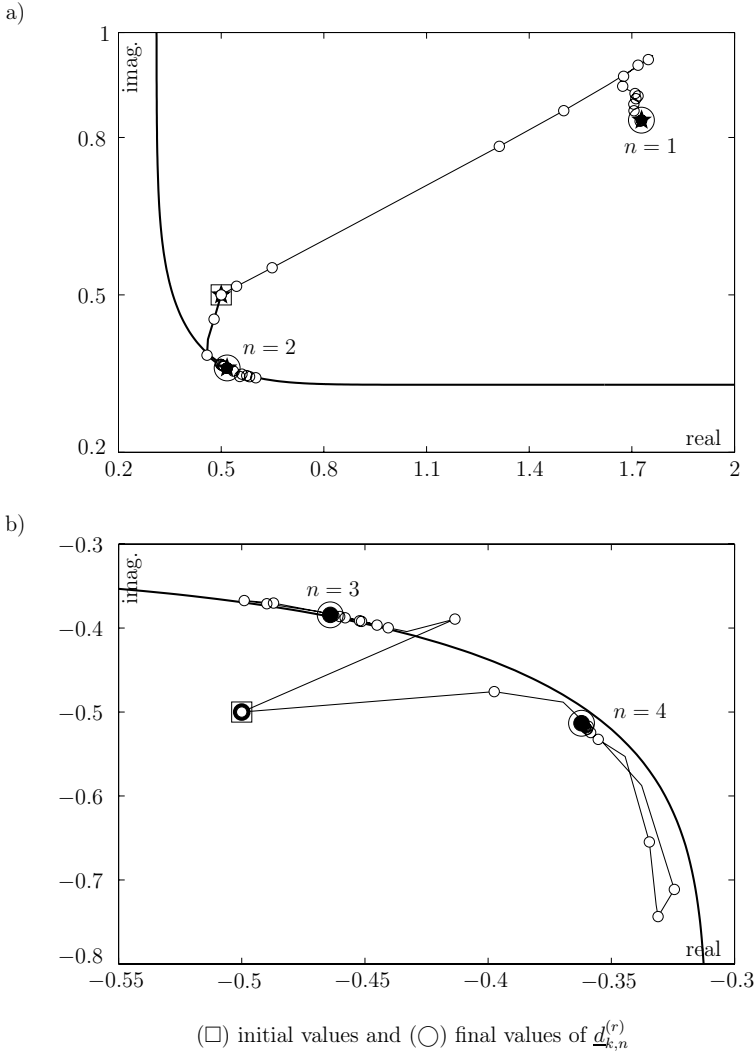e component $\underline{d}_{\text{opt},n}^{(r)}$ of $\underline{\mathbf{d}}_{\text{opt}}^{(r)}$ of (2.41) has to lie on a CCSP boundary. Otherwise, there would exist a vector $\underline{\mathbf{d}}_{\text{opt}}^{(r)'}$, resulting from the multiplication of a scalar $\kappa < 1$ and $\underline{\mathbf{d}}_{\text{opt}}^{(r)}$ which would yield a transmit energy further reduced by a factor of $1/\kappa^2$, resulting from

$$\underline{\mathbf{d}}_{\text{opt}}^{(r)'} = \kappa \underline{\mathbf{d}}_{\text{opt}}^{(r)} = \underline{\mathbf{D}}\,\underline{\mathbf{H}}\,\underline{\mathbf{t}}_{\text{opt}}^{(r)'} = \kappa \cdot \underline{\mathbf{D}}\,\underline{\mathbf{H}}\,\underline{\mathbf{t}}_{\text{opt}}^{(r)} = \underline{\mathbf{D}}\,\underline{\mathbf{H}}\,\kappa \cdot \underline{\mathbf{t}}_{\text{opt}}^{(r)} \tag{4.37}$$

and thus

$$\underline{\mathbf{t}}_{\text{opt}}^{(r)} = \frac{1}{\kappa} \cdot \underline{\mathbf{t}}_{\text{opt}}^{(r)'},\ \kappa < 1\,. \tag{4.38}$$

Hence, $\underline{\mathbf{d}}_{\text{opt}}^{(r)}$ can be characterized by the property

$$\nexists \underline{\mathbf{d}}_{\text{opt}}^{(r)'} \in \mathbb{G}_{\mathbf{a}^{(r)}}\,\Big|\,\underline{\mathbf{d}}_{\text{opt}}^{(r)'} = \kappa \underline{\mathbf{d}}_{\text{opt}}^{(r)}\ \ \text{for}\,\kappa < 1\,. \tag{4.39}$$

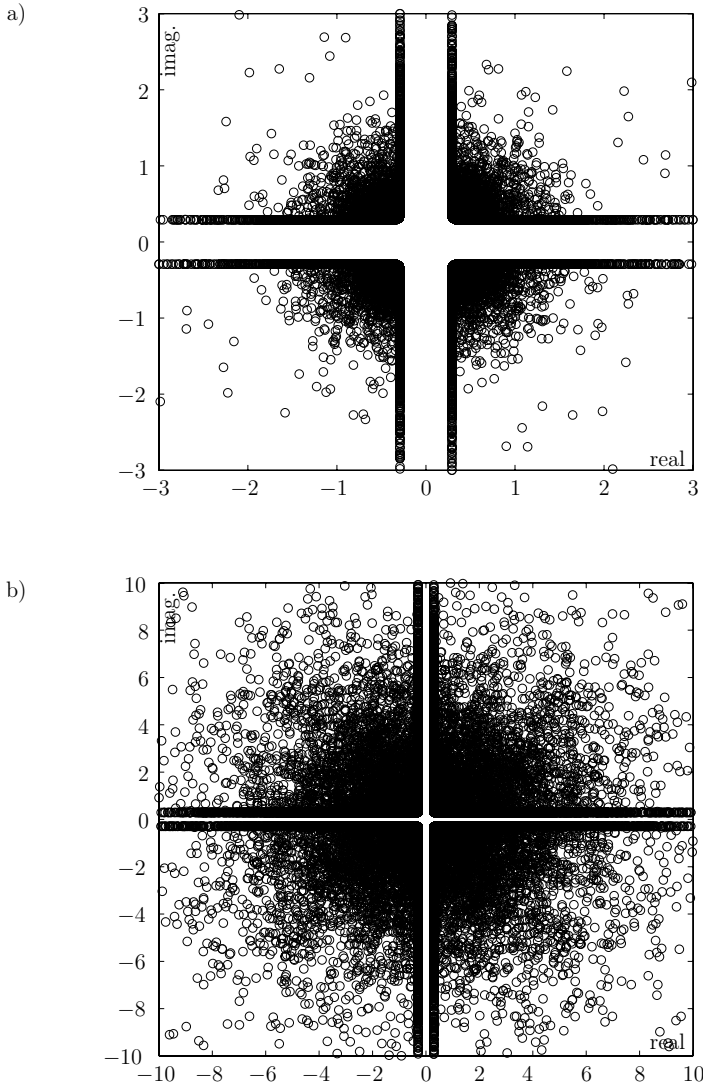### 4.3.4   Minimization of the required pseudo SNR

In this subsection, a procedure will be explained that leads to the minimum possible required pseudo SNR γ for a desired symbol error probability P_{s} [KB07b]. For a given realisation $\mathbf{a}^{(r)}$ of $\mathbf{a}$ and for given values $P_{\max}$ and σ^2, $\mathbb{G}_{\mathbf{a}^{(r)}}$ is uniquely determined. With this $\mathbb{G}_{\mathbf{a}^{(r)}}$ and under consideration of $\underline{\mathbf{D}}$ and $\underline{\mathbf{H}}$ we now solve (4.1) and determine $T_{\min}^{(r)}$ of (2.43) with $\underline{\mathbf{t}}_{\text{opt}}^{(r)}$ of (4.1), which allows us to calculate the instantaneous pseudo SNR [MBQ04]

$$\gamma_{\text{inst}}\left(P_{\max}, \mathbf{a}, \sigma^2, \underline{\mathbf{D}}, \underline{\mathbf{H}}\right) = \frac{T\left(P_{\max}, \mathbf{a}, \sigma^2, \underline{\mathbf{D}}, \underline{\mathbf{H}}\right)}{\sigma^2} \tag{4.40}$$

depending on $P_{\max}$, $\mathbf{a}$, $\underline{\mathbf{D}}$ and $\underline{\mathbf{H}}$. By repeating this procedure for the same $P_{\max}$, $\mathbf{a}$, $\underline{\mathbf{D}}$ and $\underline{\mathbf{H}}$, but different σ^2, we can arrive at the minimum instantaneous pseudo SNR

$$\gamma_{\text{inst,min}}\left(P_{\max}, \mathbf{a}, \underline{\mathbf{D}}, \underline{\mathbf{H}}\right) = \min_{\sigma^2}\left\{\frac{T\left(P_{\max}, \mathbf{a}, \sigma^2, \underline{\mathbf{D}}, \underline{\mathbf{H}}\right)}{\sigma^2}\right\} \tag{4.41}$$

sufficient to keep the symbol error probability P_{s} below $P_{\max}$. As indicated in (4.41), this minimum depends not only on $P_{\max}$, but also on $\mathbf{a}$, $\underline{\mathbf{D}}$ and $\underline{\mathbf{H}}$. In the case of a priori given

Fig. 4.9. Distribution of landing points of MESP for $P_{\max} = 10^{-3}$ and $\sigma^2 = 0.01$

a) fair channel

b) unfair channel

$\underline{\mathbf{D}}$ in the sense of RO and of stationarily varying $\mathbf{a}$ and $\underline{\mathbf{H}}$ we can form the average

$$\gamma_{\min}\left(P_{\max}, \underline{\mathbf{D}}\right) = \underset{\mathbf{a}, \underline{\mathbf{H}}}{\mathrm{E}} \left\{\gamma_{\mathrm{inst,min}}\left(P_{\max}, \mathbf{a}, \underline{\mathbf{D}}, \underline{\mathbf{H}}\right)\right\} \qquad (4.42)$$

of the minimum required instantaneous pseudo SNR $\gamma_{\mathrm{inst,min}}$ of (4.41). Now, in order to quantitatively assess MESP, based on (4.42) $P_{\max}$ should be determined depending on γ.

In order to further elucidate MESP, particularly the above steps (4.40) to (4.42), we now consider a numerical example characterized by the following parameters:

- Transparent demodulator matrix $\underline{\mathbf{D}} = \mathbf{I}^{4 \times 4}$,

- maximum symbol error probability $P_{\max} = 10^{-3}$,

- channel matrix $\underline{\mathbf{H}}_{\mathrm{fair}}$ of (2.31), and

- data $\mathbf{a}^{(r)}$, for the case of its 4-PSK representation, equivalent to

$$\mathbf{a}^{(r)} \hat{=} \frac{1}{2}(1 + \mathrm{j}, -1 + \mathrm{j}, -1 - \mathrm{j}, 1 - \mathrm{j}). \qquad (4.43)$$

Fig. 4.10 shows for this situation γ_{inst} of (4.40) versus σ^2, and we clearly recognize the occurrence of a minimum for σ^2 equal to 0.02. In Fig. 4.11 we let $\mathbf{a}$ and $\underline{\mathbf{H}}$ vary in
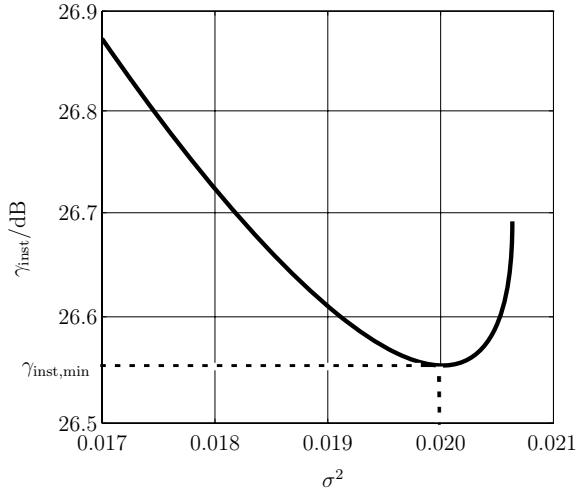

Fig. 4.10. γ_{inst} of (4.38) versus σ^2 for $P_{\max} = 10^{-3}$

a stationary manner and depict P_s versus γ as determined by the procedure explained above for the case of the fair and unfair channel matrices, respectively. In Fig. 4.11 also the symbol error probability P_s of TxZF is shown. Clearly, TxZF is inferior to MESP. However, the transmit signal generation in the case of MESP depends on the actual noise variances, and the average required transmit energy has to be determined via (4.42) in order to minimize the required pseudo SNR γ for a desired symbol error probability P_s. Therefore, as already stated above, $P_{\max}$ of (4.42) should be chosen depending on the desired value of P_s, as, depending on $P_{\max}$, different values of T of (2.34) result. In Table 4.6, the resulting values of T are shown for $P_{\max} = 10^{-3}$ and $\sigma^2 = 0.01$.
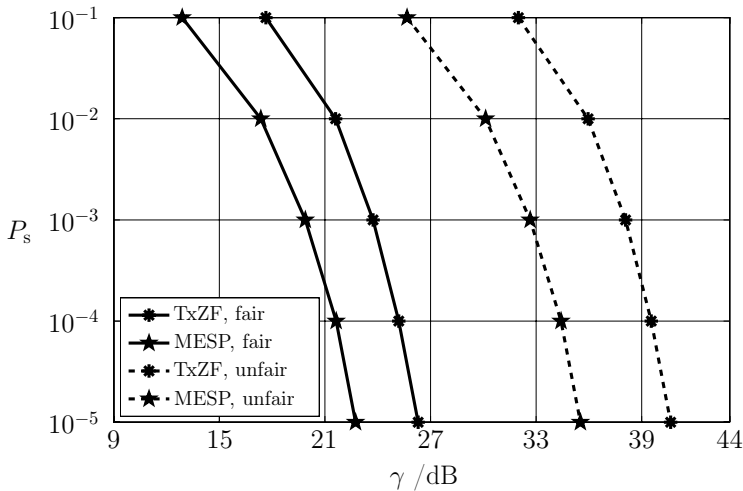
Fig. 4.11. Performance of MESP for fair and unfair channel matrices

In Table 4.6, similar to Fig. 4.3, we also depict values of T for different values P, which in the case of Approach I to selectable data representation were associated to the number of discrete representatives $\underline{v}_{m,p}$, see (2.6). However, in the case of MESP, a restriction comparable to $P < \infty$ for the case of Approach I, is to define a maximum extension of the representative domains $\mathbb{D}_m$ of (2.7). Now, in order to operate with identical decision region boundaries as in the case of Approach I, the values P for MESP in Table 4.6 are associated to the extension of the representative domains $\mathbb{D}_m$ of MESP. For a certain value P the extensions of the representative domains $\mathbb{D}_m$ are bounded to $\sqrt{P}$ for both the real and imaginary axes. The purpose of such a restriction will be discussed in Section 5.5.

| P | T | |
	fair channel	unfair channel
1	5.46	150
4	3.27	116.32
9	2.77	100.31
16	2.60	89.28
25	2.52	81.01
36	2.46	74.65
∞	2.43	46.05

Table 4.6. Average required transmit energy T of MESP for $P_\mathrm{s} = 10^{-3}$ and $\sigma^2 = 0.01$

4.4   Performance comparison

In order to energy wise judge the performance of the RO transmission systems considered in this chapter, that is TxNZF and ES for the Approach I, and MESP for Approach II to selectable data representation, in general, P_s is depicted versus γ of (2.37), as displayed in Fig. 4.12 a and b for the cases of fair and unfair channels. We can state a dramatic advantage of TxNZF, and a still remarkable advantage of MESP over TxZF. For the unfair channel this advantage is more explicit than for the fair channel. However, the superior performance of ES over TxNZF is only observed in the case of the fair channel. This is due to the computational restrictions, as for ES only values of $P \leq 36$ could be performed. In the case of the low complexity approximate approach of TxNZF and of MESP, no such computational restrictions exist and the curves displayed for TxNZF and MESP are valid for P equal to infinity, which explains how TxNZF may outperform ES. For further clarification, TxNZF for P equal to 36 is also displayed in Fig. 4.12 b, and we can see that with the same restriction of P, ES clearly outperforms TxNZF. In the case of the fair channel, the considered schemes converge within the considered values of $P \leq 36$, see Table 4.3 for TxNZF and ES and Table 4.6 for MESP. The curves displayed in Fig. 4.12 a are therefore valid for $P \geq 36$; however, no further transmit energy reductions are possible by further increasing P to values larger than 36.

The energy wise performance advantage of the precoding schemes with selectable data representation go along with modified structures of the signals arriving at the receivers. This fact has to be considered in the design of the receivers, both with respect to the data acquisition in terms of the dynamic ranges required for A/D conversion and the data detection, see Section 2.2. Concerning the data detection, for the case of Approach I no explicit modifications are required in the receivers, as the data specific representative

a)

b)
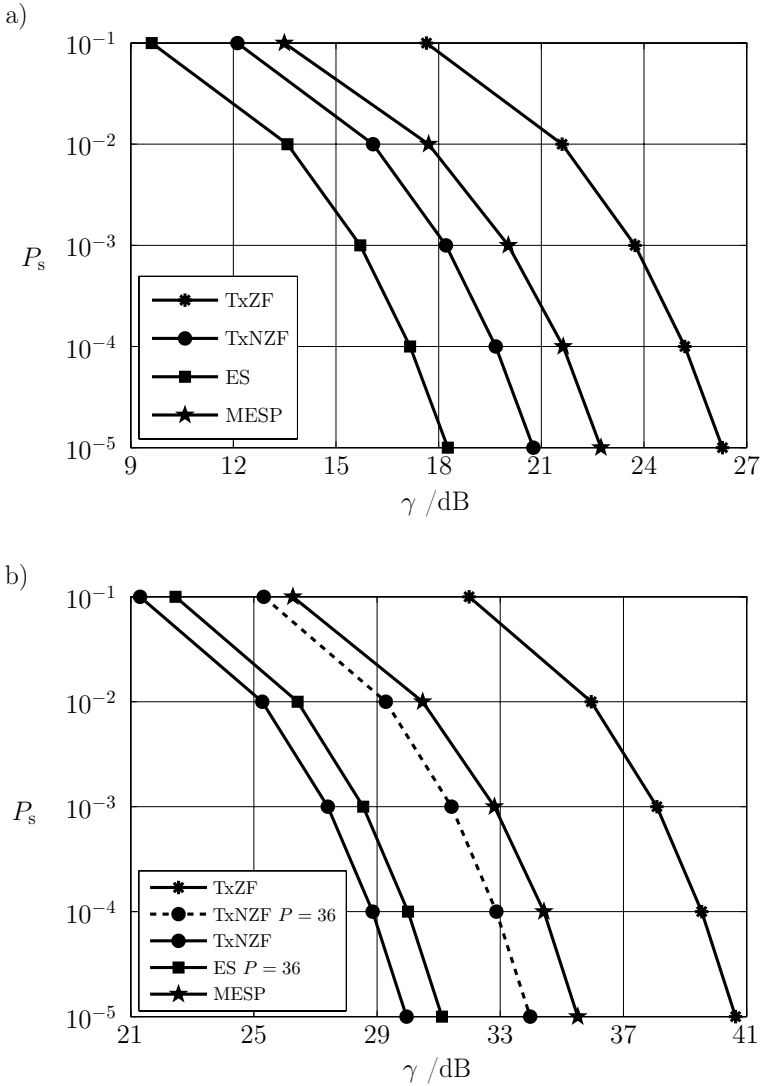
Fig. 4.12. Error probability P_s versus pseudo SNR γ

a) fair channel

b) unfair channel

sets $\mathbb{G}_{\mathbf{a}^{(r)}}$ do not modify the conventional decision regions $\mathbb{Q}_m$ of (2.17) so that only the amplitude dynamics of the receive signals have to be further taken into account [KE07]. In the case of Approach I, the receivers have to be additionally equipped with modulo-reduction units [HPS05b, HMBZ06a, KE07], which are not included in the present standards for MTs.

4.5   Résumé

Various versions of transmit energy minimization enabled by selectable data representation exist, and these can be mathematically formulated in a concise manner. The understanding of transmit energy minimization be selectable data representation can be furthered by graphical illustrations of the process of transmit signal generation and by simulation results, which show for instance the transmit energy required in order to achieve a given transmission quality.

Chapter 5
MIMO OFDM multi-user downlinks with selectable data representation

5.1 Introduction

In the previous chapters the concept of RO data transmission with selectable data representation, see Fig. 1.5, was elaborated in a very general fashion, and various aspects of this concept were studied in detail. Most importantly, it became evident that this concept allows a significant reduction of the required transmit energy as compared to RO data transmission with conventional, that is unique data representation as shown in Fig. 1.4.

In the present Chapter 5 the general rationale of RO data transmission with selectable data representation of Fig. 1.5 will be adapted to the special case of MIMO OFDM multi-user mobile radio downlinks, which, as already mentioned in Section 1.5, play an important role in the evolution of 3G and in the definition of forthcoming 4G mobile radio concepts. In the course of the chapter we will see that such an adaptation is very promising with respect to significantly reducing the required transmit energy of said downlinks. Unfortunately, it will further turn out that by such an approach the amplitude dynamics of the received signals cannot be mitigated as compared to conventional receiver oriented MIMO OFDM downlinks; rather, these dynamics are increased. Therefore, a trade-off between transmit power reduction and increased receive signal dynamics should be on the agenda.

In the following Section 5.2 we will describe the considered MIMO OFDM downlink configuration. Then, Section 5.3 will address the issue of the required transmit energy. Finally, in Sections 5.4 and 5.5 the topic of the amplitude dynamics of the received signals will be treated.

5.2 Considered configuration

5.2.1 System structure

Fig. 5.1 shows the considered MIMO OFDM downlink structure. We have an AP with multiple transmit antennas and a number of MTs with one receive antenna each. Such a downlink constitutes a broadcast system [QMBW04, KB07b], in which the AP antennas and the receive antennas of the MTs form a MIMO structure. Due to the multiplicity of channel inputs and outputs which can be simultaneously active, the channel is termed

noisy vector channel
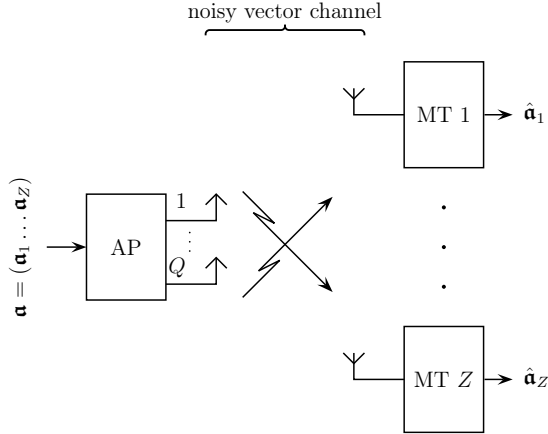
Fig. 5.1. Considered MIMO OFDM downlink structure

vector channel, and it is turned noisy by the received noise. For reasons which will become evident later, we use the symbols Q and Z for the numbers of the transmit antennas and of the MTs, respectively, which were already introduced as the dimensions of $\underline{\mathbf{H}}$ of (1.3). First, we consider a single OFDM symbol slot and a single subcarrier. The results obtained in this way can then be readily extended to realistic situations, in which we have multiple symbol slots and consider all subcarriers, the number of which we designate as N_{F}. The data $\mathfrak{a}$ fed into the AP consist of the MT specific data $\mathfrak{a}_z$, $z = 1 \ldots Z$, for the individual MTs, that is

$$\mathfrak{a} = (\mathfrak{a}_1 \ldots \mathfrak{a}_Z) . \tag{5.1}$$

At the output of MT z, $z = 1 \ldots Z$, an estimate $\hat{\mathfrak{a}}_z$ of $\mathfrak{a}_z$ is expected, which should be as reliable as possible.

The MTs are assumed to operate in a non-cooperative way, that is none of the Z MTs disposes of information on the antenna inputs or data outputs of the $Z - 1$ other MTs.

5.2.2   System model

Under the premises made in Subsection 5.2.1, the downlink structure of Fig. 5.1 can be modeled as shown in Fig. 5.2. This model results by adapting the scheme of Fig. 1.5 to the case of MIMO OFDM. In the model of Fig. 5.2 we have abstracted the self-evident OFDM typical operations of serial-to-parallel conversion, IFFT and insertion of the cyclic

Fig. 5.2. Adaptation of the structure in Fig. 1.5 to the case of MIMO OFDM multi-user downlinks

prefix in the transmitter, and of removing the cyclic prefix, FFT and parallel-to-serial conversion in the receivers. Then, see also Section 1.1, in each OFDM symbol slot and for each of the N_F subcarriers the components of the vectors

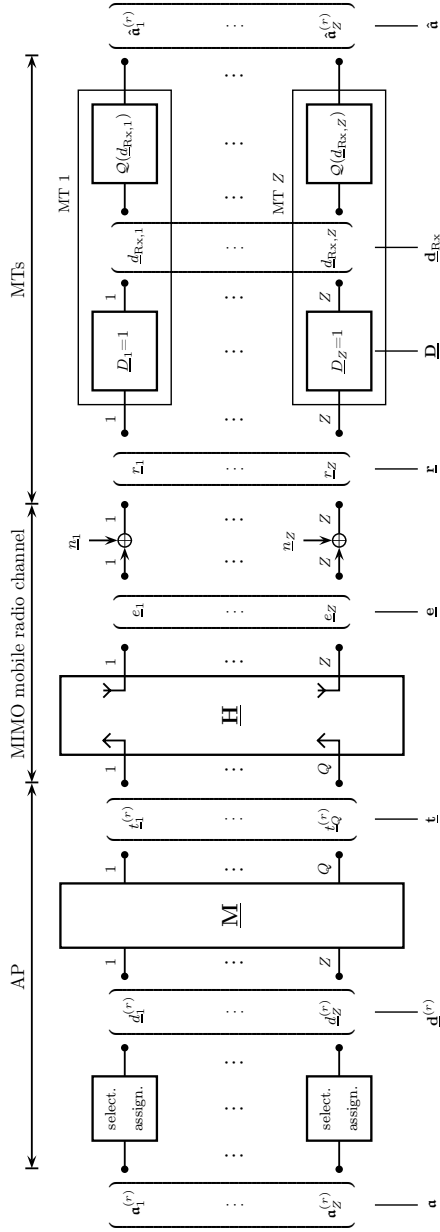$$\underline{\mathbf{t}}^{(r)} = \left(\underline{t}_1^{(r)} \ldots \underline{t}_Q^{(r)} \right)^\mathrm{T} , \tag{5.2}$$

$$\underline{\mathbf{e}} = (\underline{e}_1 \ldots \underline{e}_Z)^\mathrm{T} , \tag{5.3}$$

$$\underline{\tilde{\mathbf{n}}} = (\underline{\tilde{n}}_1 \ldots \underline{\tilde{n}}_Z)^\mathrm{T} \tag{5.4}$$

and

$$\underline{\mathbf{r}} = (\underline{r}_1 \ldots \underline{r}_Z)^\mathrm{T} \tag{5.5}$$

in the structure of Fig. 5.2 represent complex amplitudes, and the entries of the matrix $\underline{\mathbf{H}}$ stand for transfer function values. The adaptation mentioned in Subsection 5.1 comprises the two following features:

1. The procedure of selective assignment illustrated in Fig. 1.5 is split up into Z partial selective assignment procedures. Each one of these concerns the data transfer to one of the Z MTs. In the present chapter we replace the indices $n = 1 \ldots N$ of the components of $\underline{\mathbf{d}}^{(r)}$ of (1.9) by the indices $z = 1 \ldots Z$. Then, the realization $\mathfrak{a}_z^{(r)}$ of the MT specific data intended for MT z are represented by the component $\underline{d}_z^{(r)}$ of the representative vector $\underline{\mathbf{d}}^{(r)}$, that is with (2.4) we can write

$$\mathfrak{a}_z^{(r)} \to \underline{d}_z^{(r)} \in \mathbb{V}_{m_z^{(r)}} . \tag{5.6}$$

2. The demodulator matrix $\underline{\mathbf{D}}$ is a diagonal matrix with diagonal elements $\underline{D}_z$ equal to unity, that is

$$\underline{\mathbf{D}} = \underline{\mathbf{I}}^{Z \times Z} . \tag{5.7}$$

Vanishing of all off-diagonal elements of $\underline{\mathbf{D}}$ expresses the fact of non-cooperative MTs mentioned in Subsection 5.2.1, that is each MT disposes only of its own input value and has no knowledge of the input values of the $Z - 1$ other MTs.

The entry $\underline{h}_{z,q}$ of the channel matrix $\underline{\mathbf{H}}$ represents the transfer function value between the input of AP antenna q and the receive antenna output of MT z at the considered subcarrier frequency. With $\underline{\mathbf{D}}$ of (5.7) follows from (1.20) the modulator matrix

$$\underline{\mathbf{M}} = \underline{\mathbf{H}}^\mathrm{H} \left(\underline{\mathbf{H}} \, \underline{\mathbf{H}}^\mathrm{H} \right)^{-1} . \tag{5.8}$$

The inversion of $\underline{\mathbf{H}}\,\underline{\mathbf{H}}^{\mathrm{H}}$ in (5.8) can be only performed if this matrix is regular. As a necessary, but not sufficient condition for this regularity,

$$Z \leq Q \tag{5.9}$$

has to hold for $\underline{\mathbf{H}}$ of (1.3), that is $\underline{\mathbf{H}}$ has to be a square or wide matrix. In other words, the number Z of MTs should not exceed the number Q of transmit antennas at the AP.

5.3   Required transmit energy

We now assume the following:

- The channel matrices $\underline{\mathbf{H}}$ valid for each of the N_{F} subcarriers are generated independently according to the rationale displayed in Subsection 2.3.2.

- The data realizations $\mathbf{a}_z^{(r)}$ to be transmitted to the different MTs z, $z = 1 \ldots Z$, on each of the N_{F} subcarriers are independent.

Under these assumptions the average required transmit energy of the considered MIMO OFDM multi-user downlinks can be simply obtained by multiplying the values T in Tables 4.3 and 4.6 by the number N_{F} of OFDM subcarriers. Concerning the normalized standard deviations of the transmit energy, the corresponding values for the considered MIMO OFDM multi-user downlinks result from the values $\sqrt{\mathrm{var}\{T_{\mathrm{S}}\}}/T$ in Tables 4.3 and 4.6 by division by $\sqrt{N_{\mathrm{F}}}$.

5.4   Amplitude dynamics of the received signals

In this section we deal with the amplitude dynamics of the signals occurring at the receive antenna outputs of the Z MTs in the structure of Fig. 5.2. We first consider a single OFDM symbol slot and a single subcarrier. We further focus on the useful parts of these signals, which are given by the components $\underline{e}_z$ of the vector $\underline{\mathbf{e}}$ of (5.3).

We consider a sufficiently large set of snapshots, each characterized by a realization of the channel matrix $\underline{\mathbf{H}}$ and a realization $\mathbf{a}^{(r)}$ of the data $\mathbf{a}$, where $\underline{\mathbf{H}}$ and $\mathbf{a}$ vary as described in Subsection 2.3.2. Then, by applying the schemes TxZF, TxNZF, ES or MESP, respectively, we obtain Z large sets of randomly varying components $\underline{e}_z$, $z = 1 \ldots Z$, of $\underline{\mathbf{e}}$ of (5.3). Due to the characteristics of $\underline{\mathbf{H}}$ and $\mathbf{a}$ these components have zero expectations, that is

$$\mathrm{E}\{\underline{e}_z\} = 0, \; z = 1 \ldots Z, \tag{5.10}$$

and non-zero variances

$$\sigma_z^2 = \mathrm{E}\left\{\mathrm{Re}^2\left(\underline{e}_z\right)\right\} = \mathrm{E}\left\{\mathrm{Im}^2\left(\underline{e}_z\right)\right\}, \; z = 1 \ldots Z. \tag{5.11}$$

The variances σ_z^2 of (5.11), which can be determined by simulations, are the subcarrier powers at the MT antenna outputs. As examples we consider fair and unfair channel matrices with the dimensions $Z \times Q$ equal to 4×4 as described in Subsection 2.3.2 and the schemes TxZF, TxNZF, ES and MESP. The obtained variances σ_z^2, $z = 1 \ldots 4$, for these examples are listed in Table 5.1. In the case of the fair channel, all four variances σ_z^2 are equal. In the case of the unfair channel, the variances σ_1^2 and σ_2^2 as well as σ_3^2 and σ_4^2 are pairwise equal. However, the latter two are larger than the former two. This is due to the differences of the attenuations valid for MTs 1 and 2 on the one side and for MTs 3 and 4 on the other side. As can be seen from the values in Table 5.1, even though single variances σ_z^2, may assume smaller values, as for instance σ_1^2, σ_2^2 in the case of ES in the case of the unfair channels, with increasing values of P the more critical variances σ_3^2, σ_4^2 rise. The total received variances, that is the sum of all variances σ_z^2 of (5.11) is monotonically increasing with P.

Unfortunately, in the case of the unfair channel, the variances σ_3^2, σ_4^2 are considerably higher than σ_1^2, σ_2^2 and the reference case of TxZF, whereas in the case of the fair channel the ratio between the variances σ_z^2, $z = 1 \ldots 4$, and the reference case are rather small. Quantitatively spoken, the ratio as compared to the variance of TxZF scales up to values around or even more than 50 in the case of the unfair channel, whereas in the fair channel this ratio always remains below three. If we now consider, instead of a single subcarrier, all N_{F} subcarriers, then the total useful powers at the receive antenna outputs can be obtained by multiplying the values in Table 5.1 by N_{F}. The consequences of the findings above are discussed and reinterpreted in the next section.

5.5   Trade-off between transmit energy reduction and received signal dynamics

As explained in Section 5.4, MESP and TxNZF or ES enable transmit energy reductions at the cost of larger amplitudes within the receive vector $\underline{\mathbf{e}}$. Hence, the benefit of low transmit power of TxNZF, ES and MESP, in addition to their low receiver complexity, has to be bargained for larger dynamics of the receive signals, which basically requires higher amplitude resolutions, or more exactly, larger dynamic ranges of the receiver A/D-converters than in the case of TxZF. Thus, concerning the amplitude dynamics on the receiver side, TxZF represents a lower bound within the schemes considered in this thesis.

			fair channel	unfair channel	
	$A_{\max}$	P	$\sigma_1^2 = \sigma_2^2 = \sigma_3^2 = \sigma_4^2$	$\sigma_1^2 = \sigma_2^2$	$\sigma_3^2 = \sigma_4^2$
TxZF	1	1	0.25	0.25	0.25
TxNZF	2	4	0.51	0.33	1.16
	3	9	0.59	0.33	3.35
	4	16	0.60	0.33	6.17
	5	25	0.61	0.33	9.12
	6	36	0.61	0.33	11.87
ES	2	4	0.64	0.47	1.19
	3	9	0.74	0.47	3.36
	4	16	0.76	0.43	6.12
	5	25	0.76	0.40	9.01
	6	36	0.76	0.38	11.74
MESP	2	4	0.45	0.32	1.09
	3	9	0.54	0.33	2.50
	3	16	0.59	0.33	4.20
	5	25	0.61	0.33	6.01
	6	36	0.63	0.33	7.78

Table 5.1. Variances σ_z^2 of (5.11)

Now, in order to reduce the receive signal dynamics of MESP and TxNZF or ES, an amplitude limit $A_{\max}$ could be introduced during the transmit signal generation such that

$$\max\left(\mathrm{Re}\left\{\underline{e}_z\right\}, \mathrm{Im}\left\{\underline{e}_z\right\}\right) \leq A_{\max},\ z = 1\ldots Z, \tag{5.12}$$

holds for each of the components $\underline{e}_z$ of the vector $\underline{\mathbf{e}}$ of (5.3), which could be equivalently interpreted as restricting the number of multiple representatives P to a finite value in the case of TxNZF and ES, see Subsection 4.2.3. Though $A_{\max}$ could be chosen as an arbitrary continuous value, we only consider integer values for $A_{\max}$. Then, the non-

ambiguous relation between $A_{\max}$ and P is given by

$$A_{\max} = \sqrt{P}. \tag{5.13}$$

Due to the restrictions of (5.12) the variances σ_z^2 become upper bounded, and, consequently, attain smaller values. Unfortunately, the potential transmit energy reduction is reduced simultaneously as the variances σ_z^2 attain smaller values. In Fig. 5.3 a and b, this trade-off is illustrated, denoting the values of variances σ_z^2 and the mean required transmit energies T for different values of $A_{\max}$, for the case of the ensemble of channel matrices $\underline{\mathbf{H}}_{\text{fair}}$ and $\underline{\mathbf{H}}_{\text{unfair}}$, respectively. For convenience, the average transmit energies T are normalized by the value occurring in case of TxZF, termed T_{ZF}, therefore, in Figs. 5.3 a and b the transmit energy reduction with respect to TxZF is shown versus $A_{\max}$. In Figs. 5.3 a and b, also the variances σ_z^2 are normalized by the value occurring in the case of TxZF, termed σ_{ZF}^2 are displayed. However, to give an immediate impression of the additionally required number of resolution bits for the enhanced dynamic ranges, we depict $\log_2\left(\sigma_z^2/\sigma_{\text{ZF}}^2\right)$ versus $A_{\max}$. In the case of the unfair channel, the variances σ_3^2, σ_4^2 are considered, because they are larger and, therefore, more critical. The curves of the normalized average transmit energies T/T_{ZF} are displayed by solid lines and thus distinguished from the normalized variances $\sigma_z^2/\sigma_{\text{ZF}}^2$, whose curves are dashed lines.

As already mentioned in the previous section, the situation is rather dramatic in the case of unfair channel matrices, where, principally, up to six additional bits are required to provide the enhanced dynamic range as compared to the reference case of TxZF. In the case of fair channel matrices two additional bits suffice. Unfortunately, unfair channel matrices are usual for multi-user mobile radio downlinks [3GP03, SDS+05]. Thus, it can be concluded from Figs. 5.3 a and b that the transmit energy advantage is counteracted by the requirement of a larger word length of the A/D converters in the receivers, which is a drawback for practical implementation, if no further counter measures are undertaken, as for example scheduling [AH05]. Exemplary, only users with comparable channel gains could be scheduled simultaneously, such that the multi-user diversity introduced by scheduling is exploited to actively avoid unfair channel matrices. Then, the drawback of increased receive signal dynamics is only present in the slide form of the fair channel matrices. The trade-off presented may help the system designer to find a reasonable compromise between A/D converter expense and performance degradation hopefully to be combined with scheduling. This trade-off could be further elaborated by the application of more complicated cost functions rather than the simple resolute restriction of (5.12), which also is only applied subcarrierwise in the frequency domain. The determination of such cost functions is not further elaborated in this thesis and thus left aside as a topic of further research, which could refine the findings of this section.

a)

b)
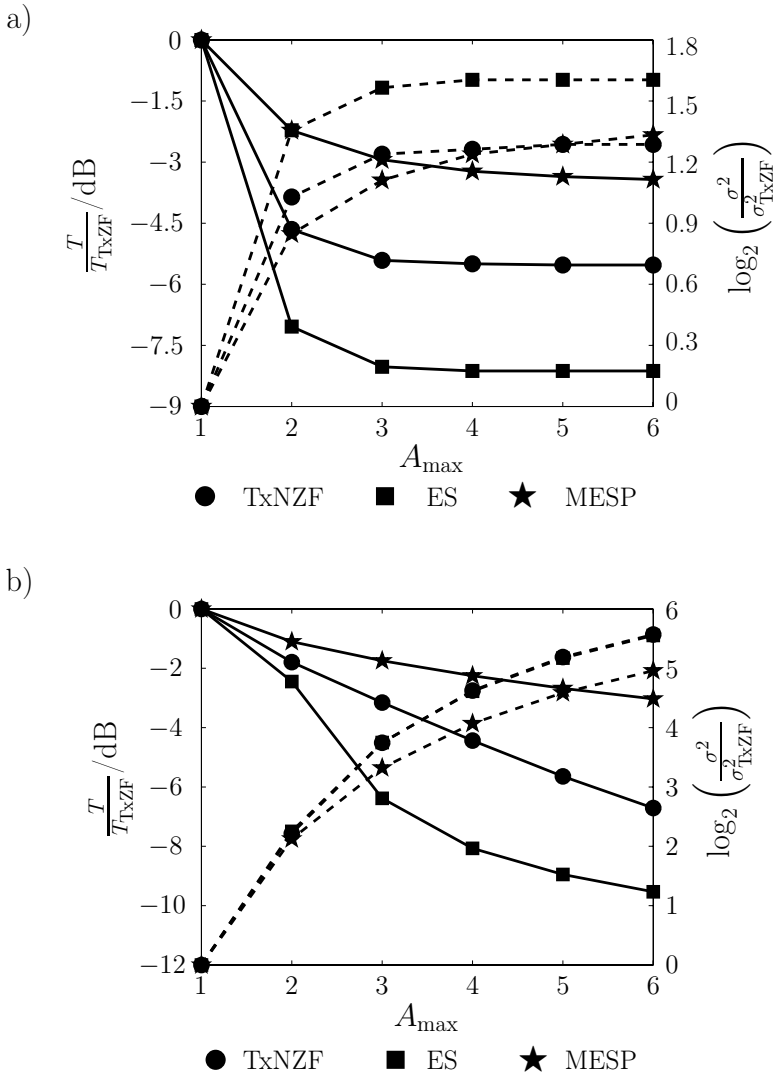
Fig. 5.3. Trade-off between transmit energies T and variance σ_z^2
of the received signals
a) fair channel
b) unfair channel

5.6   Résumé

The concept of receiver orientation in combination with selectable data representation easily lends itself for applications in MIMO OFDM multi-user downlinks. As compared to such downlinks employing unique data representation, significant transmit power reductions can be achieved. However, these reductions must be bargained for the undesired effect of increased amplitude dynamics of the received signals. Therefore, a compromise of transmit power reduction and said signal dynamics should be found in order to arrive at attractive system designs.

Chapter 6
Impact of incorrectness of the CSI available to the transmitter

6.1 Problem

In the RO transmission systems considered in this thesis, the knowledge of CSI on the transmit side in the form of the matrix $\underline{\mathbf{H}}$ of (1.3) is vital for generating the transmit vector $\underline{\mathbf{t}}$ by evaluating (4.1). As already mentioned in Section 1.5, depending on the applied duplexing schemes FDD or TDD, a number of approaches exist how to provide this information to the transmitter [JBM$^+$02, HMBZ06b]. Irrespective of which one of these approaches is chosen, we always have to accept that the true channel matrix $\underline{\mathbf{H}}$ differs from the channel matrix available in the transmitter when evaluating (4.1) - we term this matrix $\hat{\underline{\mathbf{H}}}$ - by an additive error matrix $\underline{\boldsymbol{\Delta}}_{\mathrm{H}}$, that is

$$\hat{\underline{\mathbf{H}}} - \underline{\mathbf{H}} = \underline{\boldsymbol{\Delta}}_{\mathrm{H}}. \tag{6.1}$$

If there is a difference between the channel matrices used when determining the transmit vector $\underline{\mathbf{t}}$ via (4.1) on the one side and when determining the undisturbed receive vector $\underline{\mathbf{e}}$ via (1.4) on the other side, then in the complex planes of the N components of $\underline{\mathbf{d}}$ of (1.45) the aspired landing points will not be exactly hit. These non-exact landings may entail - for a given value of the pseudo SNR γ - an increase of the error probability P_{e} of (1.1). In the present chapter we are going to investigate the degradation of the system performance due to an imperfectness of the CSI available in the transmitter.

6.2 Rationale of analysis

In Section 1.1 it is elaborated that in RO transmission systems the transmit vector $\underline{\mathbf{t}}$ results from the data $\mathfrak{a}$, the receive operator $\mathcal{D}(\underline{\mathbf{r}})$ and the channel matrix $\underline{\mathbf{H}}$ via the transmit operator according to

$$\underline{\mathbf{t}} = \mathcal{M}\left(\mathfrak{a}, \mathcal{D}(\underline{\mathbf{r}}), \underline{\mathbf{H}}\right), \tag{6.2}$$

see Fig. 1.2 c. Then, the undisturbed receive vector $\underline{\mathbf{e}}$ is given by (1.4). When investigating the impact of an incorrectness of the CSI available in the transmitter, the obvious procedure would be the following:

1. Substitute in (6.2) $\underline{\mathbf{H}}$ by $\underline{\hat{\mathbf{H}}}$ of (6.1), which yields the erroneous transmit vector $\underline{\hat{\mathbf{t}}}$.

2. Determine with this $\underline{\hat{\mathbf{t}}}$ and the correct channel matrix $\underline{\mathbf{H}}$ via (1.4) the erroneous undisturbed receive vector $\underline{\hat{\mathbf{e}}}$.

3. Determine the impact of the incorrectness of the undisturbed receive vector on the system performance.

The just described procedure is somewhat tedious, because the described determination of $\underline{\hat{\mathbf{t}}}$ is not a trivial task. This becomes evident if we, in the case of RO systems with a linear inner section, substitute in (1.20) $\underline{\mathbf{H}}$ by $\underline{\hat{\mathbf{H}}}$ of (6.1). In this case the error matrix $\underline{\boldsymbol{\Delta}}_{\mathrm{H}}$ would appear at three positions, and the influence of $\underline{\boldsymbol{\Delta}}_{\mathrm{H}}$ on the modulator matrix would not be easily recognizable. In order to circumvent this difficulty, the author proposes a more easily practicable procedure, which can be considered the inverse of the above explained approach, and which consists of the following steps:

1. Determine with the correct $\underline{\mathbf{H}}$ the exact $\underline{\mathbf{t}}$ via (6.2).

2. Determine with this $\underline{\mathbf{t}}$ and the erroneous channel matrix $\underline{\hat{\mathbf{H}}}$ of (6.1) via (1.4) the erroneous undisturbed receive vector $\underline{\hat{\mathbf{e}}}$.

3. Determine the impact of the incorrectness of the undisturbed receive vector on the system performance.

Now, the error matrix $\underline{\boldsymbol{\Delta}}_{\mathrm{H}}$ has to be considered only once, namely when determining the erroneous undisturbed receive vector $\underline{\hat{\mathbf{e}}}$ by using $\underline{\hat{\mathbf{H}}}$ of (6.1). The author conjectures that, at least for small CSI errors, both procedures yield similar results. The proof of this conjecture could be a topic of future research. In what follows we rely on the just described more simple approach.

We now set out from the realization $\boldsymbol{\mathfrak{a}}^{(r)}$ of $\boldsymbol{\mathfrak{a}}$ and the corresponding realization $\underline{\mathbf{t}}^{(r)}$ of $\underline{\mathbf{t}}$. With the transmit vector $\underline{\mathbf{t}}^{(r)}$, the error matrix $\underline{\boldsymbol{\Delta}}_{\mathrm{H}}$ and the demodulator matrix $\underline{\mathbf{D}}$ the vector of the deviations of the aspired landing points becomes, see (1.13) and (1.16),

$$\underline{\boldsymbol{\Delta}}^{(r)} = \underline{\mathbf{D}}\,\underline{\boldsymbol{\Delta}}_{\mathrm{H}}\,\underline{\mathbf{t}}^{(r)} . \tag{6.3}$$

As an overall measure of these deviations, the quantity

$$\Delta^{(r)2} = \mathrm{trace}\left(\underline{\boldsymbol{\Delta}}^{(r)}\,\underline{\boldsymbol{\Delta}}^{(r)\mathrm{H}}\right) = \mathrm{trace}\left(\underline{\mathbf{D}}\,\underline{\boldsymbol{\Delta}}_{\mathrm{H}}\underline{\mathbf{t}}^{(r)}\,\underline{\mathbf{t}}^{(r)\mathrm{H}}\underline{\boldsymbol{\Delta}}_{\mathrm{H}}^{\mathrm{H}}\underline{\mathbf{D}}^{\mathrm{H}}\right) \tag{6.4}$$

could be used. For the purpose of illustration we now consider an example, which is characterized as follows:

- Square matrices $\underline{\mathbf{H}}$, $\underline{\boldsymbol{\Delta}}_{\mathrm{H}}$ and $\underline{\mathbf{D}}$ with the dimensions $N \times N$, where N is again the dimension of the representative vectors $\underline{\mathbf{d}}^{(r)}$ of (1.9) or (1.45),

- Unitary matrix $\underline{\mathbf{D}}$, see (2.28).

Under these assumptions, (6.4) can be rewritten as [Lue96]

$$\Delta^{(r)2} = \mathrm{trace}\left(\underline{\mathbf{t}}^{(r)}\,\underline{\mathbf{t}}^{(r)\mathrm{H}}\underline{\boldsymbol{\Delta}}_{\mathrm{H}}^{\mathrm{H}}\underline{\boldsymbol{\Delta}}_{\mathrm{H}}\right). \tag{6.5}$$

6.3 Statistical evaluation

We keep the assumptions introduced at the end of the foregoing section. We further assume

- a random channel matrix of the type $\underline{\mathbf{H}}_{\mathrm{fair}}$, see Subsection 2.3.2, and

- a random error matrix $\underline{\boldsymbol{\Delta}}_{\mathrm{H}}$, which has i.i.d. bivariate Gaussian entries with equal variances $\sigma_{\Delta_{\mathrm{H}}}^2$ of all their real and imaginary parts.

Then, we obtain from (6.5) under consideration of (2.34) the mean

$$\Delta^2 = \mathop{\mathrm{E}}_{\mathbf{a},\underline{\mathbf{H}}}\left\{\Delta^{(r)2}\right\} = \mathop{\mathrm{E}}_{\mathbf{a},\underline{\mathbf{H}}}\left\{\mathrm{trace}\left(\underline{\mathbf{t}}^{(r)}\,\underline{\mathbf{t}}^{(r)\mathrm{H}}\underline{\boldsymbol{\Delta}}_{\mathrm{H}}^{\mathrm{H}}\underline{\boldsymbol{\Delta}}_{\mathrm{H}}\right)\right\} =$$

$$\mathrm{trace}\left(\underbrace{\mathop{\mathrm{E}}_{\mathbf{a},\underline{\mathbf{H}}}\left\{\underline{\mathbf{t}}^{(r)}\,\underline{\mathbf{t}}^{(r)\mathrm{H}}\right\}}_{2\cdot T\cdot\mathbf{I}^{N\times N}}\cdot\underbrace{\mathrm{E}\left\{\underline{\boldsymbol{\Delta}}_{\mathrm{H}}^{\mathrm{H}}\underline{\boldsymbol{\Delta}}_{\mathrm{H}}\right\}}_{2\cdot\sigma_{\Delta_{\mathrm{H}}}^2\cdot\mathbf{I}^{N\times N}}\right) = 4N\sigma_{\Delta_{\mathrm{H}}}^2 T. \tag{6.6}$$

As could be expected, Δ^2 of (6.6) is proportional to N and $\sigma_{\Delta_{\mathrm{H}}}^2$. As another important finding, Δ^2 is also proportional to the required mean radiated energy T of (2.34). From this follows that a reduction of T goes along with a lower sensitivity to inaccuracies of the CSI available in the transmitter, which can be considered a beneficial asset of the Approaches I and II to selectable data representation.

For the sake of a more detailed statistical analysis, we now concentrate on the componentwise mean square deviations Δ_n^2, $n = 1 \ldots N$. Due to the structure of the error matrix $\underline{\boldsymbol{\Delta}}_{\mathrm{H}}$, Δ^2 of (6.6) is equally distributed among the N components of $\underline{\mathbf{d}}^{(r)}$ of (1.9) or (1.45) so that we obtain the mean square deviations

$$\Delta_n^2 = \frac{\Delta^2}{N} = 4\sigma_{\Delta_{\mathrm{H}}}^2 \cdot T\,, \ = 1 \ldots N. \tag{6.7}$$

Consequently, as already mentioned above, the transmit vector $\underline{t}^{(r)}$ determined by (4.1) does not exactly lead to the desired landings in $\mathbb{G}_{\mathbf{a}^{(r)}}$. More precisely, with $\underline{\hat{H}}$ given by (6.1), the received vector reads

$$\underline{\hat{e}} = (\underline{H} + \underline{\Delta}_{\mathrm{H}})\, \underline{t} + \underline{n}\,, \tag{6.8}$$

and the vector containing the deviations from the desired landing points in $\mathbb{G}_{\mathbf{a}^{(r)}}$ caused by an imperfect knowledge of CSI can be statistically characterized by the variance of the real and imaginary parts of its N components. From (6.7) we obtain for this variance

$$\sigma^2_{\Delta_{\mathrm{CSI}}} = 2\sigma^2_{\Delta_{\mathrm{H}}} \cdot T\,. \tag{6.9}$$

Concerning the impact of said deviations on the error probability P_{e} of (1.1) $\sigma^2_{\Delta_{\mathrm{CSI}}}$ of (6.9) has to be added to the prevailing noise variance σ^2 so that we obtain an effective disturbance with the variance

$$\sigma^2_{\mathrm{total}} = \sigma^2_{\Delta_{\mathrm{CSI}}} + \sigma^2 \tag{6.10}$$

of both its real and imaginary parts. In other words, $\sigma^2_{\Delta_{\mathrm{CSI}}}$ can be considered a noise augmentation. We assume that the received noise vector $\underline{n}$ and the error matrix $\underline{\Delta}_{\mathrm{H}}$ of (6.1) are independent. Because both $\underline{n}$ and $\underline{\Delta}_{\mathrm{H}}$ are Gaussian, also the disturbance characterized by (6.10) is Gaussian.

6.4 Consideration for TxZF, TxNZF and ES

With the constants k_{TxZF}, k_{TxNZF} and k_{ES} the mean required transmit energy can be expressed as

$$T = a^2 \cdot k = a^2 \cdot \left\{ \begin{array}{ll} k_{\mathrm{TxZF}} & (\mathrm{TxZF}) \\ k_{\mathrm{TxNZF}} & (\mathrm{TxNZF}) \\ k_{\mathrm{ES}} & (\mathrm{ES}) \end{array} \right. . \tag{6.11}$$

From the values in Table 4.3 we obtain

$$\begin{aligned} k_{\mathrm{TxZF}} &= 5.46\,, \\ k_{\mathrm{TxNZF}} &= 1.53\,, \\ k_{\mathrm{ES}} &= 0.84\,, \end{aligned} \tag{6.12}$$

where we, in the cases TxNZF and ES set P equal to 36. With (6.9) and (6.11) the SNR at the demodulator outputs can be expressed as

$$\gamma_{\mathrm{Rx}} = \frac{a^2/2}{2\left(\sigma^2_{\Delta_{\mathrm{CSI}}} + \sigma^2\right)} = \frac{a^2/2}{2\left(\sigma^2 + k \cdot 2\sigma^2_{\Delta_{\mathrm{H}}} a^2\right)}\,. \tag{6.13}$$

If the pseudo SNR goes to infinity, then

$$\gamma_{\text{Rx},\infty} = \lim_{\gamma \to \infty} \gamma_{\text{Rx}} = \frac{1}{8\sigma_{\Delta_{\text{H}}}^2 \cdot k} \tag{6.14}$$

holds for the maximum possible γ_{Rx}. This value cannot be exceeded even if infinite transmit energy T would be available. With the values k of (6.12) we obtain from (6.14)

$$\gamma_{\text{Rx},\infty} = \frac{1}{8\sigma_{\Delta_{\text{H}}}^2} \left\{ \begin{array}{c} 1/k_{\text{TxZF}} \\ 1/k_{\text{TxNZF}} \\ 1/k_{\text{ES}} \end{array} \right. = \left\{ \begin{array}{c} \gamma_{\text{TxZF},\infty} \\ \gamma_{\text{TxNZF},\infty} \\ \gamma_{\text{ES},\infty} \end{array} \right. . \tag{6.15}$$

From (6.15) the asymptotic SNR degradations among the schemes considered in this section are given by the ratios of the specific $\gamma_{\text{Rx},\infty}$, which are equivalent to the inverses ratios of the constants k_{TxZF}, k_{TxNZF} and k_{ES} of (6.12), yielding

$$\frac{\gamma_{\text{TxZF},\infty}}{\gamma_{\text{TxNZF},\infty}} = \frac{k_{\text{TxNZF}}}{k_{\text{TxZF}}} = 0.28 \,, \tag{6.16}$$

$$\frac{\gamma_{\text{TxZF},\infty}}{\gamma_{\text{ES},\infty}} = \frac{k_{\text{ES}}}{k_{\text{TxZF}}} = 0.15 \tag{6.17}$$

and

$$\frac{\gamma_{\text{TxNZF},\infty}}{\gamma_{\text{ES},\infty}} = \frac{k_{\text{ES}}}{k_{\text{TxNZF}}} = 0.55 \,. \tag{6.18}$$

Hence, asymptotically, for the case of imperfect CSI knowledge at the APs, the advantage of reduced transmit energies by resorting to precoding with selectable data representation are doubled up by the additional advantage of lower SNR degradations due to the noise term of (6.10), see Table 4.3. This is illustrated in Fig. 6.1, which shows the dependence of $\gamma_{\text{Rx},\infty}$ on $\sigma_{\Delta_{\text{H}}}^2$ and displays how $\gamma_{\text{Rx},\infty}$ attains monotonically decreasing finite values as $\sigma_{\Delta_{\text{H}}}^2$ increases, whereas $\gamma_{\text{Rx},\infty}$ in the case of vanishing $\sigma_{\Delta_{\text{H}}}^2$ is infinite.

For the non-asymptotic case it can be quite generally stated that precoding schemes with reduced transmit energies experience lower SNR degradations so that their performance advantage becomes more pronounced in the case of imperfect CSI available at the APs. Figs. 6.2 and 6.3 show the required adjustments of a^2 and T for different $\sigma_{\Delta_{\text{H}}}^2$ required to obtain γ_{Rx} equal to 10. Exemplary, we desire γ_{Rx} equal to 10 and let $\sigma_{\Delta_{\text{H}}}^2$ vary under the assumption of a certain variance of σ^2 of (6.13). Then, for a specific $\sigma_{\Delta_{\text{H}}}^2$ different a^2 and T of (6.11) result. We set σ^2 equal to $1/40$ in order to start from unit a^2, for the case of perfect CSI available at the APs, that is vanishing $\sigma_{\Delta_{\text{H}}}^2$. As can be seen in Fig. 6.2, a^2 converges to ∞ as $\gamma_{\text{Rx},\infty}$ approaches the desired value of γ_{Rx}, which for our example is equal to 10. Accordingly, T of (6.11) converges to infinity as well, see Fig. 6.3.
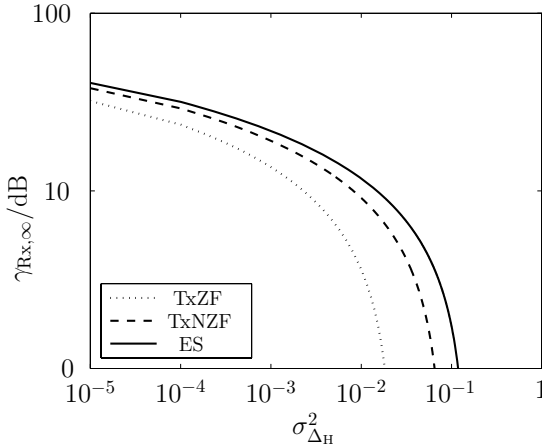
Fig. 6.1. $\gamma_{\text{Rx},\infty}$ versus $\sigma_{\Delta_{\text{H}}}^2$

Furthermore, it can be concluded from the Figs. 6.2 and 6.3 that the advantage of the schemes with reduced transmit energies can be basically exploited in two ways:

- Either with the same T, a higher value of $\sigma_{\Delta_{\text{H}}}^2$ is tolerable, which can be determined via the shift in the horizontal axis of Fig. 6.3, or

- for the same $\sigma_{\Delta_{\text{H}}}^2$, smaller transmit energies T are acceptable, which can be determined via the shift in the vertical axis of Fig. 6.3.

In Table 6.1, we determine the latter and depict the average transmit energy T for different values of $\sigma_{\Delta_{\text{H}}}^2$. In Table 6.1, additionally to the transmit energies T also their relative values in dB are depicted in brackets, which confirm that the performance advantage becomes more pronounced as $\sigma_{\Delta_{\text{H}}}^2$ increases. Finally, the desired γ_{Rx} cannot be achieved, which in Table 6.1 is denoted by the entry 'x', and consequently, no relative values are displayed.

The exclusion of MESP in the considerations of this section is due to the fact that in the case of MESP, the transmit signal generation depends on the actual noise variances and resorts to representative domains with continuous valued representatives. Therefore, the expression for the SNR at the demodulator outputs similar to (6.13) has to be determined by a more detailed analysis, which, for the sake of brevity, is omitted here. However, in principle, such an analysis would reveal similar results as obtained by the consideration above.
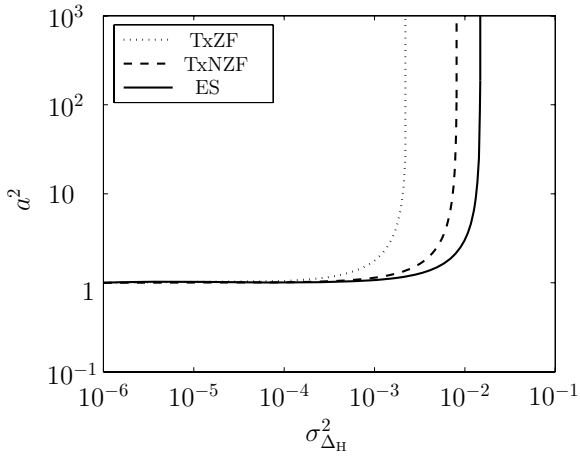
Fig. 6.2. a^2 versus $\sigma^2_{\Delta_H}$ for $\gamma_{Rx} = 10$
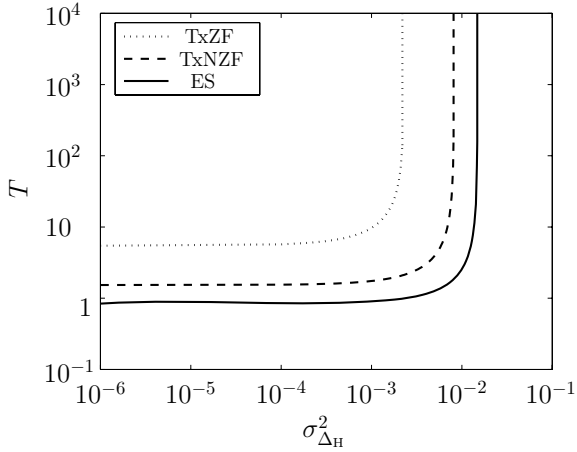
Fig. 6.3. T versus $\sigma^2_{\Delta_H}$ required for $\gamma_{Rx} = 10$

$\sigma^2_{\Delta_H} =$	0	10^{-3}	$2 \cdot 10^{-3}$	$5 \cdot 10^{-3}$	10^{-2}
TxZF	5.46 (0)	9.69 (0)	43.20 (0)	x	x
TxNZF	1.53 (-5.5)	1.74 (-7.5)	2.03 (-13.3)	3.94	x
ES	0.84 (-8.2)	0.90 (-10.4)	0.97 (-16.5)	1.27	2.56

Table 6.1. Required average transmit energy T depending on $\sigma^2_{\Delta_H}$

6.5   Résumé

An indispensable working precondition for receiver oriented transmission systems is the availability of channel state information on the transmitter side, for instance in the case of mobile radio systems at the base stations. In practice, this information has to be gained by channel estimators which are prone to errors. Therefore, the channel state information is only available in a more or less garbled form. The impact of an erroneous channel state information on the system performance scales with the radiated power. Therefore, receiver oriented transmission systems with reduced transmit power due to selectable data representation are less sensitive to erroneous channel state information than receiver oriented transmission systems with unique data representation.

Chapter 7
Summary

7.1 English

The present thesis deals with multi-user mobile radio systems, and more specifically, the downlinks (DL) of such systems. As a key demand on future mobile radio systems, they should enable highest possible spectrum efficiency. It is well known that, in principle, the utilization of multi-antennas in the form of MIMO systems, offers considerable potential to meet this demand. However, concerning the practical implementation of such MIMO multi-user downlinks, additional requirements on the concepts for future cellular and non-cellular mobile radio systems exist:

- The cost and complexity of the mobile terminals (MT) should be low, and

- with a view to checking the disturbance of other radio links and/or the mitigation of intercell interference, the transmit energies should be minimized.

Concerning the first one of these requirements, the following statements can be made:

- In the DL the receiver algorithms of the MTs should be a priori (off-line) determined under the condition of low complexity. From these, the generation of the transmit signals in the access points (AP) should follow a posteriori (on-line) under consideration of channel state information (CSI). The rationale of system design as explained above is termed receiver oriented (RO), resulting in simple receivers, which in the case of the DL are in the MTs.

- For the uplink (UL), it would be advisable to determine the transmitter algorithms of the MTs a priori (off-line) with a view to low complexity, whereas the way how the received signals are processed in the APs would then follow a posteriori (on-line) under consideration of CSI. The just mentioned rationale of system design is termed transmitter oriented (TO), resulting in simple transmitters, which in the case of the UL again are the in MTs.

To summarize, in order to keep the cost and complexity of the MTs low, one should resort to TO in the UL and to RO in the DL, so that simple MT implementations can be achieved, whereas rather complicated implementations can be tolerated in the APs.

Concerning the above mentioned energy issue, the DL is the more critical one. This is due to the growing importance of wireless Internet applications, in which the DL data

rates and, consequently, the radiated DL energies tend to be substantially higher than the corresponding UL quantities.

In this thesis, precoding schemes for MIMO multi-user mobile radio DLs are considered, where, in order to keep the MT complexity low, the rationale RO is adopted, with the main focus to further reduce the required transmit energy in such systems. Unfortunately, besides the mentioned low receiver complexity, conventional RO schemes, such as Transmit Zero Forcing (TxZF), do not offer any transmit energy reductions as compared to TO schemes. Therefore, the main goal of this thesis is the design and analysis of precoding schemes in which such transmit energy reductions become feasible - under virtually maintaining the low receiver complexity - by means of replacing the conventional unique mappings by the selectable representations of the data. Following this rationale, two basic approaches to precoding with selectable data representations are proposed:

- Approach I, a concept which extends TxZF by introducing the idea of Tomlinson-Harashima precoding (THP), that is replacing the unique valued discrete representatives of TxZF by a set of discrete valued representatives through periodic extension of the original constellation.

- Approach II, a concept in which, in the demodulators on the receive side, the "hard" spot landings on discrete valued representatives typical of TxZF are substituted by less stringent, that is "soft" landings in continuous valued representative domains.

In the case of Approach I, the optimum solution requires exhaustive search among all valid data representations. Therefore an approximate, but systematic and rather low-cost stepwise solution is adopted, based on Transmit Non-linear Zero Forcing (TxNZF), and compared to the results obtained via ES. In the case of Approach II a systematic solution is developed based on Sequential Quadratic Programming (SQP), which is termed Minimum Energy Soft Precoding (MESP). Furthermore, a procedure achieving the minimum possible transmit energy for a desired symbol error probability is explained for MESP. The performance evaluations made confirmed the potential of transmit energy reductions in the cases of TxNZF, ES and MESP. A dramatic advantage of TxNZF and ES over TxZF, and a still remarkable advantage of MESP over TxZF is observed with respect to the required transmit energy.

However, the energywise performance advantage of the precoding schemes with selectable data representation are accompanied by modified signal structures arriving at the receivers with respect to both their amplitudes and the associated decision regions. Whereas in the case of Approach I no explicit modifications are required in the receivers, in the case of Approach I the receivers have to be additionally equipped with modulo-reduction units for data detection, which, however, are not included in the present stan-

dards. With respect to the data acquisition in terms of A/D conversion, the amplitude dynamics of the received signals cannot be mitigated as compared to conventional RO schemes; rather, these dynamics are increased as the transmit energies are reduced. Therefore a trade-off between transmit power reduction and increased receive signal dynamics should be on the agenda.

Concerning the channel access scheme, Orthogonal Frequency Division Multiplex (OFDM) is presently being favored as the most promising candidate in the standardization process of the enhanced 3G and forthcoming 4G systems, because it allows a very flexible resource allocation and low receiver complexity. Receiver oriented (RO) MIMO OFDM multi-user downlink transmission, in which channel equalization is already performed in the transmitter of the AP, further contributes to low receiver complexity in the MTs. For these reasons, OFDM is adopted in the target system of the considered RO precoding schemes.

In the RO precoding schemes considered in this thesis the knowledge of CSI in the AP in the form of the channel matrix is essential. Independently of the applied duplexing schemes FDD or TDD, the provision of this information to the AP is always erroneous. However, it is shown that the impact of such deviations not only scales with the variance of the channel estimation errors, but also with the required transmit energies. Accordingly, the reduced transmit energies of the precoding schemes with selectable data representation also have the advantage of a reduced sensitivity to imperfect knowledge of CSI. In fact, these two advantages are coupled with each other.

7.2 Deutsch

Der Kontext dieser Arbeit sind Mehrteilnehmer-Mobilfunksysteme, insbesondere deren Abwärtsstrecke. Ein zentraler Aspekt zukünftiger Mobilfunksysteme ist der Wunsch nach einer möglichst hohen spektralen Effizienz, d.h. einer möglichst hohen Anzahl koexistenz-fähiger Funkverbindungen in einem möglichst kleinen Frequenzbereich. Es ist allgemein bekannt, dass die Verwendung mehrerer Antennen an den Übergangspunkten der Übertragungsstrecken zum freien Raum in Form von MIMO Systemen potentiell für diesen Zweck geeignet sind. Für die Realisierung solcher Mehrteilnehmer-Mobilfunkabwärtsstrecken mit MIMO-Antennen gelten jedoch weitere Forderungen an den Entwurf zukünftiger zellularer bzw. nicht zellularer Mobilfunksysteme:

- Kosten und Komplexität der Mobilstationen sollen gering sein, und

- im Hinblick auf die Störung anderer Funkverbindungen und/oder die Vermeidung von Interferenzen innerhalb einer Funkzelle bzw. in benachbarten Funkzellen sollte die abgestrahlte Sendeleistung minimiert werden.

Bezüglich der ersten Forderung gelten für den Systementwurf folgende grundlegende Aussagen:

- Im Entwurf der Abwärtsstrecke sollten die empfängerseitigen Signalverarbeitungsalgorithmen der Mobilstationen vor der Übertragung offline so festgelegt werden, dass sich für die Mobilstationen eine möglichst niedrige Komplexität ergibt. Im Anschluss sollte, unter Berücksichtigung der festgelegten Empfangsalgorithmen, der Entwurf der Sendesignale online erfolgen, und zwar unter Berücksichtigung von Kanalzustandsinformation. Dieses Entwurfskonzept wird als empfängerorientiert bezeichnet und führt zu besonders einfachen Empfängern, welche im Fall der Abwärtsstrecke in den Mobilstationen sind.

- Für die Aufwärtsstrecke ist es ratsam, die senderseitigen Signalerzeugungsalgorithmen im Vorfeld der Übertragung offline festzulegen, so dass möglichst einfache Senderstrukturen resultieren. Die komplementär zur Senderstruktur angewandten Verfahren zur Verarbeitung der Empfangssignale in den Zugangspunkten werden unter Berücksichtigung der Kanalzustandsinformation im Anschluss an die Übertragung online angepasst. Das soeben geschilderte Entwurfskonzept wird als senderorientiert bezeichnet und führt zu besonders einfachen Sendern, welche für den Fall der Aufwärtsstrecke wiederum in den Mobilstationen sind.

Daher sollten, um möglichst einfache Empfänger- und Senderstrukturen und somit kosten- und aufwandsgünstige Mobilstationen zu erhalten, das Konzept der Senderorientierung in

der Aufwärtsstrecke und das Konzept der Empfängerorientierung in der Abwärtsstrecke beim Systementwurf verwendet werden. In den Zugangspunkten hingegen können komplexere Strukturen toleriert werden.

Bezüglich der abgestrahlten Energie ist die Abwärtsstrecke besonders kritisch aufgrund der steigenden Bedeutung von drahtlosen Internetanwendungen. In solchen Anwendungen übersteigt die Datenrate der Abwärtsstrecke jene der Aufwärtsstrecke um Größenordnungen, und somit auch die abgestrahlte Leistung.

Aufgrund spezieller Anforderungen an die betrachteten Systeme werden in dieser Arbeit Verfahren der Sendesignalvorverarbeitung für die Mehrteilnehmer-Mobilfunkabwärtsstrecke mit MIMO-Antennen betrachtet, in denen, um die Komplexität der Mobilstationen gering zu halten, das Konzept der Empfängerorientierung übernommen wird. Das Hauptaugenmerk beim Untersuchen der in der Arbeit präsentierten neuartigen Verfahren liegt dabei auf der Reduktion der erforderlichen Sendeleistung, da konventionelle empfängerorientierte Verfahren wie z. B. die totale Interferenzeliminierung (TxZF) abgesehen von der vereinfachten Empfängerstruktur keine weiteren Vorteile bieten, insbesondere keine Freiheitsgrade zur Reduktion der erforderlichen Sendeleistung. Ziel dieser Arbeit sind daher der Entwurf und die Analyse von Verfahren zur Sendesignalvorverarbeitung, die - unter Beibehaltung der vereinfachten Empfängerstrukturen - Möglichkeiten bieten, die Sendeleistung im Vergleich zu denjenigen der konventionellen Verfahren zu reduzieren. Hierfür wird das Konzept der eindeutigen Abbildung von Datenelementen auf feste Werte innerhalb der komplexen Ebene durch das Konzept der wählbaren Repräsentation von Datenelementen ersetzt. Auf der Grundlage dieses Konzepts werden zwei Ansätze der wählbaren Datenrepräsentation eingeführt:

- Ansatz I, in dem das konventionelle Verfahren TxZF durch ein Prinzip ähnlich der Tomlinson-Harashima-Vorcodierung erweitert wird. Dadurch wird die eindeutige Abbildung der Datenelemente auf fest zugeordnete diskrete Werte innerhalb der komplexen Ebene mit einer Vielfalt von representativen diskreten Werten durch periodische Erweiterung der ursprünglichen Datenkonstellation ersetzt.

- Ansatz II, in dem in den Demodulatoren auf der Empfängerseite die 'harten' Landungen auf fest zugeordnete diskrete 'Werte', siehe TxZF, ersetzt werden durch weniger restriktive 'weiche' Landungen innerhalb von wertekontinuierlichen representativen Gebieten für die Datenelemente.

Ansatz I erfordert für die optimale Lösung eine aufwendige und erschöpfende Suche (ES) innerhalb aller gültigen representativen Werte die in der wertdiskreten Menge von Datenrepräsentanten enthalten sind. Daher wird zusätzlich eine aufwandsgünstige, systematische Lösung basierend auf einem schrittweisen Verfahren betrachtet. Diese approxi-

miert die optimale Lösung beruhend auf dem Verfahren Transmit Non-linear Zero Forcing
(TxNZF) und wird in der Arbeit mit der erschöpfenden Suche verglichen. Für Ansatz II
wird eine systematische Lösung anhand von Sequentieller Quadratischer Programmierung
(SQP) entwickelt, die Minimum Energy Soft Precoding (MESP) genannt wird. Zusätzlich
wird für MESP eine Prozedur erläutert, durch die für eine vorgegebene Fehlerwahrschein-
lichkeit die minimal mögliche Sendeleistung erreicht wird. Simulative Untersuchungen der
Leistungsfähigkeit bestätigen die erwartete Reduktion der Sendeleistungen der genann-
ten Verfahren im Vergleich zu TxZF. Hierbei ergibt sich ein drastischer Gewinn von ES
und TxNZF gegenüber TxZF und ein immerhin noch beachtlicher Gewinn von MESP
gegenüber TxZF im Hinblick auf die erforderliche Sendeleistung.

Der Vorteil reduzierter Sendeleistungen der betrachteten Verfahren wird von verän-
derten Signalstrukturen der empfangenen Werte begleitet, sowohl mit Bezug auf deren
Amplitudendynamik als auch die zugeordneten Entscheidungsgebiete. Im Gegensatz zu
Ansatz II, für den keine expliziten Anpassungen für die Zuordnung der Empfangswerte
zu Entscheidungsgebieten erfolgt, müssen im Fall von Ansatz I die Empfänger zusätz-
lich mit Modulo-Reduktionseinheiten für die Detektion ausgestattet sein, die derzeit noch
nicht standardkompatibel sind. Im Hinblick auf die veränderten Amplitudendynamiken
muss zur korrekten Datenerfassung in beiden Ansätzen der dynamische Bereich der A/D-
Wandler innerhalb der Empfänger angepasst werden, da die erhöhten Amplitudendy-
namiken als direkte Konsequenz der reduzierten Sendeleistungen erfolgen und somit nicht
verhindert werden können. Daher sollte ein Kompromiss zwischen der erzielten Reduk-
tion der Sendeleistungen und der damit verbundenen erhöhten Amplitudendynamik erzielt
werden.

Als Kanalzugriffsverfahren wird derzeit OFDM als vielversprechendster Kandidat in-
nerhalb der Standardisierungsverfahren favorisiert, sowohl für die Erweiterungen der Mo-
bilfunksysteme der dritten Generation als auch für die zukünftigen Mobilfunksysteme
der vierten Generation. Wesentliche Gründe hierfür sind die Möglichkeiten der flexiblen
Ressourcenverteilung sowie die geringe Komplexität der Empfänger in den Mobilstationen.
Empfängerorientierte MIMO-OFDM-Mehrteilnehmer-Mobilfunkabwärtsstrecken, in de-
nen die Entzerrung des Kanals bereits am Sender, d. h. in den Zugangspunkten vorgenom-
men wird, tragen darüber hinaus zu einer geringeren Komplexität der Empfänger bei.
Deshalb wird OFDM speziell im Hinblick auf dessen Verwendung für zukünftige Mobil-
funksysteme für die betrachteten empfängerorientierten Sendesignalvorverarbeitungsver-
fahren untersucht.

Die Verfügbarkeit von Kanalzustandsinformation in Form von Kanalmatrizen in den
Sendern ist für die empfängerorientierten Sendesignalvorverarbeitungsverfahren, die in
dieser Arbeit betrachtet werden, unerlässlich. Unabhängig von dem verwendeten Du-

plexverfahren, d. h. TDD oder FDD, ist die Bereitstellung dieser Information zu dem Zugangspunkt immer fehlerbehaftet, was zur Verschlechterung der Leistungsfähigkeit der betrachteten Verfahren führt. Es wird jedoch gezeigt, dass die degradierende Auswirkung solcher Fehler nicht nur von der Varianz dieser Abweichungen abhängt, sondern auch mit der benötigten Sendeleistung skaliert. Daher haben die reduzierten Sendeleistungen der Sendesignalvorverarbeitungsverfahren mit wählbarer Datenrepräsentation auch den Vorteil einer geringeren Anfälligkeit gegenüber fehlerhafter Kanalkenntnis in den Zugangspunkten.

Appendix A

Derivations of closed-form analytic expressions

A.1 PDFs of the singular values of i.i.d. distributed complex Gaussian matrices

In this section, an analytical approach based on random matrix theory [Ede89], feasible for the case of the ensemble of matrices of the type $\underline{\mathbf{H}}_{\text{fair}}$, which will be pursued.

In order to apply results from random matrix theory [Ede89] we first consider the Gram matrix

$$\underline{\mathbf{W}} = \underline{\mathbf{H}}_{\text{fair}}\underline{\mathbf{H}}_{\text{fair}}^{\text{H}}, \tag{A.1}$$

whose positive square roots are equivalent to the singular values of $\underline{\mathbf{H}}_{\text{fair}}$. Due to this relation, the marginal PDFs of the singular values can be obtained via transformation of the marginal PDFs of the corresponding eigenvalues. If $\underline{\mathbf{H}}_{\text{fair}}$ has i.i.d. bivariate Gaussian distributed entries of both its real and imaginary parts with equal unit variances σ_{H}^2, which is in accordance with the assumptions above, see Section 2.2, then the matrix $\underline{\mathbf{W}}$ is known to be complex Wishart distributed [Jam64, Ede89] and therefore is termed Wishart matrix hereafter. The Wishart matrix $\underline{\mathbf{W}}$ is self-adjoint and Hermitian, hence its eigenvalues are non-negative and real, with joint PDF $p_{\mathbf{v}}(\nu_1 \ldots \nu_G)$ of the ordered eigenvalues $\nu_1 \geq \nu_2 \ldots \nu_{G-1} \geq \nu_G$ given by [Jam64, Ede89]

$$p_{\mathbf{v}}(\nu_1 \ldots \nu_G) = K_{G,S} \prod_{i=1}^{G} e^{-\nu_i} \nu_i^{(S-G)} \prod_{i<j}^{G} (\nu_i - \nu_j)^2 \tag{A.2}$$

with

$$G = \min(Q, N) \tag{A.3}$$

and

$$S = \max(Q, N) \tag{A.4}$$

where $K_{G,S}$ is a scalar constant [Ede89] given by

$$K_{G,S} = \frac{\pi^{G(G-1)}}{\Gamma_G(S)\Gamma_{mG}(G)}. \tag{A.5}$$

$\Gamma_G(a)$ denotes the complex multivariate gamma function

$$\Gamma_G(a) = \pi^{G(G-1)/2} \prod_{i=1}^{G} \Gamma(a - i + 1) \tag{A.6}$$

which is calculated by repeatedly evaluating the gamma function

$$\Gamma(x) = \int_0^{\infty} t^{(x-1)} e^{-t} dt \,. \tag{A.7}$$

With these quantities, the marginal PDF of the g-th largest eigenvalue of $\underline{\mathbf{W}}$ is then given by [Jam64]

$$p_{v_g}(\nu_g) = K_{\text{norm}} \cdot \int_{\nu_g}^{\infty} \left\{ \int_{\nu_{g-1}}^{\infty} \cdots \right.$$

$$\left\{ \int_{\nu_3}^{\infty} \left\{ \int_{\nu_2}^{\infty} \left\{ \int_0^{\nu_g} \cdots \left\{ \int_0^{\nu_{G-1}} p(\nu_1 \ldots \nu_G) d\nu_G \right\} \cdots \right. \right. \right. \tag{A.8}$$

$$\left. d\nu_{g+1} \right\} d\nu_1 \right\} d\nu_2 \right\} \ldots d\nu_{g-2} \right\} d\nu_{g-1} \,,$$

where K_{norm} is a constant that normalizes the PDF to have the property.

$$\int_0^{\infty} p_{\nu_g}(\nu_g) d\nu_g = 1 \tag{A.9}$$

For clarification of (A.8), following statements shall be made [Wen02]: Since the eigenvalues are ordered, $\nu_1 \geq \cdots \geq \nu_G$, the marginal PDF $p_{v_g}(\nu_g)$ of an arbitrary eigenvalue ν_g is found by integrating out the order $G - 1$ eigenvalues from (A.2) one by one in a certain order, e.g. starting by integrating out the smallest eigenvalue ν_G. Since $0 \leq \nu_G \leq \nu_{G-1}$, the integration limits that should be used to find the marginal PDF $p(\nu_1 \ldots \nu_{G-1})$ are

$$p(\nu_1 \ldots \nu_{G-1}) = \int_0^{\nu_{G-1}} p(\nu_1 \ldots \nu_G) d\nu. \tag{A.10}$$

Now, since ν_G has been integrated out, the smallest eigenvalue is ν_{G-1}, which is bounded by $0 \leq \nu_{G-1} \leq \lambda_{G-2}^2$. Hence, the joint PDF of the $G - 2$ largest eigenvalues is found from

$$p(\nu_1 \ldots \nu_{G-2}) = \int_0^{\nu_{G-2}} p(\nu_1 \ldots \nu_{G-1}) d\nu_{G-1}. \tag{A.11}$$

This procedure is iterated until we reach the joint PDF of the g largest eigenvalues $p(\nu_1, \ldots, \nu_k)$. By integrating out the largest eigenvalue, which is bounded as $\nu_2 \leq \nu_1 < \infty$,

we find

$$p(\nu_2 \ldots \nu_g) = \int_{\nu_2}^{\infty} p(\nu_1 \ldots \nu_g) d\nu_1 \tag{A.12}$$

and then proceed iteratively until only the marginal PDF for the eigenvalue $p_{\nu_g}(\nu_g)$ remains. This iterative manner for finding $p_g(\nu_g)$ can be written compactly as (A.8).

The procedure explained above is now applied to the ensemble of 4×4 matrices of the type $\underline{\mathbf{H}}_{\mathrm{fair}}$ considered in this thesis. Then, according to (A.2) the joint PDF of the ordered eigenvalues is given by

$$p(\nu_1, \nu_2, \nu_3, \nu_4) =$$
$$\frac{1}{24} e^{-\nu_1 - \nu_2 - \nu_3 - \nu_4} (\nu_1 - \nu_2)^2 (\nu_1 - \nu_3)^2 (\nu_1 - \nu_4)^2 (\nu_2 - \nu_3)^2 (\nu_2 - \nu_4)^2 (\nu_3 - \nu_4)^2. \tag{A.13}$$

To find the marginal PDF of the smallest eigenvalue, we integrate out the three largest as

$$p_{v_4}(\nu_4) = \int_{\nu_4}^{\infty} \left\{ \int_{\nu_3}^{\infty} \left\{ \int_{\nu_2}^{\infty} p(\nu_1 \ldots \nu_4) d\nu_1 \right\} d\nu_2 \right\} d\nu_3 = 4e^{-4\nu_4}. \tag{A.14}$$

The two middle eigenvalues have the marginal PDF's

$$p_{v_3}(\nu_3) = \int_{\nu_3}^{\infty} \left\{ \int_{\nu_2}^{\infty} \left\{ \int_{0}^{\nu_3} p(\nu_1 \ldots \nu_4) d\nu_4 \right\} d\nu_1 \right\} d\nu_3$$
$$= 12e^{-3\nu_3} - 12e^{-4\nu_3} - 12e^{-3\nu_3}\nu_3 + \frac{5}{6}e^{-3\nu_3}\nu_3^5 \tag{A.15}$$
$$+ 6e^{-3\nu_3}\nu_3^2 + \frac{28}{6}e^{-3\nu_3}\nu_3^3 + \frac{23}{6}e^{-3\nu_3}\nu_3^4 + \frac{1}{2}e^{-3\nu_3}\nu_3^6$$

and

$$p_{\nu_2}(\nu_2) = \int_{\nu_2}^{\infty} \left\{ \int_{0}^{\nu_2} \left\{ \int_{0}^{\nu_1} p(\nu_1 \ldots \nu_4) d\nu_1 \right\} d\nu_3 \right\} d\nu_4$$
$$= -\frac{8}{3}e^{-2\nu_2} + \frac{8}{6}e^{-2\nu_2} - 24e^{-2\nu_2}\nu_2 + 12e^{-4\nu_2} + \frac{4}{9}e^{-2\nu_2}\nu_2^6 - \frac{1}{6}e^{-3\nu_2}\nu_2^6$$
$$- \frac{4}{3}e^{-2\nu_2}\nu_2^5 - \frac{23}{3}e^{-3\nu_2}\nu_2^4 + \frac{1}{72}e^{-2\nu_2}\nu_2^8 - \frac{5}{3}e^{-3\nu_2}\nu_2^5 - \frac{1}{18}e^{-2\nu_2}\nu_2^7 + 24e^{-2\nu_2} \tag{A.16}$$
$$+ 24e^{-2\nu_2}\nu_2^2 - \frac{28}{3}e^{-3\nu_2}\nu_2^3 - 12e^{-3\nu_2}\nu_2^2 - 24e^{-3\nu_2} + 24e^{-3\nu_2}$$

and the PDF of the largest eigenvalue ν_1 is given by

$$p_{\nu_1}(\nu_1) = \int_0^{\nu_1} \left\{ \int_0^{\nu_2} \left\{ \int_0^{\nu_3} p(\nu_1 \ldots \nu_4) d\nu_2 \right\} d\nu_3 \right\} d\nu_4$$

$$= 4e^{-\nu_1} + \frac{21}{6}e^{-\nu_1}\nu_1^4 + \frac{1}{6}e^{-\nu_1}\nu_1^6 - \frac{1}{2}e^{-\nu_1}\nu_1^5 - 12e^{-\nu_1}\nu_1 - \frac{34}{3}e^{-\nu_2}\nu_2^3$$

$$+18e^{-\nu_1}\nu_1^2 + 12e^{-3\nu_1} - 12e^{-2\nu_1} + 24e^{-2\nu_1}\nu_1 - \frac{4}{9}e^{-2\nu_1}\nu_1^6 + \frac{1}{18}e^{-2\nu_2}\nu_2^7 \qquad \text{(A.17)}$$

$$+6e^{-3\nu_1}\nu_1^2 - 12e^{-3\nu_1}\nu_1 + \frac{4}{3}e^{-2\nu_1}\nu_1^5 - \frac{4}{3}e^{-2\nu_1}\nu_1^4 + \frac{14}{3}e^{-3\nu_1}\nu_1^3 - 4e^{-4\nu_2}$$

$$+\frac{8}{3}e^{-2\nu_1}\nu_1^3 - 24e^{-2\nu_1}\nu_1^2 + \frac{1}{12}e^{-3\nu_1}\nu_1^6 + \frac{23}{6}e^{-3\nu_1}\nu_1^4 - \frac{1}{72}e^{-2\nu_1}\nu_1^8 + \frac{5}{6}e^{-3\nu_2}\nu_2^5 .$$

The marginal PDF's $p_{\nu_g}(\nu_g)$ of the eigenvalues ν_g now have to be transformed into the marginal PDF's $p_{\lambda_g}(\lambda_g)$ of the singular values λ_g. With the relation

$$\lambda_g = +\sqrt{\nu_g}, \qquad \text{(A.18)}$$

the marginal PDF's $p_{\lambda_g}(\lambda_g)$ of the singular values λ_g are given by the random variable transformation [Pap91]

$$p_{\lambda_g}(\lambda_g) = 2 \cdot \lambda_g \cdot p_{\nu_g}(\lambda_g^2) \qquad \text{(A.19)}$$

yielding

$$p_{\lambda_4}(\lambda_4) = 2 \cdot \lambda_4 \cdot p_{\nu_4}(\lambda_4^2) = 8 \cdot e^{-4 \cdot \lambda_3^2}, \qquad \text{(A.20)}$$

$$p_{\lambda_3}(\lambda_3) = 2 \cdot \lambda_3 \cdot p_{\nu_3}(\lambda_3^2) =$$
$$\left(24(1 - e^{-\lambda_3^2})\lambda_3 - 24\lambda_3^3 + 12\lambda_3^5 + \frac{28}{3}\lambda_3^7 + \frac{23}{3}\lambda_3^9 + \frac{5}{3}\lambda_3^{11} + \frac{1}{6}\lambda_3^{13} \right) e^{-3 \cdot \lambda_3^2}, \qquad \text{(A.21)}$$

$$p_{\lambda_2}(\lambda_2) = 2 \cdot \lambda_2 \cdot p_{\nu_2}(\lambda_2^2) = \left(24(1 - 2e^{-\lambda_2^2} + 1e^{-2\lambda_2^2})\lambda_2 - 48(1 - e^{-\lambda_2^2})\lambda_2^3 - \right.$$
$$24(2 - e^{-\lambda_2^2})\lambda_2^5 - (\frac{16}{3} + \frac{56}{3}e^{-\lambda_2^2})\lambda_2^7 + (\frac{8}{3} - \frac{46}{3}e^{-\lambda_2^2})\lambda_2^9 - \qquad \text{(A.22)}$$
$$\left. (\frac{8}{3} + \frac{10}{3}e^{-\lambda_2^2})\lambda_2^{11} + (\frac{8}{9} - \frac{1}{3}e^{-\lambda_2^2})\lambda_2^{13} - \frac{1}{9}\lambda_2^{15} + \frac{1}{36}\lambda_2^{17} \right) e^{-2 \cdot \lambda_2^2}$$

and

$$p_{\lambda_1}(\lambda_1) = 2 \cdot \lambda_1 \cdot p_{\nu_1}(\lambda_1^2) =$$

$$\left(4(2 - 6e^{-\lambda_1^2} + 6e^{-2\lambda_1^2} - e^{-3\lambda_1^2})\lambda_1 - 24(1 - 2e^{-\lambda_1^2} + e^{-2\lambda_1^2})\lambda_1^3 + \right.$$
$$(\frac{108}{3} - 48e^{-\lambda_1^2} + 12e^{-2\lambda_1^2})\lambda_1^5 - (\frac{68}{3} - \frac{16}{3}e^{-\lambda_1^2} - \frac{28}{3}e^{-2\lambda_1^2})\lambda_1^7 +$$
$$(\frac{21}{3} - \frac{8}{3}e^{-\lambda_1^2} + \frac{23}{3}e^{-2\lambda_1^2})\lambda_1^9 - (1 - \frac{8}{3}e^{-\lambda_1^2} - \frac{5}{3}e^{-2\lambda_1^2})\lambda_1^{11} + \qquad \text{(A.23)}$$
$$\left. (\frac{1}{18} + \frac{8}{9}e^{-\lambda_1^2} + \frac{1}{6}e^{-2\lambda_1^2})\lambda_1^{13} + \frac{1}{9}e^{-\lambda_1^2}\lambda_1^{15} - \frac{1}{36}e^{-\lambda_1^2}\lambda_1^{17} \right) e^{-\lambda_1^2} .$$

A.2   PDF of the required transmit energy of TxZF

The transmit energy required for TxZF can be expressed as

$$T = \frac{1}{2}\sigma_d^2 \sum_{g=1}^{G} \frac{1}{\lambda_g^2}\,, \tag{A.24}$$

see (3.65). However, in the following we only consider the sum of the inverses

$$X = \sum_{g=1}^{G} \frac{1}{\lambda_g^2} \tag{A.25}$$

and its distribution, as with $p_X(X)$ the distribution of T simply can be obtained the transformation

$$p_T(T) = \frac{2}{\sigma_d^2} \cdot p\left(\frac{2X}{\sigma_d^2}\right)\,. \tag{A.26}$$

For the distribution of X we have to consider again the joint PDF $p_{\mathbf{v}}(\nu_1 \ldots \nu_G)$ of the ordered their eigenvalues as the values $\lambda_g, 1 \ldots G$ are not independent of each other, that is

$$p_{\mathbf{v}}(\nu_1 \ldots \nu_G) \neq p_{v_1}(\nu_1) \ldots p_{v_G}(\nu_G) \tag{A.27}$$

holds for the joint and marginal PDFs of the eigenvalues. We now derive the PDF of X by transforming the set of variables $\mathbf{v} = (v_1 \ldots v_G)$ of the joint PDF of (A.2) into a new set of random variables $\mathbf{x} = (x_1 \ldots x_G)$ according to

$$x_1 = \sum_{g=1}^{G} \frac{1}{v_g} = \sum_{g=1}^{G} \frac{1}{\lambda_g^2}\,,$$

$$x_2 = v_2,\ x_3 = v_3, \ldots, x_G = v_G\,, \tag{A.28}$$

that is we only transform the first eigenvalue v_1 and do not modify the others. Then, the $v_1 \ldots v_m$ can be expressed by $x_1 \ldots x_m$ as

$$v_1 = f_1(x_1 \ldots x_G) = \frac{1}{x_1 - \sum_{g=2}^{G} \frac{1}{x_g}}\,,$$

$$v_2 = f_2(x_1 \ldots x_G) = x_2,\ v_3 = f_3(x_1 \ldots x_G) = x_3,\ v_G = f_G(x_1 \ldots x_G) = x_G\,. \tag{A.29}$$

Then, with (A.2) and the absolute value of the Jacobian

$$|J| = \left| \det \begin{pmatrix} \frac{\partial f_1}{\partial x_1} & \cdots & \frac{\partial f_1}{\partial x_G} \\ \vdots & \ddots & \vdots \\ \frac{\partial f_G}{\partial x_1} & \cdots & \frac{\partial f_G}{\partial x_G} \end{pmatrix} \right|$$

$$= \left| \det \begin{pmatrix} -\left(v_1 - \sum_{g=2}^{G} \frac{1}{v_g}\right)^{-2} & 0 & \cdots & 0 \\ -\left(v_2 - \sum_{g=2}^{G} \frac{1}{v_g}\right)^{-2} & v_2^2 & 1 & 0 & \vdots \\ \vdots & & 0 & \ddots & 0 \\ -\left(v_g - \sum_{g=2}^{G} \frac{1}{v_g}\right)^{-2} & v_G^2 & 0 & 0 & 1 \end{pmatrix} \right| \tag{A.30}$$

$$= \frac{1}{\left(v_1 - \sum_{g=2}^{G} \frac{1}{v_g}\right)^2}$$

the joint PDF $p_{\mathbf{x}}(x_1 \ldots x_G)$ of $x_1 \ldots x_G$ reads [Wha71]

$$p_{\mathbf{x}}(x_1 \ldots x_G) = |J| \cdot p_{\mathbf{v}}\left(v_1 = \frac{1}{x_1 - \sum_{g=2}^{G} \frac{1}{x_g}}, v_2 = x_2 \ldots v_G = x_G\right),$$

see (A.29). Setting

$$X = x_1 \tag{A.31}$$

the PDF of X can be determined by integrating out $x_2 \ldots x_G$ to obtain

$$p_X(X) = K_{\text{norm}} \int_0^\infty \cdots \int_0^\infty$$

$$\prod_{z=2}^{g} e^{-\frac{1}{x_1 - \sum_{g=2}^{G} \frac{1}{x_g}}} \left(\frac{1}{x_1 - \sum_{g=2}^{G} \frac{1}{x_g}}\right)^{(S-g)} \left(\frac{1}{x_1 - \sum_{g=2}^{G} \frac{1}{x_g}} - x_z\right)^2 \tag{A.32}$$

$$\prod_{i=2}^{g} e^{-x_i} x_i^{(S-g)} \prod_{i<j}^{g} (x_i - x_j)^2 \, dx_2 \ldots dx_G$$

which, however, is non-trivial and cannot be solved in a close form. Therefore, only numerical results were displayed in Subsection 3.4.3, as the author is not aware of another

approach to determining $p_X(X)$.

Appendix B
Frequently used abbreviations and symbols

B.1   Abbreviations

3G	3rd Generation
4G	4th Generation
AP	Access Point
BER	Bit Error Rate
CCSP	Contours of Constant Symbol Error Probability
Ch	Channel
CO	Channel Oriented
CSI	Channel State Information
DL	Downlink
ES	Exhaustive Search
EVD	Eigenvalue Decomposition
FDD	Frequency Division Duplexing
FFT	Fast Fourier Transformation
IFFT	Inverse Fast Fourier Transformation
MESP	Minimum Energy Soft Precoding
MF	Matched Filter
MIMO	Multiple-Input Multiple-Output
MMSE	Minimum Mean Square Error
MT	Mobile Terminal
NA	Noise Adder
NLP	Nonlinear Programming
OFDM	Orthogonal Frequency Division Multiplexing
PSK	Phase Shift Keying
PDF	Probability Density Function
QP	Quadratic Programming
RO	Receiver Oriented
Rx	Receiver
RxMF	Receive Matched Filter
RxZF	Receive Zero Forcing
SER	Symbol Error Rate
SQP	Sequential Quadratic Programming
SNR	Signal to Noise Ratio

SNIR	<u>S</u>ignal to <u>N</u>oise and <u>I</u>nterference <u>R</u>atio
SVD	<u>S</u>ingular <u>V</u>alue <u>D</u>ecomposition
TDD	<u>T</u>ime <u>D</u>ivision <u>D</u>uplex
THP	<u>T</u>omlinson-<u>H</u>arashima <u>P</u>recoding
TO	<u>T</u>ransmitter <u>O</u>riented
Tx	<u>T</u>ransmitter
TxMF	<u>T</u>ransmit <u>M</u>atched <u>F</u>ilter
TxMMSE	<u>T</u>ransmit <u>M</u>inimum <u>M</u>ean-<u>S</u>quare <u>E</u>rror
TxNZF	<u>T</u>ransmit <u>N</u>on-linear <u>Z</u>ero <u>F</u>orcing
TxPZF	<u>T</u>ransmit <u>P</u>artial <u>Z</u>ero <u>F</u>orcing
TxZF	<u>T</u>ransmit <u>Z</u>ero <u>F</u>orcing
UL	<u>U</u>p<u>l</u>ink
VR	<u>V</u>oronoi <u>R</u>egion
WLAN	<u>W</u>ireless <u>L</u>ocal <u>A</u>rea <u>N</u>etwork
ZF	<u>Z</u>ero <u>F</u>orcing

B.2   Symbols

$\alpha_k^{(r)}$	step length of the SQP procedure
a	grid parameter
$\mathfrak{a}$	data
$\mathfrak{a}^{(r)}$	realization instance of $\mathfrak{a}$
$\underline{\mathbf{a}}^{(r)}$	complex mapping of $\mathfrak{a}^{(r)}$, column vector
$A_{\max}$	maximum magnitude restriction
$\underline{\mathfrak{A}}$	matrix containing all vectors $\underline{\mathbf{a}}^{(r)}$
$d_{\mu,\nu}$	distances from the origin
$\underline{\mathbf{d}}^{(r)}$	unique representative vector of $\mathfrak{a}^{(r)}$
$\underline{\mathbf{d}}^{(r,l)}$	selectable representative vector of $\mathfrak{a}^{(r)}$
$\mathbf{d}_k^{(r)}$	vector resulting from the k-th iteration of the SQP procedure
$\underline{\mathbf{d}}_n^{(r)}$	n-th component of $\underline{\mathbf{d}}^{(r)}$
$\underline{\mathbf{d}}_{\mathrm{opt}}^{(r)}$	energy wise optimum representive vector
$\underline{\mathbf{d}}_{\mathrm{Rx}}$	demodulator output vector
$\underline{\mathbf{D}}$	demodulator matrix
$\underline{D}_z$	diagonal elements of demodulator matrix $\underline{\mathbf{D}}$
$\underline{\mathbf{D}}_n$	partial demodulator matrix of index n
$\underline{\mathbf{D}}_{\mathrm{RxMF}}$	demodulator matrix

δ	mean noise raise
$\overline{\delta}$	overall noise raise
δ_n	component specific noise raise
$\underline{\boldsymbol{\Delta}}$	deviation of the aspired landing points
$\underline{\boldsymbol{\Delta}}_n$	component specific interference compensation
$\underline{\boldsymbol{\Delta}}_{\mathrm{H}}$	additive error matrix
$\Delta^{(r)2}$	total mean square error due to $\underline{\boldsymbol{\Delta}}_{\mathrm{H}}$
Δ^2	mean of the quantity $\Delta^{(r)2}$
$\mathcal{D}(.)$	receive operator
$\underline{\mathfrak{D}}$	matrix containing all vectors $\underline{\mathbf{d}}^{(r)}$
$\mathbb{D}_m$	representative domain
$\mathbb{D}_{m,p}$	subset of $\mathbb{D}_m$ in the case of multiple representative domains
$\underline{\mathbf{e}}$	undisturbed receive vector
$\underline{\mathbf{e}}^{(r)}$	data specific undisturbed receive vector
$\underline{\hat{\mathbf{e}}}$	erroneous undisturbed receive vector
erfc	error function
η	mean energy raise
η_n	component specific energy raise
$\overline{\eta}$	overall energy raise
ε	minimum sufficient decrease of the objective function
$\underline{\mathbf{F}}$	core modulator matrix
$\underline{\mathbf{F}}_{\mathrm{irrel}}$	irrelevant part of core modulator matrix
$\underline{\mathbf{F}}_{\mathrm{rel}}$	relevant part of core modulator matrix
$\underline{\mathbf{F}}_{\mathrm{TxMF}}$	core transmit matched filter
F	objective function
ϕ_k	angle between search direction and Gradient
G	number of existing singular values
$g_k^{(r)}$	search direction of the SQP procedure
$\underline{\mathbf{G}}$	core demodulator matrix
$\underline{\mathbf{G}}_{\mathrm{irrel}}$	irrelevant part of core demodulator matrix
$\underline{\mathbf{G}}_{\mathrm{rel}}$	relevant part of core demodulator matrix
$\underline{\mathbf{G}}_{\mathrm{RxMF}}$	core transmit matched filter
$\mathbb{G}_{\mathfrak{a}^{(r)}}$	data specific representative set of $\mathfrak{a}^{(r)}$
$\mathbb{G}_{\mathfrak{a}^{(r)}}^{\mathbb{R}}$	real valued equivalent of $\mathbb{G}_{\mathfrak{a}^{(r)}}$
γ	pseudo SNR
γ_{inst}	instantaneous pseudo SNR
$\gamma_{\mathrm{inst,min}}$	minimum instantaneous pseudo SNR

γ_{Rx}	SNR at the receiver output
Γ	Gamma function
Γ_{G}	multivariate Gamma function
$\underline{\mathbf{H}}$	channel matrix
$\underline{\mathbf{H}}_{\text{fair}}$	fair channel matrix
$\underline{\mathbf{H}}_{\text{unfair}}$	unfair channel matrix
$\underline{\hat{\mathbf{H}}}$	erroneous channel matrix
$\mathbf{I}$	identity matrix
$\underline{i}_n$	total component specific interference
$\underline{i}_{n'}^{(r)}$	partial component specific interference
k	transmit energy coefficient
$K_{G,S}$	normalization function of the joint PDF $p_{\mathbf{v}}(\nu_1 \dots \nu_G)$
K_{norm}	normalization constant
κ	real scaling factor
L	number of data specific realizations of $\mathfrak{a}^{(r)}$
λ_g	singular value
$\overline{\lambda}_g$	average singular value
$\boldsymbol{\Lambda}$	matrix of the singular values
$\boldsymbol{\Lambda}_{\text{fair}}$	core channel matrix containing singular values of $\underline{\mathbf{H}}_{\text{fair}}$
$\boldsymbol{\Lambda}_{\text{unfair}}$	core channel matrix containing singular values of $\underline{\mathbf{H}}_{\text{unfair}}$
$\boldsymbol{\Lambda}_{\text{irrel}}$	irrelavant partial core matrix
$\boldsymbol{\Lambda}_{\text{rel}}$	relevant partial core matrix
$\mathbf{m}^{(r)}$	integer representative vector of $\mathfrak{a}^{(r)}$
$m_n^{(r)}$	n-th element of vector $\mathbf{m}^{(r)}$
M	cardinality of $\mathbb{V}$
$\underline{\mathbf{M}}$	modulator matrix
$\underline{\mathbf{M}}_{\text{n}}$	partial modulator matrix
$\underline{\mathbf{M}}_{\text{TxMF}}$	TxMF modulator matrix
$\mathcal{M}(.)$	transmit operator
ν_g	eigenvalue
$\underline{\mathbf{n}}$	noise vector at the demodulator output
$\underline{\tilde{\mathbf{n}}}$	noise vector at the channel output
N	dimension of $\underline{\mathbf{d}}^{(r)}$
N_{F}	number of subcarriers
$p_{\text{T}}(T)$	PDF of T
P	number of discrete valued representatives or representative domains, respectively, from which the components of $\underline{\mathbf{d}}^{(r,l)}$ are taken

P_{e}	probability of erroneous transmission
$P_{\max}$	maximum symbol error probability
P_{out}	outage probability
P_{r}	radiated power of $\underline{\mathbf{t}}$
P_{s}	symbol error probability
P_0	error probability of corner regions
Q	dimension of the transmit vector
$\mathcal{Q}(.)$	quantization operator
$\mathbb{Q}_m$	decision regions
$\underline{\mathbf{r}}$	disturbed receive vector
R	number of possible realizations of the data (cardinality)
$\underline{\mathbf{R}}_{\mathrm{d}}$	autocorrelation matrix of data representative vectors
$\underline{\mathbf{R}}_{\mathbf{n}}$	autocorrelation matrix of noise at the demodulator output
$\underline{\mathbf{R}}_{\tilde{\mathbf{n}}}$	autocorrelation matrix of noise at the demodulator input
$\mathbf{S}_n$	selection matrix
σ^2	variance of the real and imaginary parts of $\underline{\tilde{\mathbf{n}}}$
σ_{d}^2	variance of the data
σ_{e}^2	variance of the entire received vector $\underline{\mathbf{e}}$
$\sigma_{\mathrm{e},z}^2$	component-wise variance of the useful received vector $\underline{\mathbf{e}}$
σ_{h}^2	variance of the components of the channel matrix $\underline{\mathbf{H}}$
σ_n^2	component specific variances in the case of RxZF
$\sigma_{\mathrm{RxMF},n}^2$	component specific variances in the case of RxMF
$\sigma_{\mathrm{total}}^2$	total received noise variance
$\sigma_{\Delta_{\mathrm{CSI}}}^2$	noise variance due to CSI errors
$\sigma_{\Delta_{\mathrm{H}}}^2$	variance of the CSI errors
σ_{Z}^2	variance of magnitude dynamics
σ_{ZF}^2	variance of magnitude dynamics in the case of TxZF
$\underline{\mathbf{t}}$	complex transmit vector
$\underline{\hat{\mathbf{t}}}$	erroneous transmit vector
$\underline{\mathbf{t}}^{(r)}$	specific transmit vector of $\underline{\mathbf{d}}^{(r)}$
$\underline{\mathbf{t}}_n^{(r)}$	component specific transmit vector
$\underline{\mathbf{t}}_{0,n}^{(r)}$	normalized component specific transmit vector
$\underline{\mathbf{t}}_{\mathrm{opt}}^{(r)}$	transmit vector causing the minimum transmit energy
T	average required transmit energy
T_{ZF}	average required transmit energy in the case of TxZF
T_1	minimum required transmit energy
T_2	maximum required transmit energy

T_{min}	minimum of average required transmit energy
T_{s}	snapshot specific transmit energy
$T^{(r)}$	transmit energy of $\underline{\mathbf{t}}^{(r)}$
$T_{\mathrm{min}}^{(r)}$	minimum required transmit energy of transmit vector $\underline{\mathbf{t}}_{\mathrm{opt}}^{(r)}$
$T_n^{(r)}$	component specific transmit energies in the case of TxZF
$T_{\mathrm{TxMF},n}^{(r)}$	component specific transmit energies in the case of TxMF
$\underline{\mathbf{u}}_z$	left side singular vector
$\underline{\mathbf{U}}$	left side unitary matrix of the SVD
$\underline{\mathbf{U}}_{\mathrm{fair}}$	left side singular matrix of $\underline{\mathbf{H}}_{\mathrm{fair}}$
$\underline{\mathbf{U}}_{\mathrm{unfair}}$	left side singular matrix of $\underline{\mathbf{H}}_{\mathrm{unfair}}$
υ	comparison between $T(\underline{\mathbf{H}})$ and T to find the elimination criterion
$\mathbf{v}$	ratio of instantaneous to average required transmit energy
$\mathbf{v}_{\mathrm{threshold}}$	elimination threshold
$\underline{\mathbf{v}}_z$	right side singular vector
$\underline{\boldsymbol{v}}_m$	unique representative value
$\underline{\boldsymbol{v}}_{m,p}$	selectable representative value
$\underline{\mathbf{V}}$	right side unitary matrix of the SVD
$\underline{\mathbf{V}}_{\mathrm{fair}}$	right side singular matrix of $\underline{\mathbf{H}}_{\mathrm{fair}}$
$\underline{\mathbf{V}}_{\mathrm{unfair}}$	right side singular matrix of $\underline{\mathbf{H}}_{\mathrm{unfair}}$
$\mathbb{V}$	representative set of $\mathfrak{a}$
$\mathbb{V}_m$	partial representative set of $\mathbb{V}$
X	sum of the reciprocals of the eigenvalues
$\underline{\mathbf{W}}$	Wishart matrix
Z	dimension of the receive vector

References

[3GP03]   *Spatial Channel Model for Multiple Input Multiple Output (MIMO)*
            Simulations.   3GPP   TR   25.996   V6.1.0,   [Online].   Available:
            http://www.3gpp.org/ftp/Specs/html-info/25996.htm, 2003.

[AH05]   Ajib, W.; Haccoun, D.: An overview of scheduling algorithms in MIMO-
            based fourth-generation wireless systems. *IEEE Network*, vol. 19, 2005, pp.
            43–48.

[BBC87]   Benedetto, S.; Biglieri, E.; Castellani, V.: *Digital Transmission Theory.*
            New York: Prentice-Hall, 1987.

[BBT02]   Berezdivin, R.; Breinig, R.; Topp, R.: Next-generation Wireless Communica-
            tions Concepts and Technologies. *IEEE Communications Magazine*, vol. 40,
            2002, pp. 108–116.

[Bel63]   Bello, P. A.: Characterization of randomly time-variant linear channels.
            IEEE Transactions on Communications Systems, vol. 11, 1963, pp. 360–393.

[BF99]   Barreto, A. N.; Fettweis, G.: On the downlink capacity of TDD CDMA
            using a Pre-Rake. *Proceedings IEEE Global Telecommunications Conference*
            (GLOBECOM'99), vol. 1a, Rio de Janeiro, 1999, pp. 117–121.

[Big75]   Biggs, M. C.: Constrained Minimization Using Recursive Quadratic Pro-
            gramming. *Towards Global Optimization*, 1975, pp. 341–349.

[Bin90]   Bingham, J. A. C.: Multicarrier Modulation for Data Transmission: An
            Idea Whose Time Has Come. *IEEE Communications Magazine*, 1990, pp.
            5–14.

[BMWT00]   Baier, P. W.; Meurer, M.; Weber, T.; Tröger, H.: Joint Transmission (JT),
            an alternative rationale for the downlink of time division CDMA using multi-
            element transmit antennas. *Proceedings IEEE 6th International Symposium*
            on Spread Spectrum Techniques & Applications (ISSSTA'00), vol. 1, Parsip-
            pany, 2000, pp. 1–5.

[BPD00]   Brandt-Pearce, M.; Dharap, A.: Transmitter-based multiuser interference
            rejection for the downlink of a wireless CDMA system in a multipath envi-
            ronment. *IEEE Journal on Selected Areas in Communications*, vol. 18, 2000,
            pp. 407–417.

[BQT+03]   Baier, P. W.; Qiu, W.; Tröger, H.; Jötten, C. A.; Meurer, M.; Lehmann, G.: Modelling and Optimization of Receiver Oriented Multi-user MIMO Downlinks for Frequency Selective channels. *Proceedings 10th International Conference on Telecommunications (ICT'03)*, vol. 2, Papeete, 2003, pp. 1547–1554.

[BS02]   Boche, H.; Schubert, M.: A general duality theory for uplink and downlink beamforming. *Proceedings IEEE Vehicular Techn. Conf. (VTC) Fall, Vancouver, Canada*, vol. 1, 2002, pp. 87–91.

[CLM01]   Choi, R. L.; Letaief, K. B.; Murch, R. D.: Miso cdma transmission with simplified receiver for wireless communication handsets. *IEEE Transactions on Communications*, vol. 49, 2001, pp. 888–898.

[CM02]   Choi, R. L. U.; Murch, R. D.: Transmit MMSE pre-rake preprocessing with simplified receivers for the downlinks of MISO TDDCDMA systems. *Proceedings IEEE Global Telecommunications Conference (GLOBECOM'02)*, vol. 1, Taipei, 2002, pp. 429–433.

[CM04]   Choi, L. U.; Murch, R. D.: A transmit preprocessing technique for multiuser MIMO systems using a decomposition approach. *IEEE Transactions on Wireless Communications*, vol. 3, 2004, pp. 20–24.

[Cos83]   Costa, M. H. M.: Writing on dirty paper. *IEEE Transactions on Information Theory*, vol. 29, 1983, pp. 439–441.

[CS99]   Conway, J. H.; Sloane, N. J. A.: *Sphere Packings, Lattices and Groups*. New York/Berlin/Heidelberg: Springer, 1999.

[CS03]   Caire, G.; Shamai, S.: On the achievable throughput of a multiantenna gaussian broadcast channel. *IEEE Transactions on Information Theory*, vol. 49, 2003, pp. 1691–1706.

[CT91]   Cover, T. M.; Thomas, J. A.: *Elements of Information Theory*. Wiley & Sons, 1991.

[Ede89]   Edelman, A.: *Eigenvalues and condition numbers of random matrices*. Dissertation, Dept. of Mathematics, MIT University, 1989.

[EN93]   Esmailzadeh, R.; Nakagawa, M.: Pre-rake diversity combination for direct sequence spread spectrum mobile communications systems. *IEICE Transaction Communication*, vol. E76-B, 1993, pp. 1008–1015.

[ESN93]   Esmailzadeh, R.; Sourour, E.; Nakagawa, M.: Pre-rake diversity combing in time division duplex CDMA mobile communication. *Proceedings IEEE International Conference on Communications (ICC'93)*, 1993, pp. 463–467.

[ESZ00]   Erez, U.; Shamai, S.; Zamir, R.: Capacity and Lattice-Strategies for Cancelling known Interference. *Proceedings International Symposium on Information Theory and Its Applications (ISITA 2000)*, Honolulu, 2000, pp. 681–684.

[ESZ05]   Erez, U.; Shamai, S.; Zamir, S.: Capacity and lattice strategies for canceling known interference. *IEEE Transactions on Information Theory*, vol. 51, 2005, pp. 3820–3833.

[Fis02]   Fischer, R. F. H.: *Precoding and Signal Shaping for Digital Transmission.* New York: John Wiley & Sons, Inc., 2002.

[FK03]   Fazel K., K. S. (Hrsg.): *Multi-Carrier and Spread Spectrum Systems.* Chichester: John Wiley & Sons, 2003.

[Fle70]   Fletcher, R.: A New Approach to Variable Metric Metric Algorithms. *Computer Journal*, vol. 13, 1970, pp. 317–322.

[Flo95]   Floudas, C. A.: *Nonlinear and Mixed-Integer Optimization.* Oxford: Oxford University Press, 1995.

[FWLH02a] Fischer, R. F. H.; Windpassinger, C.; Lampe, A.; Huber, J. B.: MIMO Precoding for Decentralized Receivers. *Proceedings IEEE International Symposium on Information Theory (ISIT'02)*, Lausanne, Switzerland, 2002, pp. 496.

[FWLH02b] Fischer, R. F. H.; Windpassinger, C.; Lampe, A.; Huber, J. B.: Space time transmission using Tomlinson-Harashima precoding. *Proceedings 4th International ITG Conference on Source and Channel Coding 2002 (SCC'2002)*, Berlin, 2002, pp. 139–147.

[GC02a]   Georgouilis, S.; Cruickshank, D.: Transmitter based inverse filters for MAI and ISI mitigation in a TDD/CDMA downlink. *Proceedings IEEE 56th Vehicular Technology Conference (VTC'02-Fall)*, Vancouver, 2002, pp. 1818–1822.

[GC02b]   Ginis, G.; Ciioffi, J. M.: Vectored transmission for digital subscriber line systems. *IEEE Journal on Selected Areas in Communications*, vol. 20, 2002, pp. 1085–1104.

[GP80]   Gelfand, S. I.; Pinsker, M. S.: Coding for channel with random parameters. *Problems Information and Control*, vol. 9, 1980, pp. 19–31.

[GvL96]   Golub, G. H.; van Loan, C. F.: *Matrix Computations*. Baltimore: The Johns Hopkins University Press, 1996.

[Hay83]   Haykin, S.: *Communication Systems*. New Jersey: John Wiley & Sons Inc., 1983.

[HIRF05]   Habendorf, R.; Irmer, R.; Rave, W.; Fettweis, W.: Nonlinear multiuser pre-coding for non-connected decision regions. *Proceedings 6th IEEE Workshop on Signal Processing Advances in Wireless Communications (SPAWC)*, New York City, 2005, pp. 535–539.

[HL05]   Han, S. H.; Lee, J. H.: An overview of peak-to-average power ratio reduction techniques for multicarrier transmission. *IEEE Wireless Communications*, vol. 12, 2005, pp. 56–65.

[HM72]   Harashima, H.; Miyakawa, H.: Matched-transmission technique for channels with intersymbol interference. *IEEE Transactions on Communications*, vol. 20, 1972, pp. 774–780.

[HMBZ06a]   Hahn, J.; Meurer, M.; Baier, P. W.; Zirwas, W.: Spectrum and energy efficient MIMO OFDM multi-user downlinks for B3G and 4G mobile radio systems. *Proceedings 13th Int. Conference on Telecommunications (ICT'06)*, 2006.

[HMBZ06b]   Hahn, J.; Meurer, M.; Baier, P. W.; Zirwas, W.: Spread-spectrum based low-cost provision of downlink channel state information to the access points of FDD OFDM mobile radio systems. *Proceedings IEEE 9th International Symposium on Spread Spectrum Techniques and Applications (ISSSTA'06)*, Manaus, 2006, pp. 512–518.

[HPS05a]   Hochwald, B. M.; Peel, C. B.; Swindlehurst, A. L.: A vector-pertutbation technique for near-capacity multiantenna multiuser communication - Part I: channel inversion and regularization. *IEEE Transactions on Communications*, vol. 53, 2005, pp. 195–202.

[HPS05b]   Hochwald, B. M.; Peel, C. B.; Swindlehurst, A. L.: A vector-pertutbation technique for near-capacity multiantenna multiuser communication - Part II: Perturbation. *IEEE Transactions on Communications*, vol. 53, 2005, pp. 537–544.

[HRF06]   Habendorf, R.; Rave, W.; Fettweis, G.: Nonlinear Predistortion with Reduced Peak-to-Average Power Ratio. *Proceedings 9th International Symposium on Wireless Personal Multimedia Communications*, San Diego, 2006.

[HSB03]   Hauenstein, T.; Schubert, M.; Boche, H.: On power reduction strategies for the multi-user downlink with decetralized receivers. *Proceedings IEEE 57th Vehicular Technology Conference (VTC'03-Spring)*, Jeju, 2003, pp. 1007–1011.

[Hug00]   Hughes, B. L.: Differential space-time modulation. *Transactions on Information Theory*, vol. 46, 2000, pp. 2567–2578.

[HvHJ$^+$]   Haustein, T.; von Helmolt, C.; Jorswieck, E.; Jungnickel, V.; Pohl, V.: Performance of MIMO systems with channel inversion. *Proceedings IEEE 55th Vehicular Technology (VTC'02-Spring)*.

[IEE]   *Worldwide Interoperability for Microwave Access.* [Online]. Available: http://www.wimaxforum.org.

[IEE99]   *Supplement to the IEEE standard for Information technology-part 11: Wireless LAN medium access control (MAC) and physical layer (PHY) specifications: High-speed physical layer in the 5 GHz band.* Technical Report IEEE Std 802.11a-1999, 1999.

[IEE05]   *Air interface for fixed and mobile broadband wireless access systems.* IEEE P802.16e/D12, 2005.

[IHRF03]   Irmer, R.; Habendorf, R.; Rave, W.; Fettweis, G.: Nonlinear Multiuser Transmission using Multiple Antennas for TDD-CDMA. *Proceedings IEEE 6th International Symposium on Wireless Personal Multimedia Communications 2003 (WPMC'03)*, vol. 3, Yokosuka, 2003, pp. 251–255.

[INBF01]   Irmer, R.; Noll-Barreto, A.; Fettweis, G.: Transmitter precoding for spread-spectrum signals in frequency-selective fading channels. *Proceedings 3G Wireless*, San Francisco, 2001, pp. 939–944.

[IRF03]   Irmer, R.; Rave, W.; Fettweis, G.: Minimum BER Transmission for TDD-CDMA in frequency-selective channels. *Proceedings IEEE International Symposium On Personal, Indoor And Mobile Radio Communications (PIMRC'03)*, vol. 2, Beijing, 2003, pp. 1260–1264.

[Jam64]   James, A. T.: Distribution of matrix variate and latent roots derived from normal samples. *Ann. Math. Stat.*, vol. 35, 1964, pp. 475–501.

[JBM+02]   Jötten, C. A.; Baier, P. W.; Meurer, M.; Weber, T.; Haardt, M.: Efficient
            Representation and Feedback Signaling of Channel State Information in Fre-
            quency Division Duplexing MIMO Systems. *Proceedings 5th International
            Symposium on Wireless Personal Multimedia Communications (WPMC'02)*,
            Honolulu, 2002, pp. 444–448.

[Jia04]   Jiang, J.: *Capacity-Approaching Data Transmission in MIMO Broadcast
            Channels – A Cross-Layer Approach –*. Dissertation, Virginia Polytechnic
            Institute and State University, 2004.

[JVG04]   Jindal, N.; Vishwanath, S.; Goldsmith, A.: On the Duality of Gaussian
            Multiple-Access and Broadcast Channels. *IEEE Transactions on Informa-
            tion Theory*, vol. 50, 2004, pp. 768–783.

[JVP98]   Jang, W. M.; Vojcic, B. R.; Pickholtz, R. L.: Joint Transmitter-Receiver Op-
            timization in Synchronous Multiuser Communications over Multipath Chan-
            nels. *IEEE Transactions on Communications*, vol. 46, 1998, pp. 269–278.

[KB07a]   Keskin, F.; Baier, P. W.: Energy efficient MIMO OFDM multi-user down-
            links: THP based versus soft precoding. *Proceedings IEEE joint conference
            (ICT-MICC '07) of 14th IEEE International Conference On Telecommu-
            nications (ICT '07) and 8th IEEE Malaysia International Conference on
            Communications (MICC '07)*, Penang, 2007.

[KB07b]   Keskin, F.; Baier, P. W.: Minimum energy precoding in receiver oriented
            MIMO multi-user mobile radio downlinks. *Proceedings IEEE 65th Vehicular
            Technology Conference (VTC'07)*, Dublin, 2007, pp. 2073–2077.

[KE07]   Keskin, F.; Egelhof, A.: On the receive signal dynamics in energy efficient
            MIMO OFDM multi-user mobile radio downlinks. *Proceedings IEEE 6th
            Workshop on Multi-Carrier Spread Spectrum 2007 (MC-SS '07)*, München,
            2007, pp. 247–256.

[KHB07]   Keskin, F.; Hahn, J.; Baier, P. W.: Minimum energy soft precoding. *IEE
            Electronics Letters*, vol. 43, 2007, pp. 356–358.

[Kle96]   Klein, A.: *Multi-user detection of CDMA signals – algorithms and their
            application to cellular mobile radio*. Fortschrittberichte VDI, Reihe 10, Nr.
            423. Düsseldorf: VDI-Verlag, 1996.

[KM00]   Kowalewski, F.; Mangold, P.:   Joint predistortion and transmit
          diversity.   *Proceedings IEEE Global Telecommunications Conference
          (GLOBECOM'00)*, vol. 1, San Francisco, 2000, pp. 245–249.

[KSS99]   Karimi, H. R.; Sandell, M.; Salz, J.: Comparison between transmitter and
          receiver array processing to achieve interference nulling and diversity. *Proceedings IEEE 10th International Symposium on Personal, Indoor and Mobile Radio Communications (PIMRC'99)*, Osaka, 1999, pp. 997–1001.

[LHS03]   Love, D. J.; Health, R. W.; Strohmer, T.:   Grassmannian beamforming
          for multiple-input multiple-output wireless systems. *IEEE Transactions on Information Theory*, vol. 49, 2003, pp. 2735–2747.

[LSF03]   Lampe, L. H.-J.; Schober, R.; Fischer, R.:   Coded differential space-time
          modulation for flat fading channels. *IEEE Transactions on Wireless Communications*, vol. 2, 2003, pp. 582–590.

[Lue96]   Luetkepohl, H.: *Handbook of Matrices.* Wiley & Sons, 1996.

[Mat06]   Mathworks, T.: Optimization toolbox. *Users Guide*, 2006.

[MBQ04]   Meurer, M.; Baier, P. W.; Qiu, W.: Receiver Orientation versus Transmitter
          Orientation in Linear MIMO Transmission Systems. *EURASIP Journal on Applied Signal Processing*, vol. 9, 2004, pp. 1191–1198.

[MBW+00] Meurer, M.; Baier, P. W.; Weber, T.; Lu, Y.; Papathanassiou, A.:   Joint
          transmission: advantageous downlink concept for CDMA mobile radio systems using time division duplexing. *IEE Electronics Letters*, vol. 11, 2000, pp. 900–901.

[Meu05]   Meurer, M.: *Empfängerorientierte Funkkommunikation - Grundzüge, Potential und Ausgestaltung einer unkonventionellen Übertragungstechnik für die Mobilkommunikation.* Habilitation, Lehrstuhl für hochfrequente Signalübertragung und -verarbeitung, Technische Universität Kaiserslautern, 2005.

[MFP97]   Masoomzadeh-Fard, A.; Pasupathy, S.: Combined equalization and differential detection using precoding. *IEEE Transactions on Communications*, vol. 45, 1997, pp. 274–278.

[MGS98]   Montalbano, G.; Ghauri, I.; Slock, D. T. M.: Spatio-temporal array processing for CDMA/SDMA downlink transmission. *Proceedings 32th Asilomar Conference on Signals, Systems and Computers*, vol. 2, Pacific Grove, 1998, pp. 1337–1341.

[MR98]   May, T.; Rohling, H.: Reducing the Peak-to-Average Power in OFDM Radio Tranmission Systems. *Proceedings IEEE (VTC'98)*, Ottawa, 1998, pp. 2474–2478.

[MSN97]   Matsutani, H.; Sanada, Y.; Nakagawa, M.: A forward link intracell orthogonalization technique using multicarrier pre-decorrelation for CDMA wireless local communication system. *Proceedings IEEE 8th International Symposium on Personal, Indoor Mobile Radio Communications (PIMRC'97)*, vol. 1, Helsinki, 1997, pp. 125–129.

[MTWB01]   Meurer, M.; Tröger, H.; Weber, T.; Baier, P. W.: Synthesis of joint detection (JD) and joint transmission (JT) in CDMA downlinks. *IEE Electronics Letters*, vol. 37, 2001, pp. 919–920.

[MWQ04]   Meurer, M.; Weber, T.; Qiu, W.: Transmit Nonlinear Zero Forcing: Energy Efficient Receiver Oriented Transmission in MIMO CDMA Mobile Radio Downlinks. *Proc. IEEE 8th International Symposium on Spread Spectrum Techniques & Applications (ISSSTA'04)*, Sydney, 2004, pp. 260–269.

[NW99]   Nocedal, J.; Wright, S. J.: *Numerical Optimization*. New York: Springer, 1999.

[Pap96]   Papageorgiou, M.: *Optimierung*. Munich: R. Oldenbourg Verlag, 1996.

[PHS03]   Peel, C. B.; Hochwald, B. M.; Swindlehurst, A. L.: Achieving near-capacity in multi-antenna multi-user systems. *Proceedings 41st Allerton Conference on Communication, Control and Computing*, Monticello, 2003.

[PJU06]   Psaltopoulos, G. K.; Joham, M.; Utschick, W.: Comparison of lattice search techniques for nonlinear precoding. *Proceedings International ITG - IEEE Workshop on Smart Antennas, WSA 2006*, 2006.

[PMWB00]   Papathanassiou, A.; Meurer, M.; Weber, T.; Baier, P. W.: A novel multiuser transmission scheme requiring no channel estimation and no equalization at the mobile stations for the downlink of TD-CDMA operating in the TDD mode. *Proceedings IEEE 52nd Vehicular Technology Conference (VTC'00-Fall)*, Bosten, 2000, pp. 203–210.

[Pow83]   Powell, M. J. D.: Variable Metric Methods for Constrained Optimization. *Mathematical Programming: The State of the Art*, 1983, pp. 288–311.

[Pro95]   Proakis, J. G.: *Digital-Communications*. New York: McGraw-Hill, 1995.

[Qiu05]   Qiu, W.:   *Transmit power reduction in MIMO multi-user mobile radio downlinks by the rationale receiver orientation.* Dissertation, Lehrstuhl für hochfrequente Signalübertragung und -verarbeitung, Technische Universität Kaiserslautern, 2005.

[QMBW04]   Qiu, W.; Meurer, M.; Baier, P. W.; Weber, T.:   Power Efficient CDMA Broadcast System Doing Without any Channel Knowledge at the Receivers, a Non-obvious Modification of THP. *Proceedings IEEE joint conference (APCC/MDMC'04) of 10th Asia-Pacific Conference on Communications (APCC2004) and 5th International Symposium on Multi-Dimensional Mobile Communications (MDMC2004)*, Beijing, 2004, pp. 793–799.

[QTM02]   Qiu, W.; Tröger, H.; Meurer, M.: System model of joint transmission (JT) in multi-user MIMO transmission systems. *COST 273 TD(02) 008*, London, 2002.

[QTMJ03]   Qiu, W.; Tröger, H.; Meurer, M.; Jötten, C. A.:   Performance analysis of a channel oriented concept for multi-user MIMO downlinks with frequency selective channels. *Proceedings IEEE 57th Vehicular Technology Conference (VTC'03-Spring)*, Jeju, Korea, 2003, pp. 539–543.

[RG96]   Rohling, H.; Grünheid, R.: OFDM transmission technique with flexible sub-carrier allocation. *Proceedings IEEE International Conference on Telecommunications*, Istanbul, Turkey, 1996, pp. 567–571.

[RG02]   Rohling, H.; Galda, D.: OFDM - a good candidate for the 4th generation mobile communications. *Proceedings of the International Seminar on Special Topics on Advanced Communication Technologies*, Antalya, Turkey, 2002.

[Sal67]   Saltzberg, B. R.: Performance of an Efficient Parallel Data Transmission. *IEEE Transactions on Communications*, vol. 15, 1967, pp. 805–811.

[SB93]   Steiner, B.; Baier, P. W.:   Low Cost Channel Estimation in the Uplink Receiver of CDMA Mobile Radio Systems. *Die Frequenz*, vol. 47, 1993, pp. 11–12.

[Sch85]   Schittkowski, K.:   NLQPL: A FORTRAN-Subroutine Solving Constrained Nonlinear Programming Problems. *Annuals of Operations Research*, vol. 5, 1985, pp. 485–500.

[SDS+05]   Salo, J.; Del Galdo, G.; Salmi, J.; Kyösti, P.; Milojevic, M.; Laselva, D.; Schneider, C.:   *MATLAB implementation of the 3GPP*

Spatial Channel Model (3GPP TR 25.996). [Online]. Available: http://www.tkk.fi/Units/Radio/scm/, 2005.

[Sha58] Shannon, C. E.: Channels with side information at the transmitter. *IBM Journal of Research and Development*, vol. 2, 1958, pp. 289–293.

[SJ67] Stein, S.; Jones, J. J.: *Modern Communication Principles.* New York: Mc Graw-Hill, 1967.

[SWBC02] Sklavos, A.; Weber, T.; Baier, P. W.; Costa, E.: Beyond 3G radio interface JOINT: Optimum uplink data detection when applying OFDM. *Proceedings 7th International OFDM-Workshop (InOWo'02)*, Hamburg, 2002, pp. 11–15.

[TC94] Tang, Z.; Cheng, S.: Interference cancellation for DS-CDMA systems over flat fading channels through pre-decorrelating. *Proceedings IEEE 5th International Symposium on Personal, Indoor and Mobile Radio Communications (PIMRC'94)*, vol. 2, The Haag, 1994, pp. 435–438.

[Tom71] Tomlinson, M.: New automatic equalizer Quadratic Programming. *Electronics Letters*, vol. 7, 1971, pp. 138–139.

[Trö03] Tröger, H.: *Empfängerorientierte Mehrteilnehmer-Übertragungsverfahren für die Abwärtsstrecke zellularer Mobilfunksysteme.* Dissertation, Lehrstuhl für hochfrequente Signalübertragung und -verarbeitung, Universität Kaiserslautern, 2003.

[UY01] Ulukus, S.; Yates, R. D.: Signature Squence Optimization in Asynchronous CDMA Systems. *Proceedings IEEE International Conference on Communications (ICC'01)*, Helsinki, 2001, pp. 545–549.

[VJ98] Vojcic, B. R.; Jang, W. M.: Transmitter precoding in synchronous multiuser communications. *IEEE Transactions on Communications*, vol. 46, 1998, pp. 1346–1355.

[vNP00] van Nee, R. D. J.; Prasad, R.: *OFDM for Wireless Multimedia Communications.* Boston: Artech House, 2000.

[VT03] Viswanath, P.; Tse, D.: Sum capacity of the Multiple Antenna Gaussian Broadcast Channel and Uplink-Downlink Duality. *IEEE Transactions on Information Theory*, vol. 49, 2003, pp. 1912–1921.

[WE71]   Weinstein, S. B.; Ebert, P. M.: Data Transmission by Frequency Division
            Multiplexing Using the Discrete Fourier Transform. *IEEE Transactions on
            Communications*, vol. 19, 1971, pp. 628–634.

[Wen02]   Wenestrom, M.: *On MIMO systems and adaptive arrays for wireless com-
            munication.* Dissertation, Dept. Elect. Eng., Uppsala University, 2002.

[WFH04]   Windpassinger, C.; Fischer, R. F. H.; Huber, J. B.: Lattice-reduction-aided
            broadcast precoding. *IEEE Transactions on Communications*, vol. 52, 2004,
            pp. 2057–2060.

[Wha71]   Whalen, A. D.: *Detection of Signals in Noise.* New York: Academic Press,
            1971.

[WLM+03]   Weber, T.; Liu, Y.; Maniatis, I.; Meurer, M.; Costa, E.: Performance of a
            Multiuser OFDM Mobile Radio System with Joint Detection. *Proceedings
            8th International OFDM Workshop (InOWo '03)*, Hamburg, 2003, pp. 191–
            195.

[WM03]   Weber, T.; Meurer, M.: Optimum joint transmission: Potentials and duali-
            ties. *Proceedings 6th International Symposium on Wireless Personal Multi-
            media Communications 2003 (WPMC'03)*, vol. 1, Yokosuka, 2003, pp. 79–83.

[WMS03]   Weber, T.; Meurer, M.; Sklavos, A.: Optimum nonlinear joint transmission.
            COST 273 TD(03)008, Barcelona, 2003.

[WMZ04]   Weber, T.; Meurer, M.; Zirwas, W.: Low Complexity Energy Efficient Joint
            Transmission for OFDM Multiuser Downlinks. *Proceedings IEEE 15th Inter-
            national Symposium on Personal, Indoor and Mobile Radio Communications
            (PIMRC'04)*, vol. 2, Barcelona, 2004, pp. 1095–1099.

[Wun03]   Wunder, G.: *A theoretical framework for the peak-to-average power control
            problem in OFDM transmission.* Dissertation, Technische Universität Berlin,
            2003.

[Yan05]   Yang, H.: A Road to Future Broadband Wireless Access: MIMO-OFDM-
            Based Air Interface. *IEEE Communications Magazine*, 2005, pp. 53–60.

[ZF86]   Zurmühl, R.; Falk, S.: *Matrizen und ihre Anwendungen.* vol. 2.5. Berlin:
            Springer-Verlag, 1986.

Tabellarischer Lebenslauf

Name:	Faruk Keskin
Adresse:	Seydlitzstr. 17
	67061 Ludwigshafen
Geburtsdatum:	09.08.1980
Staatsangehörigkeit:	türkisch
Schulbildung:	1987-1991 Grundschule Gräfenau Ludwigshafen a. Rh.
	1991-2000 Carl-Bosch Gymnasium Ludwigshafen a. Rh.
Schulabschluss:	Allgemeine Hochschulreife
Studium:	2000-2005
	Studium der Informationstechnik
	an der Technischen Universität Kaiserslautern
	Vertiefungsrichtung Kommunikationssysteme
Studienabschluß:	Diplom
Berufstätigkeit:	seit Dezember 2005
	wissenschaftlicher Mitarbeiter am Lehrstuhl
	für hochfrequente Signalübertragung und -verarbeitung
	an der Technischen Universität Kaiserslautern